Addis Ababa University
Addis Ababa Institute of Technology
School of Civil and Environmental Engineering

FINITE ELEMENT BASED INVESTIGATION OF BELLED PIERS IN EXPANSIVE SOILS

by

Gideon Amha Gebremedhin

B.Sc. (Civil Engineering, Addis Ababa University, 2011)

Advisor: Henok Fikre (Ph.D.)

Sponsor: Ministry of Education(MOE)

April, 2017

A Thesis submitted at Addis Ababa Institute of Technology
in partial fulfillment of the requirements for
the Degree of Master of Science in Geotechnical Engineering

The undersigned have examined the thesis entitled **'Finite Element Based Investigation of Belled Piers in Expansive Soils'** presented by **Gideon Amha Gebremedhin**, a candidate for the degree of Master of Science and hereby certify that it is worthy of acceptance.

Advisor	Signature	Date
Internal Examiner	Signature	Date
External Examiner	Signature	Date
Chair Person	Signature	Date

UNDERTAKING

I certify that the research work titled "**Finite Element Based Investigation of Belled Piers in Expansive Soils**" is my own work. The work has not been presented elsewhere for assessment. Where material has been used from other sources, it has been properly acknowledged /referred.

_____

Gideon Amha Gebremedhin

Acknowledgment

I would like to pay owed gratitude to my advisor, Dr. Henok Fikre (Ph.D.) for his endless patience. Douglas Adams famously remarked "*I love deadlines — I like the whooshing sound they make as they fly by....*"; two years and three deadlines later my advisor has been kind enough to presume that my glacial pace was less from a leaning toward laziness than a thirst for thoroughness, a certain excess of inquisitiveness, or a propensity to ponder rather than produce.

Late in his life, Albert Einstein wrote "*Many times a day I realize how my own endeavors rely on the labors of others, and how earnestly I must exert myself to give in return as much as I have received and am still receiving...*"; Salsawi Ferede, Fatema Safaa Noori, Ashenafi Yilikal, Belay Zeleke, Tenaw Workie, Admassu Tirualem, Alemayehu Bekele, Anteneh Mitiku, Askale Gebreyes, Samuel Tadesse (Ph.D.), Messele Haile (Ph.D.), Ameyou Temesgen, Alpha Seifu (M. D.), Elias Yilma, Kidus Ayalneh, Besrat Eshetu, Kaleab Woldeyohannes; I hope to give in return as much as I have received.

I would like to thank the Ministry of Education of Ethiopia for sponsoring this work.

Without the constant support of my family, this work would not be possible.

Contents

List of Figures

List of Tables

Abstract

Expansive soils are a worldwide challenge. Straight shaft drilled pier foundation and the belled drilled pier foundation are rational and reliable solutions to combat the problem of expansive soils. The belled drilled pier foundation is especially preferred when deep depths of the swelling zone exist and large uplift forces have to be resisted. Various investigations have studied the behavior of straight shaft drilled pier foundations when they are employed in expansive soils, while very few investigations exist for belled drilled pier foundations employed in expansive soils. The only in-depth investigation concerned with the study of the behavior of belled piers in expansive soils is the elastic pier approach. Yet, this approach has limitations and is majorly focused on straight shaft piers. Concerning the design of belled piers in expansive soils, the rigid pier design method is commonly used. However, this method has limitations as well. To address the limitations of the elastic pier approach and the rigid pier design, a finite element based investigation of the behavior of belled piers in expansive soils is conducted using the finite element software Abaqus. The finite element model was validated using several mechanisms. The effect of various parameters affecting belled pier behavior in expansive soils was investigated. A cost comparison among different types of piers was conducted. Finally, trend lines that can serve as design charts were developed. The parametric investigations indicated that when designing belled piers in expansive soils increasing the shaft diameter is preferred to increasing the length or the bell size; the limiting diameter for belled piers is much higher than that for straight shaft piers; most belled piers in expansive soils in Ethiopia do not need tensile reinforcement and the applied load needed to fully eliminate tensile stresses in belled piers is less than that needed in straight shaft piers. The cost comparison indicated that for smaller values of the swelling pressure and the depth of the swelling zone, straight shaft piers are more cost effective; while for medium to large values of the swelling pressure and the depth of the swelling zone, large bell size belled piers are more cost effective. The trend lines indicated that in Ethiopia belled piers with the minimum possible values of the shaft diameter, base to shaft diameter ratio and length can be used.

Keywords: Expansive soils; Belled piers; Elastic pier approach; Rigid pier design; Finite element model; Parametric investigation; Cost comparison; Trend lines

Chapter 1

Introduction

1.1 Background

Karl Terzaghi writing in 1951 (Murthy 2002), on 'The Influence of Modern Soil Studies on the Design and Construction of Foundations' commented on foundations as follows:

> "Foundations can appropriately be described as a necessary evil. If a building is to be constructed on an outcrop of sound rock, no foundation is required. Hence, in contrast to the building itself which satisfies specific needs, appeals to the aesthetic sense, and fills its matters with pride, the foundations merely serve as a remedy for the deficiencies of whatever whimsical nature has provided for the support of the structure at the site which has been selected. On account of the fact that there is no glory attached to the foundations, and that the sources of success or failures are hidden deep in the ground, building foundations have always been treated as step children; and their acts of revenge for the lack of attention can be very embarrassing".

Expansive soils cause more damage to structures, particularly light buildings and pavements, than any other natural hazard, including earthquakes and floods (Jones and Holtz 1973). The estimated damage to buildings, roads, and other structures built on expansive soils, for example, exceeds 15 billion dollars in the US annually (Al-Rawas and Goosen 2006). Out of some surveyed buildings constructed on expansive soils in Addis Ababa, Ethiopia, 64 % were adversely affected; they showed cracks associated with expansive soils (Sisay and Haile 2004). The design of foundations for light structures on expansive soils is perhaps one of the most challenging problems facing foundation engineers (Nelson 2007).

Expansive soils are generally found in arid and semiarid regions that cover vast areas around the world. Due to the presence of some hydrophilic clay minerals such as montmorillonite, these soils exhibit significant volume changes upon wetting or drying. Principally, swelling occurs when water infiltrates between the clay particles, causing them to separate

(Aljorany and Noori 2013). The differential movement caused by swell or shrinkage of expansive soils can increase the probability of damage to the foundation and superstructure. Differential movements redistribute the structural loads causing concentration of loads on portions of the foundation and large changes in moments and shear forces in the structure not previously accounted for in standard design practice (U.S. Army Corps of Engineers 1983).

There are many measures to mitigate expansive soil troubles. Some of these measures deal with altering the chemical or mineralogical structure of swelling clay skeleton by blending lime, cement, or fly ash. Others are by installing tension-resistant members to absorb the swelling pressure, such as piles, piers, and belled piers or recently, granular pile anchor (GPA) (Aljorany and Noori 2013).

The drilled pier foundation is a rational solution to combat the problem of expansive soils; however, the design and construction must be closely controlled (Chen 1988). Adequate anchorage length has to be provided in the zone unaffected by moisture change. The drilled pier foundation may prove economical in areas where considerable expansion is to be expected, and the additional cost can be balanced against the saving in future maintenance (Teferra 1992). For sites with high to very high expansion potential the most reliable method for foundation design is the use of pier and grade beam system (Nelson 2007).

Drilled piers, when made with an enlarged base, are commonly referred to as belled piers (Chen 1988). The bell (enlarged base) serves like an anchor, increasing uplift capacity of the pier. Increased uplift capacity of these piers makes them useful for use in foundation of structures constructed in expansive soils. The greatest advantage of the belled pier is that the resistance against uplift will not be affected by loss of friction in the zone unaffected by wetting. If, for some reason, such as the rise of ground water, the skin friction in this zone is lost, then straight shaft pier uplift is unavoidable. With belled piers, the total weight of the soil above the bell, will not be affected by moisture change. Hence, there is always an added factor of safety of this system against uplift (Chen 1988). Belled piers are normally used when large uplift forces have to be resisted (Murthy 2002).

Different methods exist to analyze drilled pier foundations in expansive soil, among which the finite-element method (FEM) provides a good option in theoretical analysis (Xiao et al. 2011). FEM relies on the discretisation of the geometry of the structure to solve system of equations, effectively subdividing the structure in an assembly of simple (finite) elements. FEM has the following advantages (PRE Technologies 2014):

- Comprehensive result sets, generating the physical response of the system at any location, including some which might have been neglected in an analytical approach.
- Safe simulation of potentially dangerous, destructive or impractical load conditions and failure modes.

- Optimal use of a model. Often, several failure modes or physical events can be tested within a common model.
- The simultaneous calculation and visual representation of a wide variety of physical parameters such as stress or time, enabling the designer to rapidly analyze performance and possible modifications.
- Extrapolation of existing experimental results via parametric analyses of validated models.
- Relatively low investment and rapid calculation time for most applications.

One such FEM software is Abaqus. Abaqus is a software suite for finite element analysis and computer-aided engineering, originally released in 1978. The product is popular with non-academic and academic institutions in engineering alike due to the wide material modelling capability, and the program's ability to be customized. Abaqus is preferred in geotechnical engineering, due to its powerful capability in non-linear analysis (Zhan et al. 2012). Abaqus also provides a good collection of multiphysics capabilities, such as coupled acoustic-structural and structural-pore capabilities, making it attractive for belled pier analysis in expansive soils.

1.2 Statement of the problem

Expansive soils are a worldwide challenge. With the rapid development in urban infrastructure, expansive soil problems have become more evident; there is therefore a need to address the problems associated with these soils (Al-Rawas and Goosen 2006). One solution is to use belled pier foundations.

Various researches and books have investigated the behavior of straight shaft piers in expansive soils (Poulos and Davis 1980; Chen 1988; Challa and Poulos 1991; Nelson and Miller 1992; Mohamedzein et al. 1999; Fan et al. 2007; Nelson et al. 2007; Kaufmann et al. 2010; Xiao et al. 2011; Nelson et al. 2012; Aljorany and Noori 2013). However, very few investigations exist concerning belled piers in expansive soils. Though some design approaches exist (Poulos and Davis 1980; Chen 1988 and O'Neill 1988) the only in-depth investigation of the behavior of belled piers in expansive soils was presented by Poulos and Davis (1980) by considering the soil as an elastic medium known as the elastic pier approach. This approach was later somewhat modified by Nelson and Miller (1992) and Nelson et al. (2007) to make it more easily usable by the design engineer.

The most common design approach for belled piers in expansive soils is O'Neill's (1988) approach (see Section 2.5.1). This approach has the following limitations:

- Pier heave is considered to be zero. If some pier heave were to be allowed, more economical designs can be obtained.
- No soil-pier slip is considered. But, some soil-pier slip is certain to exist in the actual soil-pier interaction.
- Bell friction is neglected.
- Interface shear stress is considered as a constant maximum value throughout the length of the belled pier in the swelling zone.
- For large bell sizes, increase in shaft diameter does not reduce the corresponding required length for a safe design. This results in uneconomical designs for large bell size belled piers.
- Does not enable to determine the maximum tensile stresses developed inside the belled piers accurately.

The elastic pier approach investigation (Poulos and Davis 1980; Nelson and Miller 1992; Nelson et al. 2007) in relation to belled piers in expansive soils has the following limitations:

- The plastic behavior of the soil is not considered.
- Investigations are presented for belled piers with bell sizes of bell to shaft diameter (db/d) of 2 only.
- Relationships with time have not been investigated.
- Bell friction is neglected.
- No suggestions have been given on whether to use small bell sizes or large bell sizes.
- The interface shear stress between the pier and the soil is an approximation.

Therefore, it is necessary to conduct a study that addresses these limitations of both O'Neill's (1988) design approach and the elastic pier approach investigation (Poulos and Davis 1980; Nelson and Miller 1992; Nelson et al. 2007). This work attempts to do so.

1.3 Objectives

1.3.1 General Objective of the study

The main objective of the work is to conduct an in-depth investigation of the behavior of belled piers in expansive soils and therefore enable geotechnical engineers to conduct the

appropriate designs and make the correct decisions when they are faced with the problem of employing belled piers in expansive soils. This objective will be met using the FEM software Abaqus.

1.3.2 Specific Objectives of the study

The specific objectives of the study are listed as follows:

- Investigate the effect of parameters that can affect belled pier behavior in expansive soils. These parameters include:
  - Length of the belled piers.
  - Shaft diameter of the belled piers.
  - Bell size of the belled pier.
  - Interface shear stress on the bell (bell friction).
  - Depth of the swelling zone of the expansive soil.
  - Time.
  - The elastic modulus and undrained cohesion of the soil.
  - Applied loads coming from the super structure.
- Conduct a cost comparison among different types of piers.
- Develope trend lines that can be used to design belled piers in expansive soils.

1.4 Scope and Limitations of the study

The effect of the installation process of belled piers on belled pier behavior in expansive soils was not investigated in the work. The installation process effect is more significant for driven piles than it is for bored piles (piers). Nevertheless, the extent of its effect may need to be investigated.

1.5 Thesis Layout

Chapter 1 Introduction states why the work is necessary and presents a general background for the work.

Chapter 2 Literature Review reviews previous works related to the current work by categorizing them under specific topics.

Chapter 3 Methodology and Validation explains the procedures employed to conduct the work and validates these procedures.

Chapter 4 Material and Contact Properties presents the material and contact properties used in the formulation of the finite element modelling.

Chapter 5 Results and Discussions presents the major findings of the work and discusses them by considering previous works.

Chapter 6 Conclusions and Recommendations summarizes the major findings of the work and presents suggestions for future works.

Chapter 2

Literature Review

2.1 Chapter Introduction

In this chapter, previous works related to the current work are reviewed. The reviewing process is done by categorizing the works under specific topics.

2.2 Expansive Soils Related

2.2.1 Expansive Soils General

Expansive soils occur in many parts of the world but particularly in arid and semi-arid regions. In these regions, evaporation rates are higher than the annual rainfall so that there is almost always a moisture deficiency in the soil. The addition of water will cause ground heave in soils possessing swelling potential. This characteristic causes considerable construction defects if not adequately taken care of. Semi-arid regions are characterized by short periods of rainfall followed by long periods of draught causing cyclic swelling and shrinking phenomena. The ground heave that results from soil swelling potential is a multifactorial phenomenon that involves a combination of the type of material, type and amount of clay minerals, microfabric, initial moisture content, and initial dry density. (Al-Rawas and Goosen 2006).

2.2.2 Identification and Classification of Expansive Soils

Al-Rawas and Goosen (2006) presented the following identification and classification schemes for expansive soils.

Table 2.1: Identification of Expansive Soils (Al-Rawas and Goosen 2006)

Colloid content (%)	*Plasticity index (%)*	*Shrinkage limit (%)*	*Degree of expansion*	*Probable expansion (% total volume change)*
<15	<18	<10	Low	<10
13–23	15–28	10–20	Medium	10–20
20–31	25–41	20–30	High	20–30
>28	>35	>30	Very high	>30

Table 2.2: Classification of Expansive Soils (Al-Rawas and Goosen 2006)

Degree of expansion	*Holtz and Gibbs' (1956) classification of percent swell*	*Seed et al's (1962) classification of percent swell*
Low	0–10	0–1.5
Medium	10–20	1.5–5
High	20–35	5–25
Very high	>35	>25

2.2.3 Swelling Pressure

Swelling pressure is the pressure required to hold the expansive soil at constant volume when water is added. Knowledge of swelling pressure is essential for the design of a variety of geotechnical structures on expansive soils. The swelling pressure is evaluated in the laboratory by a number of testing methods which include oedometer method, suction measurements, triaxial methods, etc. Out of all the methods, laboratory oedometer testing method is extensively used to determine the swelling pressure due to its simplicity and operational ease. Soundara and Robinson (2012) list three different oedometer methods for the determination of swelling pressure as explained below:

Method A The sample is inundated and allowed to swell vertically at a small seating pressure until primary swell is completed. The sample is then loaded in intervals similar to the procedure of conventional consolidation testing until the specimen reaches its initial thickness. The pressure required to bring back the sample to its initial thickness is regarded as the swelling pressure (σ'_{cs}). This method is also often termed as Swell-consolidation method.

Method B Three identical samples are loaded with different pressures near the expected swelling pressure and submerged in water. The vertical movements are plotted against

the applied pressure and the pressure corresponding to zero volume change is taken as swelling pressure. While only one sample is enough to determine the swelling pressure in method A, at least three identical samples are needed in method B. This method is also often called as different pressure method.

Method C In this method, also called as Constant volume method, a specimen is maintained at constant height by adjusting the vertical pressure after the specimen is inundated in free water. The pressure required to maintain constant volume is the swelling pressure (σ'_{cv}).

Each of the methods is equally sensible, but gives entirely different swelling pressure values for the same placement conditions of the soil. Soundara and Robinson (2012) stated that method A gives the highest value, method B gives the least value and method C gives an intermediate value. According to Soundara and Robinson (2012) the possible reason for difference in the swelling pressure values was attributed to the fabric change that occurs in the sample, which depends on the test method.

Nelson et al. (2007) presented a relationship between σ'_{cv} and σ'_{cs} in the form of:

$$\sigma'_{cv} = \sigma'_i + \lambda(\sigma'_{cs} - \sigma'_i) \tag{2.1}$$

Where λ is a coefficient dependent upon the mineralogy of the clay soil.

Definitions of the other variables are presented in Figure 2.1.

Where

σ'_{cv} = constant volume swelling pressure

σ'_{cs} = swell-consolidation swelling pressure

σ'_i = setting pressure

Murthy (2002) presented that the maximum swelling pressure may be as high as 2MPa.

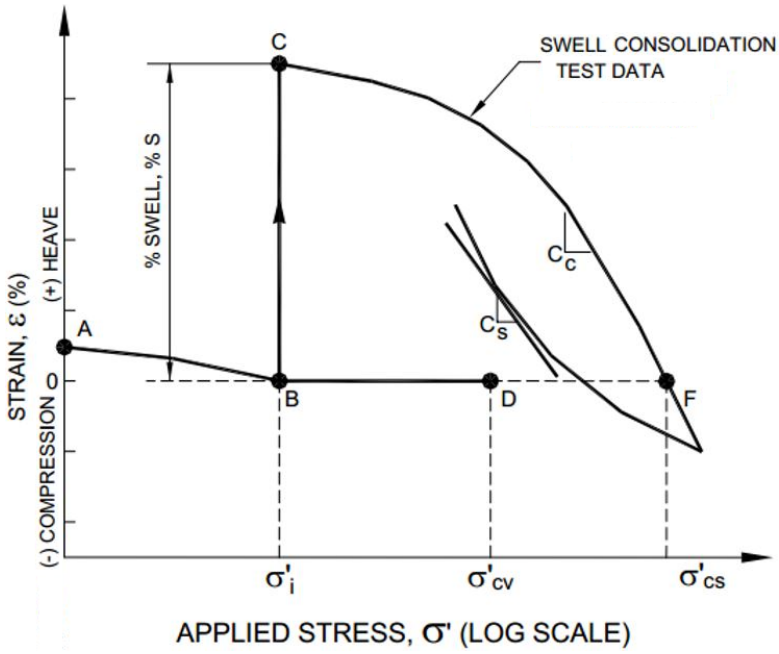

Figure 2.1: Terminology and Notation for Oedometer Tests (Nelson et al. 2007)

2.2.4 Depth of the Swelling Zone

According to Nelson et al. (2007), the following definitions were presented in relation to the term active zone or swelling zone:

Active Zone is that zone of soil that is contributing to heave due to soil expansion at a particular point in time. The depth of the active zone will vary as heave progresses, and therefore varies with time.

Zone of Seasonal Moisture Fluctuation is that zone of soil in which water contents change due to climatic changes.

Depth of Wetting is the depth to which water contents have increased due to external factors. Such factors could include capillary rise after the elimination of evapotranspiration from the surface, infiltration due to irrigation or precipitation, or introduction of water from offsite. Underground sources may include broken water lines, perched water tables, flow through more permeable strata that are recharged at distant locations, or a number of other factors.

Depth of Potential Heave is the depth to which the overburden vertical stress equals or exceeds the swelling pressure of the soil. This represents the maximum depth of Active Zone that could occur.

According to Nelson and Miller (1992), by developing plots of water content as a function of depth over several wet and dry seasons, the depth of the swelling zone may be estimated for

any site. The depth at which the water content becomes nearly constant with depth should define the depth of the swelling zone. Nelson and Miller (1992) presented that in arid or semiarid locations, by considering the Front Range of Colorado, the depth of the swelling zone is about 6m.

According to Nelson and Miller (1992), analytical problems generally are associated with underestimation of the depth of the swelling zone and estimates of depth of the swelling zone less than 3m should be considered suspect.

Chen (1988) presented that the depth of the swelling zone can reach as much as 8m.

Soundara and Robinson (2012) presented that the depth of the swelling zone is the depth at which the overburden pressure equals the swelling pressure of the soil.

Kaufmann et al. (2010) presented the depth of the swelling zone (n) as a function of time. The depth of the swelling zone is determined by equalizing the incoming volume of water and the heave at a specific time calculated as consolidation settlements of preconsolidated clay (Kaufmann et al. 2010). The following equation is presented (Kaufmann et al. 2010):

$$n = 2\sqrt{c_k t} \tag{2.2}$$

Where c_k is the coefficient of consolidation and t is the consolidation time or the life expectancy of the structure.

Bowles (2001) presented various empirical equations to estimate the swelling pressure of which none of the presented empirical equations depend on the thickness of the swelling zone and therefore, the amount of the swelling pressure is not affected by the thickness of the swelling zone.

Chen (1988) explored the effect of the thickness of the swelling zone on the amount of volume change and swelling pressure using samples with thickness ranging from 13mm to 38mm. The magnitude of the volume change was found to be proportional to the sample thickness while the swelling pressure remained constant.

2.2.5 Free Field Heave

Free-field heave is the heave that will occur at the surface of the expansive soil if no surcharge or stress is applied. Because the stress imposed by the weight of an unloaded slab-on-grade is small, slab heave is also approximately equal to the free-field heave (Nelson et al. 2007). According to Nelson and Miller (1992), to predict the free field heave of a soil profile, the swelling zone is divided into a number of layers, n, of thickness, z. Then, the general equation for the free field heave will be (Nelson and Miller 1992):

$$\rho = \sum_{i=1}^{n} \left[\frac{C_s z_i}{(1+e_o)_i} \log\left(\frac{\sigma'_f}{\sigma'_{sc}}\right) \right]_i \tag{2.3}$$

where:

$\rho =$ free-field heave

$C_s =$ swelling index

$\sigma'_f =$ final effective stress state

$\sigma\prime_{sc} =$ swelling pressure from the swell consolidation oedometer test

$e_o =$ initial void ratio

$z_i =$ layer thickness

Nelson and Miller (1992) presented that the expansive soil heave has a maximum value at the surface and has a value of zero at the depth of the swelling zone.

2.2.6 Relationship between Vertical and Volumetric Swell Strains

Puppala et al. (2013) presented that from volumetric swell tests, the ratio between vertical and volumetric swell strains was close to 0.5.

Al-Shamrani and Al-Mhaidib (1999) presented that the average ratio between vertical and volumetric swell strains at all time intervals was around 0.55.

2.3 Pier-Soil Contact and Interface Stresses

The contact or interface stresses between the pier and the expansive soil are presented in Figure 2.2 (Nelson and Miller 1992).

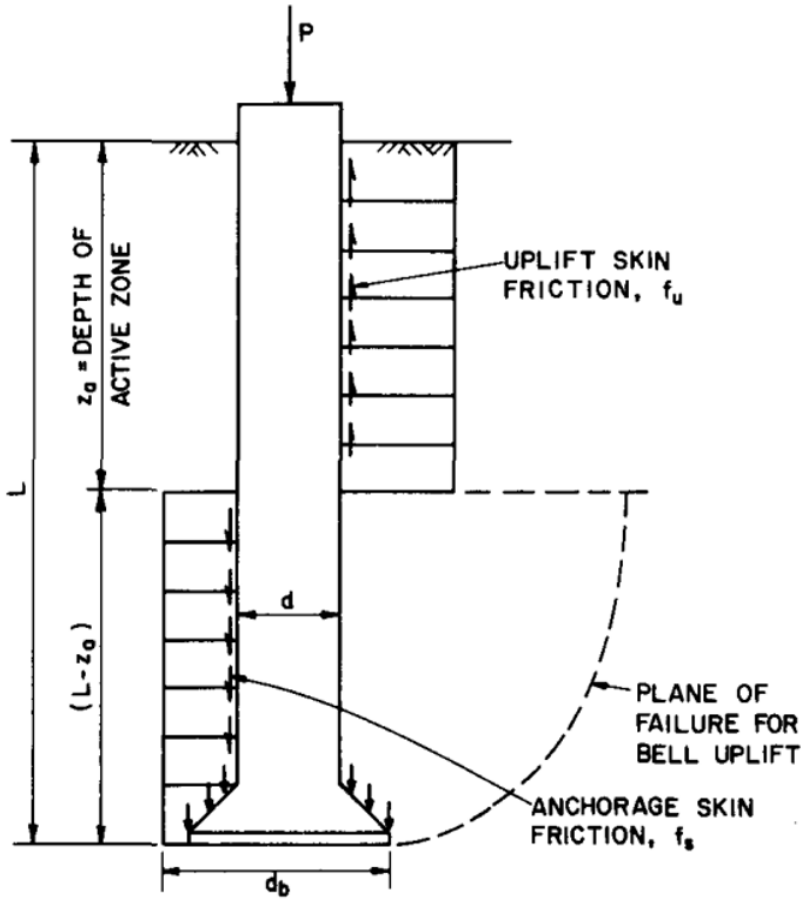

Figure 2.2: Stresses acting on a Pier in Expansive Soil (Nelson and Miller 1992)

Chen (1988) assumed that the uplift stress developed in the swelling (active) zone is constant throughout the swelling zone. This uplift stress has a value of $\alpha_s \sigma_s$, where α_s is the coefficient of uplift between concrete and soil usually taken to be 0.15 and σ_s is the swelling pressure of the soil.

O'Neill (1988) considered that for a short interval at the bottom of the swelling zone there will be a transition zone where the uplift stress increases from zero (at the bottom) to a limiting constant value that exists throughout the upper part of the swelling zone. The length of this transition zone, however, is small and not within the accuracy with which the depth of the swelling zone can be determined. It is prudent, therefore, to assume that the uplift stress is constant throughout the swelling depth (O'Neill 1988).

Poulos and Davis (1980); Nelson and Miller (1992) considered the pier-soil interface friction stress to be:

- A linear distribution where the interface stress is zero at the top of the pier shaft and $0.01Es$ at the bottom of the pier shaft. Where Es is the modulus of elasticity of the soil.

- $0.005Es$ throughout the length of the pier shaft. This condition prevails unless other-

wise specified (Poulos and Davis 1980; Nelson and Miller 1992).

According to Poulos and Davis (1980); Nelson and Miller (1992) the bearing stress on the bells of the belled piers was assumed to vary from $0.36Es$ at $L = 5d$ to $0.64Es$ at $L = 20d$. Where L is the total length of the belled pier and d is the shaft diameter of the belled pier.

2.4 Belled Pier Related

2.4.1 Belled Pier Dimensions

Chen (1988) presented that shaft of a belled pier must be sufficiently large to allow cleanout and inspection. The minimum shaft size is $0.6m$, although $0.8m$ is desirable. Straight shaft piers can have a minimum shaft size of $0.3m$. The ideal bell is in the shape of a frustum with a vertical side at the bottom. The vertical side may be $0.15m$ to $0.3m$ high. The sloping side of the bell should be at an angle at least $60degrees$ with the horizontal. Most drillers are capable of providing bells with diameters equal to three times the diameter of the shaft. (Chen 1988).

2.4.2 Advantages of Belled Piers

Chen (1988) mentioned that the advantages of belled piers include increased bearing capacity and increased uplift capacity. According to Chen (1988), the greatest advantage of the belled pier is that the resistance against uplift will not be affected by loss of friction in the zone unaffected by wetting. If, for some reason, such as the rise of ground water, the skin friction in this zone is lost, then straight shaft pier uplift is unavoidable. With belled piers, the total weight of the soil above the bell, will not be affected by moisture change. Hence, there is always an added factor of safety of this system against uplift (Chen 1988).

In areas where the upper soils are highly expansive, bedrock is shallow, and there is a strong possibility of development of a perched water table condition, the use of a belled pier system should be favorably considered. Since a belled pier system relies entirely upon the anchorage of the lower portion of the pier in the zone unaffected by wetting against uplift, this type of pier can be used for columns with very light load. The magnitude of dead load pressure exerted on the pier is not a factor. (Chen 1988).

2.4.3 Disadvantages of Belled Piers

According to Chen (1988), the most prominent disadvantage of belled piers is the cost and the difficulty of inspection. Bells can be formed mechanically with a special belling device. In hard bedrock, a mechanical device may be unsuccessful. When it is necessary to send a man down the hole with a jackhammer to complete the bell, the cost can be prohibitive.

In the Denver area (USA) where the cost of pier drilling is exceedingly competitive, it is estimated that in a favorable drilling condition, the cost of belling can easily exceed the cost of drilling an extra 3m of pier shaft. The advantage of anchorage in a bell pier system can easily be offset by drilling an additional 3m into bedrock with a straight-shaft pier (Chen 1988).

Cleaning a belled pier is much more difficult than cleaning a straight-shaft pier. Proper cleaning of a belled pier can only be accomplished by sending a man down the hole with a shovel. The condition of the bottom of the straight-shaft pier can be inspected from the ground level with a torch or a mirror, but the condition of the bell cannot be inspected from ground level. (Chen 1988).

The difficulty of belled pier construction increases markedly where the materials immediately overlying bedrock are subject to caving. It is nearly impossible to bell in granular soil. The problem is further complicated if ground water is encountered. (Chen 1988).

2.5 Belled Pier Design

Two procedures exist for the design of belled piers. These are the rigid pier design and the elastic pier design (Nelson and Miller 1992) and are presented as follows:

2.5.1 Rigid Pier Design

Chen (1988) and O'Neill (1988) presented similar methods of analysis for the rigid pier design. The stresses acting on a pier in expansive soil are shown in Figure 2.2. The principle of the design is that the interface friction stress and the bearing stress below the depth of potential heave plus the dead load, P, must resist the uplift pressures produced by the swelling pressures exerted on the pier above that point. O'Neill (1988), as quoted in Nelson and Miller (1992), following this principle, presented the following equation for the design of a belled pier in expansive soil:

$$L = Z_a + \frac{4\alpha_1 \sigma'_s Z_a - dkq_{dl} - d\beta cN_u}{4f_s + d\beta\gamma} \tag{2.4}$$

where:

$L =$ total length of the belled pier

$d =$ shaft diameter of the belled pier

$d_b =$ base (bell) diameter of the belled pier

$Z_a =$ depth of the swelling zone

$\alpha_1 =$ coefficient of uplift between the pier (concrete) and the soil

$\sigma'_s =$ swelling pressure of the soil

$k.q_{dl} =$ minimum dead load stress on the belled pier (Nelson et al. 2007)

$\beta =$ $(d_b/d)^2$–1

$c =$ cohesion of the soil

$N_u =$ values given in Table 2.3

$f_s =$ interface friction stress in the non-swelling zone

$\gamma =$ unit weight of the soil

Table 2.3: Values of N_u (Nelson and Miller 1992)

$\frac{(L - z_a)}{d_b}$	N_u
1.7	4
2.5	6
≥5.0	9

According to Nelson and Miller (1992), the rigid pier design method does not provide the ability to predict pier movement. It is implicit in the way that the equations are developed that if sufficient anchorage is provided, the movement will be within tolerable limits.

Nelson et al. (2007) observed that the rigid pier design works well if the stratum of expansive soil is not thick and is underlain by a stable non-expansive stratum. However, in a deep deposit of expansive soil, the required pier length is approximately twice the depth of potential heave. In such cases the design rigid pier length is generally not practical for a light structure, and it would be appropriate to use a shorter pier if the predicted heave of the shorter pier is within tolerable limits. In that case an elastic pier design would be appropriate (Nelson et al. 2007).

2.5.2 Elastic Pier Design

Elastic pier design is presented in Nelson et al. (2007). The heave prediction methodology presented therein, is based on a theoretical treatment of pier heave in an elastic medium developed by Poulos and Davis (1980). The material presented by Poulos and Davis was modified somewhat by Nelson and Miller (1992) and later by Nelson et al. (2007) to make it more easily usable by the design engineer.

According to Nelson et al. (2007), the uplift skin friction along the side of the pier may be considered to be uniform along the length of the pier or may increase with depth. A case for the uniform distribution would be the situation where the soil within the depth of potential

heave has generally the same swelling pressure throughout. A case for the linearly increasing distribution would be where several strata of soils exist with the deeper soils having a higher expansion Potential. Another case would be where the soundness of a claystone stratum increases with depth as a result of weathering of the upper material, such that the swelling pressure increases with depth.

Figure 2.3 shows normalized pier heave plotted as a function of the ratio of pier length to depth of potential heave for a belled pier having a bell diameter twice that of the shaft. The two curves presented in that Figure are for the two cases where the soil-pier skin friction is constant with depth (A) and where it varies linearly with depth (B). Figure 2.4 shows the normalized maximum tensile force in belled piers plotted as a function of the ratio of pier length to depth of potential heave. The maximum tensile force is normalized to a force, P_{FS}, computed by applying the uplift friction over the entire length of the pier. For the case where the skin friction varies linearly with depth, this force, P_{FS}, is equal to, $-0.5 f_{um} L \pi d$ and for the case where the skin friction is uniform with depth, this force, P_{FS}, is equal to, $-f_{um} L \pi d$ where f_{um} is equal to $0.01 Es$. (Nelson et al. 2007).

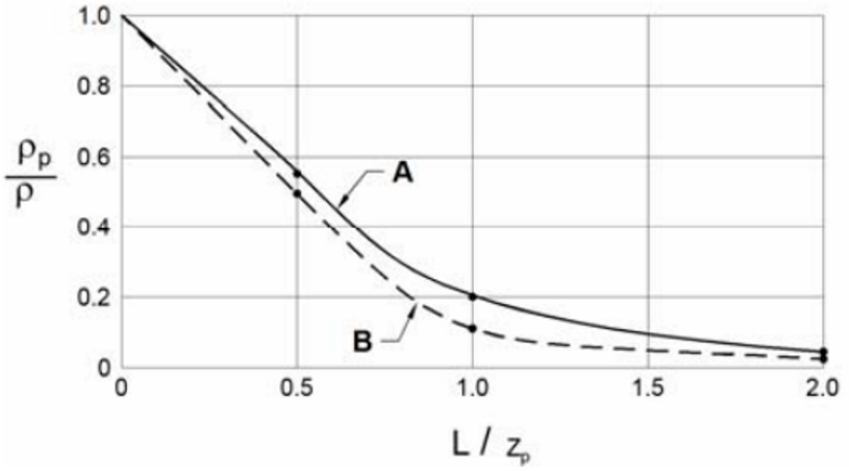

Figure 2.3: Normalized Belled Pier Heave vs. L/z_p (Nelson et al. 2007)

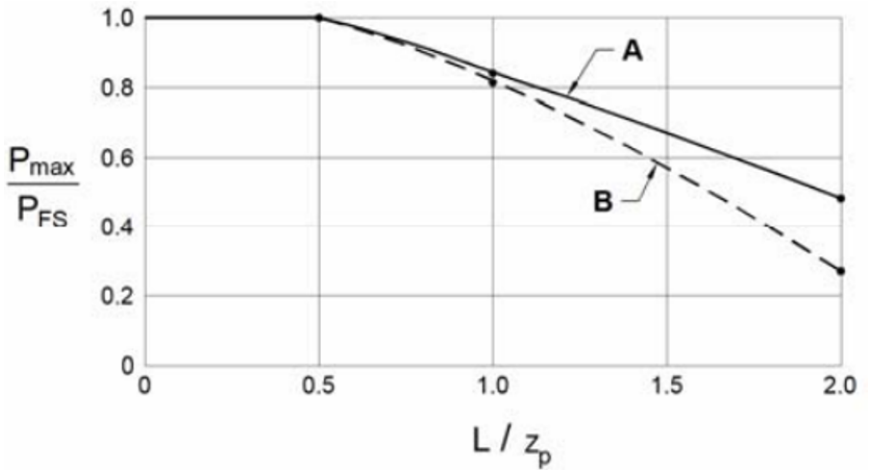

Figure 2.4: Normalized Force in Belled Piers vs. L/z_p (Nelson et al. 2007)

where

$\rho_p =$ pier heave

$\rho =$ soil heave

$L =$ pier length

$z_p =$ depth of the swelling zone

2.6 Investigation of Straight Shaft Piers (Piles) in Expansive Soils

Various authors have investigated the behavior of straight shaft piers in expansive soils.

Nelson et al. (2012) presented a general design procedure for straight shaft piers in expansive soils including a finite-element-based analysis tool. The design procedure allows for pier analysis within complex soil profiles, where soil properties and water content vary with depth or piers with complex construction details, such as segmented micropiles. Nelson et al. (2012) determined that the pier heave and the tensile force are particularly sensitive to the value of Young's modulus of the heaving soil. The coefficient of skin friction (α) also has a significant impact on both the pier heave and the tensile force.

Xiao et al. (2011) presented an analytical solution to analyze straight shaft pier (pile)-soil interaction in expansive soils. The results of the work are summarized as follows (Xiao et al. 2011):

- Increasing pile lengths decrease the upward pile displacements, but if the length is too long, the upward displacements become much less sensitive to the length elongate. On the other hand, the length increase would cause larger tensile stresses distributing

along the pile shaft, although the stresses become less and less sensitive to the pile length. Both stresses and displacements therefore should be controlled in designing the pile in expansive soil, which requires a comprehensive analysis and does not only rely on a single index.

- Piles with a small diameter ($d \approx 0.04L$) are able to effectively reduce the upward shaft displacement; however, diameters exceeding $0.04L$ have little effect on decreasing shaft displacement. Also, free piles with smaller diameters under swelling pressure produce less tensile stress, although the stresses become less and less sensitive to the pile diameters after d over $0.04L$.

- As irrigation (saturation) increases, the upward shaft movements and axial tensile force keep increasing, and both indexes are less and less sensitive to the amount of incoming water. That is because the swelling potential of the expansive soil is being consumed during the irrigation.

- The loads for stopping the upward pile movements are proposed to be around 2.5 times the maximum tensile stress of a free pile under swelling pressure in an expansive soil foundation. A further investigation reveals this 2.5 times seems independent of the pile length, given that other parameters are fixed.

Kaufmann et al. (2010), investigated straight shaft pier (pile)-soil interaction in expansive soils using the FEM software Plaxis. According to Kaufmann et al. (2010), the swelling of the surrounding soil has shown to imply upward shear stresses at the soil–pile interface. This leads to tensile vertical stresses in the pile. Furthermore, the pile has shown to be elongated to a maximum value after 35-40 years followed by some shrinkage up to the end of the swelling period of 340 years. It appears that the development of plastic interface implies the shrinkage of the pile because of the slip at the pile surface. This affects the internal stresses in the pile where the maximum values are observed after 35-50 years. Hence, when designing unloaded piles with a life expectancy of 100 years, the tensile stresses in the pile can be evaluated after the first 33–50 % of the design period. (Kaufmann et al. 2010).

Fan et al. (2007) presented elastic differential equations of load-transfer of single straight shaft pier in expansive soil either with applied loads on pile-top or only under the soil swelling, based on the theory of pile-soil interaction and the shear-deformation method. The derivation of analytic solution to load-transfer for single pile in expansive soil was obtained by means of superposition principle under expansive soils swelling. The analyzed results by Fan et al. (2007) show that this analytic solution can achieve high precision with few parameters required, indicating its' simplicity and practicability in engineering application. The employed method can contribute to determining the greatest tension along pile shaft resulting from expansive soils swelling and provide reliable bases for engineering design. The

method can be employed to obtain various distributive curves of axial force, settlements and skin friction along the pile shaft with the changes of active depth, vertical movements of the surface and loads of pile-top. (Fan et al. 2007).

Nelson et al. (2007) investigated the effect of time of saturation on pier heave (straight shaft pier). According to Nelson et al. (2007), rate of heave of the piers will depend on the rate at which subsoil become wetted. Analyses of rate of wetting front movement, for a typical case where there is a constant source of water at the ground surface (continuous saturation), have shown that to move downward a distance of 10 meters can require 20 to 30 years or more. As time progresses, the depth of wetting, and hence, distress to the building, will continue. Figure 2.5 shows slab and pier heave as a function of time for the rate of wetting front movement. Data for only the first ten years after development of a wetting front are shown. It is particularly interesting to note that, whereas slab movement begins almost immediately after a wetting front has begun to develop, pier movement does not begin until several years later. Furthermore, the length of the pier influences both the time at which pier movement begins and the amount of pier movement.

According to Nelson et al. (2007), design of foundations for extreme ultimate conditions is not always practical and economical in engineering practice. When large values of heave are predicted, the depth of potential heave may be very deep, and the time required for the saturation to reach large depths of potential heave may exceed the design life of the structure. Thus, design of foundations for buildings on expansive soils must consider the saturation that will occur during the design life of the structure, and the amount of expected heave that such saturation will produce. Nelson et al. (2007) observed that by considering the effect of time of saturation and design life of the structure, the required pier length can be reduced.

Nelson et al. (2010) presented prediction of pier heave with time using a hyperbolic curve fitting technique. It was indicated that using observed data collected over a period of less than 3 years in the hyperbolic curve fitting technique provided reasonable accuracy for pier heave prediction with time.

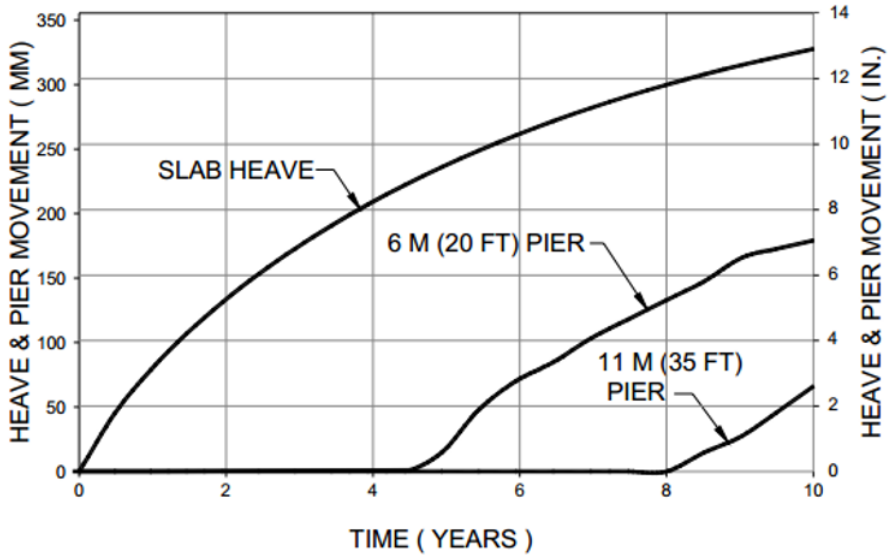

Figure 2.5: Time of Saturation and Pier Heave (Nelson et al. 2007)

Xu and Poulos (2001) employed a 3D coupled boundary element approach to analyze the response of vertical piles subjected to passive loadings including soil swelling. A number of theoretical expressions for soil movements were developed and presented. The authors found reasonable agreement between some existing published solutions and their presented solutions.

Mohamedzein et al. (1999) considered a two dimensional axisymmetric finite element model for analysis of short pile (straight shaft pier) in expansive soils. The pile material was modeled as linear elastic and the soil was assumed to be a nonlinear elastic material. Heave-induced strains were computed in terms of change in soil suction. According to Mohamedzein et al. (1999) the proposed model gave reasonable values of vertical upward movement of piles in expansive soils when compared to the results obtained from the field experiments. This proposed finite element program was proposed be used to find the distribution of tensile stresses in a pile needed for design against tensile failure; and the optimum pile length and diameter needed to resist upward movements due to soil heave. Based on the parametric study conducted using the finite element program mentioned, the following results were presented (Mohamedzein et al. 1999):

- An increase in pile length decreases the upward vertical movement of the pile due to soil heave. The upward vertical movement also decreases with the increase in axial compressive load. The decrease in heave due to increase in pile length is more significant than that due to increase in axial compressive load.

- The maximum axial tensile stress increases when the pile length increases for piles installed completely in the zone of soil heave.

- The tensile stress decreases as the axial load increases and eventually the pile may be subjected only to compressive stresses.
- The maximum tensile stress in the axially loaded pile usually occurs near the mid height of the pile. For loaded piles tensile stresses occur throughout the lower two thirds of the pile length within the active zone.

Challa and Poulos (1991) carried out tests on test model piles (straight shaft piers) in a model expansive clay medium to measure movement and tensile force developed in the piles by the swelling of the clay. Measurements have also been made of the distribution with the depth of swelling movement in the clay at various times after commencement of the swelling. The results are summarized as follows (Challa and Poulos 1991):

- For relatively early times, the soil swelling profile appears to vary almost lineally with depth from a maximum at the surface to zero at the base of the clay.
- The pile head movement increases as the soil heave increases, but tends to approach a constant value if the pile is founded in a stable sand layer below the swelling clay.
- Swelling of the soil may induce substantial tensile forces in the pile. The maximum tensile force tends to increase with increasing depth of the swelling clay relative to the pile length, with increasing amount of soil movement, and with increasing limiting shaft friction and end bearing capacities of the pile.

2.7 Pier related modelling with Abaqus

Zhan et al. (2012) modelled straight shaft pier foundations in non-expansive soils using Abaqus. The ability of Abaqus to model pier-soil contact was studied. The pier-soil contact was modelled using Coulomb frictional model in conjugate with "hard" contact model, both provided in Abaqus. For pier-sand interaction, the tangential behavior was modelled by providing the frictional coefficient, μ, (which is dependent on the angle of friction of the sand soil) in the Coulomb frictional model. For pier-clay interaction, the tangential behavior was modelled by providing a frictional coefficient, μ, but the interface shear stress was limited by providing a limit shear stress value (which is dependent on the cohesion of the clay soil) in the Coulomb frictional model. See Figures 2.6 and 2.7.

Next, Zhan et al. (2012) compared shaft and base resistances of the pier outputted by Abaqus (using the contact modelling technique mentioned in the previous paragraph) to the shaft and base resistances calculated by numerical analysis. A perfect agreement was observed. Therefore, it was concluded that Coulomb frictional model in conjugate with "hard" contact model is capable of modelling the pier-soil interaction.

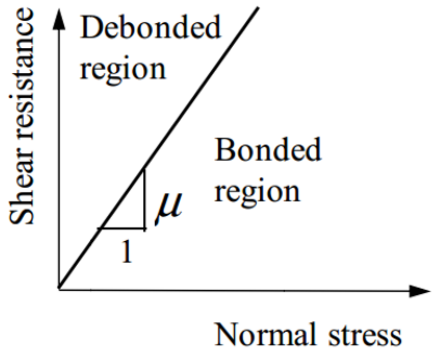

Figure 2.6: Modelling Pier-Sand Contact in Abaqus (Zhan et al. 2012)

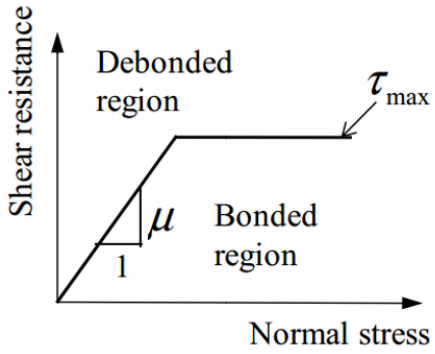

Figure 2.7: Modelling Pier-Clay Contact in Abaqus (Zhan et al. 2012)

Zhan et al. (2012) also checked the capability of two mesh element types, provided in Abaqus, to accurately model pier-soil interaction. The two mesh elements were CAX4 (a first order mesh element) and CAX8 (a second order mesh element). CAX4 predicted both the shaft and base resistances of the pier accurately, as checked against numerical analysis, while CAX8 was able to predict the base resistance accurately but not the shaft resistance.

Aljorany and Noori (2013) modelled straight shaft pier foundations in expansive soils using Abaqus. The soil was modelled by considering elastic, plastic and swelling properties. The swelling property of the soil was modelled using Moisture Swelling model in conjugate with Sorption model, both provided in Abaqus. The Sorption model represents the suction-saturation relationship of the soil. However, the pier-soil contact was not modelled explicitly and pier-soil slip was not considered.

Helwany (2007) modelled straight shaft pier foundations in non-expansive soils using Abaqus. The soil was modelled by considering elastic and plastic properties. The plastic property of the soil was modelled using Cap Plasticity model (in conjugate with a Cap Hardening curve) provided in Abaqus. Cap Plasticity model represents the modified Drucker-Prager model. Good agreements with numerical analysis results were observed in relation to pier capacity and pore pressure development in the soil. However, pier-clay contact was not modeled explicitly by providing limit shear stresses.

2.8 Miscellaneous

2.8.1 Drained and Undrained Conditions

Chen et al. (2008) evaluated axial uplift data for straight-sided drilled shafts (piers) in a wide variety of soil profiles. The database included 42 sites with 77 field uplift load tests, including 21 sites with 40 tests in drained loading and 21 sites with 37 tests in undrained loading. Six representative interpretation criteria were used to evaluate the data. It was observed that upward pier movement was similar in both drained and undrained cases.

Kaufmann et al. (2010), investigated straight shaft pier (pile)-soil interaction in expansive soils using the FEM software Plaxis and observed that the choice of drained or undrained strength parameters does not influence the heave of the expansive soil significantly.

2.8.2 Allowable Pier Heave

Nelson et al. (2007), presented that the allowable pier heave can be approximated to be $50mm$. From experience Nelson et al. (2007) showed that a differential movement between adjacent piers is usually half to one times of the predicted total heave. Therefore, the assumption of $50mm$ of the total movement could result in a differential movement of 25 to $50mm$. Normally, the maximum tolerable differential movement ranges from 25 to $50mm$ depending on the type and configuration of the pier and grade beam foundation. The actual maximum tolerable differential movement should be discussed with a structural engineer. (Nelson et al. 2007).

2.8.3 Design Approaches for Pier Design

There are two approaches to designing belled piers embedded in expansive soils against uplift. The first approach is to consider only a condition where there is no applied load acting on the belled pier, i.e. free belled pier (Tomlinson and Woodward 2008). Only this condition is considered because it is assumed to be the governing condition. The second approach is to consider a condition where there is applied load acting on the belled pier in addition to the condition where there is no applied load acting on the belled pier (Murthy 2002).

2.8.4 Tensile Strength of Concrete

Mosely (2007), based on the European code, presented the tensile strength of concrete (f_{ctk}) as follows:

$$f_{ctk} = 0.21 f_{ck}^{\frac{2}{3}} \tag{2.5}$$

where f_{ck} is the cylindrical strength of the concrete.

2.8.5 Required Area of Steel in Piers for tensile reinforcement

Nelson et al. (2007) presented the required area of steel in piers (belled or straight shaft) to serve as tensile reinforcement as follows:

$$A_s = \frac{0.23 T_{max}}{f_s} \tag{2.6}$$

Where

$A_s =$ required area of steel in in^2

$T_{max} =$ maximum tensile force in the pier in KN

$f_s =$ allowable design stress of reinforcement steel in ksi

Note that $1in = 25.4mm$ and $1ksi = 6895KPa$.

U.S. Army Corps of Engineers (1983) presented the minimum percent steel for piers (belled or straight shaft) should be 1% of the pier shaft concrete cross-sectional area.

2.8.6 Piled Rafts and Pier Groups in Expansive soils

Poulos (1993) presented that for soils subjected to expansive (upward) movement, additional tensile loads are transferred to the piers when piled rafts or pier groups are considered, both because of the direct action of the expansive soil and also because of additional pressures generated on the underside of the raft or the pile (pier) cap. In both cases, the movement of the pile raft or cap is greater than that of the corresponding free-standing pile (pier) group. It is therefore clear that, in circumstances where external vertical soil movements are likely to develop, the use of a piled raft or pier group foundations is best avoided.

2.8.7 Elastic Properties of Soil

Zhan et al. (2012) considered the modulus of elasticity or Young's modulus of the soil to be $1000Cu$ where Cu is the undrained cohesion of the soil. Bowles (2001) considered the modulus of elasticity or Young's modulus to vary from $750Cu$ to $1200Cu$ for lightly overconsolidated clay and within the range of $50MPa$ to $100MPa$ for hard clays. Bowles (2001) considered the Poisson's ratio to vary from 0.4 to 0.5 for clay soils.

Chapter 3

Methodology and Validation

3.1 Chapter Introduction

In this chapter, the methodologies employed to conduct the work are presented. The validation of these methodologies is also presented.

3.2 Formulation of the Hypothetical Site

The main objective of the work is to conduct an in-depth investigation of the behavior of belled piers in expansive soils using the FEM software Abaqus. To meet this objective, belled piers are modelled in a hypothetical site. This belled piers-hypothetical site combination is assumed to represent the usual case of belled piers employed in expansive soils. This hypothetical site is assumed by considering an actual site located in Addis Ababa, Ethiopia around the "Bole" area. Expansive soils are known to occur in abundance in this area. It was observed that the soil at the actual site was clay soil having a very deep depth.

Assumptions of the hypothetical site:

- Initially, the soil at the hypothetical site is assumed to have the same properties up to the depth of embedment of the belled pier. Later, the effect of variations of the Young's modulus (Es) and undrained cohesion (Cu) of the soil is investigated by considering different values of Es and Cu.
- The properties of the soil at the hypothetical site are determined by taking a representative samples from the actual site.
- The ground water table (GWT) is assumed to be just below the swelling zone. This is to account for the most critical condition.
- The GWT doesn't cause saturation of the swelling zone.

3.3 Determination of Material and Contact properties

In this Section, the methodologies employed to determine the material and contact properties that are used in the formulation of the finite element model in Abaqus are discussed. The actual values of the material and contact properties are presented in chapter 4.

3.3.1 Soil Properties

As mentioned before, the soil properties are determined by taking a representative sample form the actual site and represent the soil properties of the hypothetical site.

3.3.1.1 Soil Sampling

Soil samples were taken from a site located in Addis Ababa, Ethiopia around the "Bole" area. Samples were taken from a depth of $9m$ below ground level. Both disturbed and undisturbed samples were taken.

3.3.1.2 Basic Index Properties

The basic index properties of the soil are determined by conducting laboratory testing and using basic soil parameter relations. For the laboratory testing, ASTM D 2216 (moisture content), ASTM D 2937-00 (unit weight), ASTM D 854-00 (specific gravity) were followed.

3.3.1.3 Grain size and Distribution

To determine the grain size and distribution, wet sieve and hydrometer analysis tests were carried out according to ASTM D 422.

3.3.1.4 Atterberg Limits

The Atterberg limits were determined in the laboratory following ASTM D 4318.

3.3.1.5 Free Swell

The free swell test was carried out following the recommendation given by Chen (1988).

3.3.1.6 One Dimensional Consolidation Test

The one dimensional consolidation test related properties are determined by laboratory testing and corresponding calculations. The laboratory testing is done according to ASTM D 2435. Samples remolded at the natural condition of the soil were considered to represent the actual field conditions.

The preconsolidation pressure, Pc, was determined from the void ratio versus logarithm of pressure plot (e-log P plot) using the method proposed by Casagrande (1936) by applying remolding corrections proposed by Schmertmann (1955). The swelling pressure is determined by considering the swell-consolidation method according to Nelson and Miller (1992). The recompression index (Cr) is taken to be equal to $0.05Cc$ where Cc is the compression index (Bowles 2001). The swelling index (Cs) is also taken to be equal to $0.05Cc$ (Helwany 2007). The coefficient of volume compressibility (m_v) is assumed to be constant.

3.3.1.7 Elastic Properties

The modulus of elasticity and Poisson's ratio of the soil are determined following the recommendations given by Zhan et al. (2012) and Bowles (2001). The coefficient of earth pressure at rest (k_o) is computed from $\frac{\nu}{1-\nu}$ where ν is the Poisson's ratio of the soil (Bowles 2001).

3.3.1.8 Plastic Properties

The undrained cohesion (Cu) of the soil is determined from Figure 3.1 from the over consolidation ratio considering Varved clay (Bowles 2001) while the undrained angle of friction (ϕ_u) is taken to be equal to zero considering a saturated clay soil.

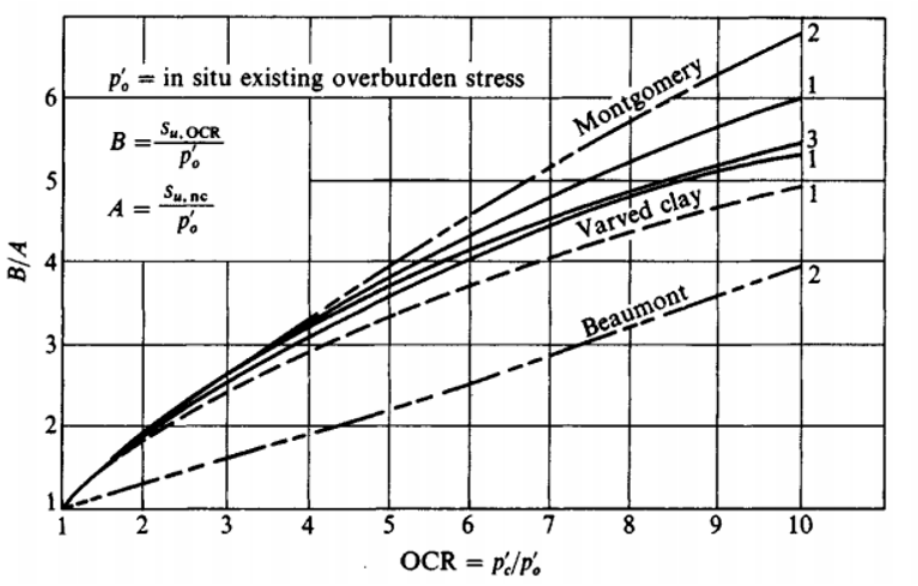

Figure 3.1: Determination of Undrained Cohesion (Cu) (Bowles 2001)

Where:

$S_{u,OCR} =$ value of the undrained cohesion (Cu) for over consolidation

$S_{u,nc} =$ value of the undrained cohesion for normal consolidation as determined from the average of $(0.45P_I^{1/2})p'_o$, $(0.11 + 0.037I_p)p'_o$ and $0.5w_Lp'_o$

$P_I =$ Plastic Index

$I_P =$ Plastic index in percent

$w_L =$ Liquid limit

$p'_o =$ effective overburden pressure (in situ existing overburden stress)

$p'_c =$ preconsolidation pressure

$OCR =$ over consolidation ratio

3.3.1.9 Swelling Property, Unsaturated Property and Permeability

The unsaturated soil property is defined by the unsaturated soil's soil water characteristic curve, SWCC curve (relationship between the soil's saturation level and the soil's negative pore pressure level). The soil water characteristic curve of the soil is predicted by the program SEEP/W using the grain size (modified Kovacs) estimation method.

The estimation function is developed by defining the degree of saturation for two main components. The first component contributes to the amount of water that is stored in a soil by capillary forces that exist at relatively small negative pore-water pressures. The second component contributes to the volumetric water content function at large negative pore-water pressures where the amount of water that exists in the soil is primarily a function of adhesion. Both of these components can be evaluated from the negative porewater pressure and material property information such as particle-size, the shape of the particles and the porosity. (Seepage Modeling with SEEP/W 2007).

The swelling property is defined by defining a relationship between the soil's saturation level and the soil's volumetric swelling strain level. Laboratory testing, according to Bowles (2001), is conducted to find this relationship. Samples where compacted at constant densities but varying saturation levels and the consolidometer was used to determine the vertical swell strains. The vertical swell strains are later converted into volumetric swell strains by considering Puppala et al. (2013).

The permeability property of the soil is defined as a function of the saturation level of the soil and is presented in equation 3.1 (Averjanov 1950):

$$K_{un} = K_{sat} S^{3.5} \tag{3.1}$$

Where:

$K_{un} =$ unsaturated permeability

$K_{sat} =$ saturated permeability; Bowles (2001) is considered

$S =$ saturation level

3.3.2 Pier Properties

The pier material is assumed to be reinforced concrete. Furthermore, the pier is assumed to have elastic properties only. Therefore, elastic properties typical of concrete are considered.

3.3.3 Contact Properties

The contact properties are determined using the recommendations given by Chen (1988) and finite element analysis to determine the maximum value of the swelling pressure.

3.4 Formulation of the Finite Element Model in Abaqus

3.4.1 Model and Parts

The finite element model in Abaqus has three parts, namely, the belled pier, the swelling zone and the non-swelling zone. Since these parts are symmetric with respect to both actions acting on them and shape, an axisymmetric modelling is chosen where one half of the belled pier-soil combination is modelled in two dimensions as shown in Figure 3.2. The dimensions of the soil are chosen in a way that the boundary effect on the belled pier behavior is minimized; the width of the soil is taken to be $10.5db$ and the length to be $L + 10db$ where db is the diameter of the base of the belled pier and L is the length of the belled pier (Zhan et al. 2012).

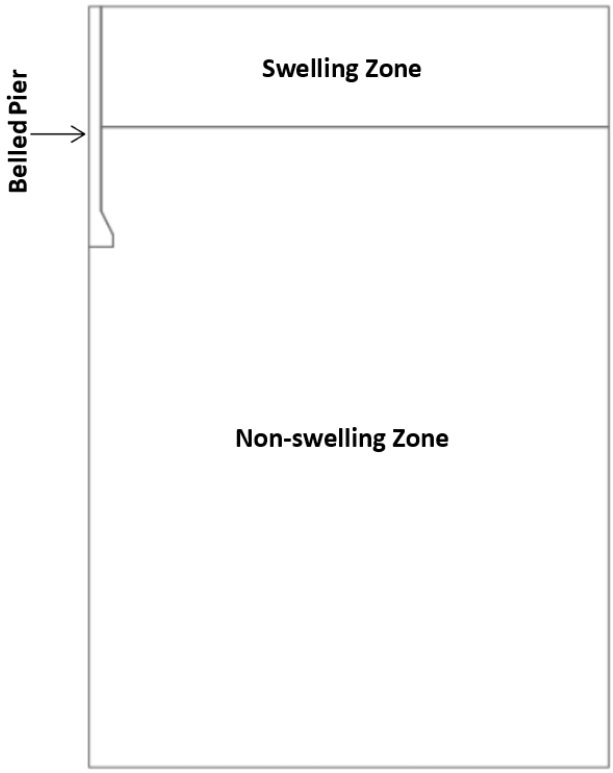

Figure 3.2: Model and Parts in Abaqus

3.4.2 Material Properties

The belled pier is assumed to have elastic properties only. While the soil has elastic, plastic and swelling properties.

The elastic properties of the belled pier and the soil in Abaqus are defined by specifying the Young's modulus and Poisson's ratio of the two materials. The elastic behavior for both the belled pier and the soil is assumed to be linear and isotropic. The total stress is defined from the total elastic strain as $\sigma = D^{el}\varepsilon^{el}$ where σ is the total stress ("true," or Cauchy stress in finite-strain problems), σ^{el} is the fourth-order elasticity tensor, and ε^{el} is the total elastic strain (log strain in finite-strain problems). (Abaqus documentation 2014).

The plastic property of the soil is modelled in Abaqus using the modified Drucker-Prager (Cap plasticity) model by specifying the Cap plasticity model parameters. The Cap plasticity model parameters are presented in Chapter 4. The Cap plasticity model can be used in conjunction with the elastic material model in Abaqus (Abaqus documentation 2014).

The Cap plasticity model in Abaqus is intended to model cohesive geological materials that exhibit pressure-dependent yield, such as soils and rocks. It is appropriate to model soil behavior because it is capable of considering the effect of stress history, stress path, dilatancy, and the effect of the intermediate principal stress. The Cap plasticity model is based on the addition of a cap yield surface to the Drucker-Prager plasticity model. The

addition of the cap yield surface to the Drucker-Prager model serves two main purposes: it bounds the yield surface in hydrostatic compression, thus providing an inelastic hardening mechanism to represent plastic compaction; and it helps to control volume dilatancy when the material yields in shear by providing softening as a function of the inelastic volume increase created as the material yields on the Drucker-Prager shear failure surface. (Abaqus documentation 2014).

The yield surface of the modified Drucker–Prager/cap plasticity model consists of three parts: a Drucker–Prager shear failure surface, an elliptical cap, which intersects the mean effective stress axis at a right angle, and a smooth transition region between the shear failure surface and the cap, as shown in Figure 3.3 (Helwany 2007).

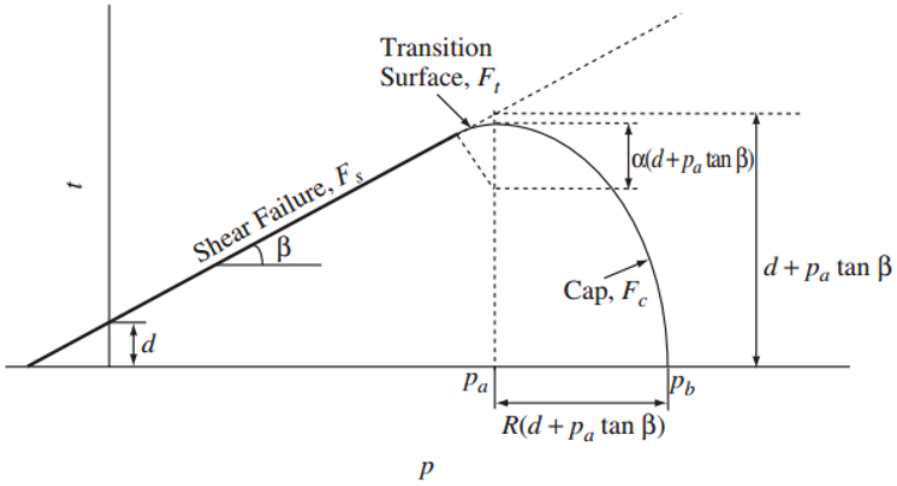

Figure 3.3: Yield surfaces of the modified Cap plasticity model in the p–t plane (Abaqus documentation 2014)

In the modified Cap plasticity model, the onset of plastic behavior is determined by the Drucker–Prager failure surface and the cap yield surface. The Drucker–Prager failure surface is given by:

$$Fs = t - p\tan\beta - d = 0 \tag{3.2}$$

where

$t =$ the t-plane

$p =$ the p-plane

$\beta =$ the soil's angle of friction in the p–t plane equal to $\frac{6\sin\phi}{3-\sin\phi}$

$d =$ the soil's cohesion in the p–t plane equal to $c\sqrt{3}$

$\phi =$ angle of friction

$c =$ cohesion

As shown in the Figure 3.3, the cap yield surface is an ellipse with eccentricity of R in the p–t plane. The cap yield surface is dependent on the third stress invariant, r, in the deviatoric plane as shown in Figure 3.4 (Helwany 2007). The cap surface hardens (expands) or softens (shrinks) as a function of the volumetric plastic strain. When the stress state causes yielding on the cap, volumetric plastic strain (compaction) results, causing the cap to expand (hardening). But when the stress state causes yielding on the Drucker–Prager shear failure surface, volumetric plastic dilation results, causing the cap to shrink (softening). (Helwany 2007).

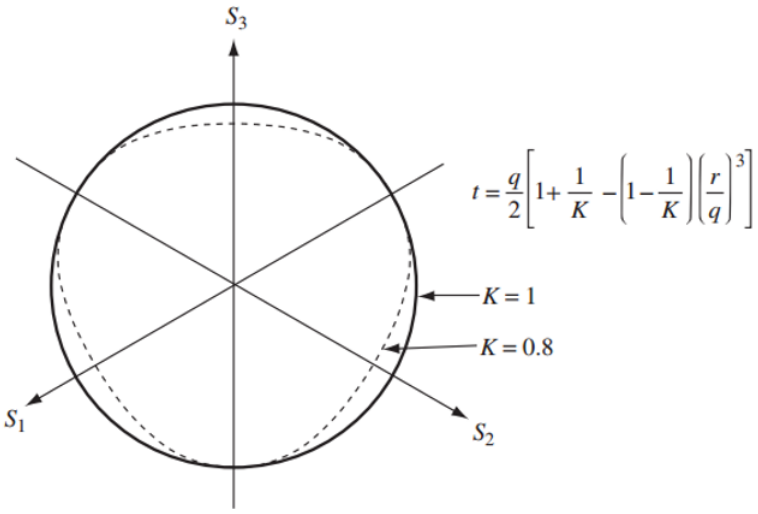

Figure 3.4: Projection of the modified cap yield/flow surfaces on the Π-plane (Abaqus documentation 2014)

The cap yield surface is given as:

$$F_t = \sqrt{(p - p_a)^2 + \left[t - \left(1 - \frac{\alpha}{\cos\beta}\right)(d + p_a \tan\beta)\right]^2} - \alpha\,(d + p_a \tan\beta) = 0 \qquad (3.3)$$

where α is a small number (typically, 0.01 to 0.05) used to define a smooth transition surface between the Drucker–Prager shear failure surface and the cap and p_a is an evolution parameter that controls the hardening–softening behavior as a function of the volumetric plastic strain. The hardening–softening behavior is simply described by a piecewise linear function relating the mean effective (yield) stress (p_b) and the volumetric plastic strain (ε_{vol}^{pl}) and is given in equation 3.4. This function can easily be obtained from the results of one isotropic consolidation test with several unloading–reloading cycles. Consequently, the evolution parameter, p_a, can be calculated from equation 3.5.

$$\varepsilon_{vol}^{pl} = \frac{C_c - C_s}{2.3\,(1 + e_o)} \ln \frac{p_b}{p'_o} \tag{3.4}$$

where

$C_c =$ compression index

$C_s =$ swelling index

$e_o =$ natural void ratio

$p'_o =$ initial mean effective yield stress

$$p_a = \frac{p_b - Rd}{1 + R \tan \beta} \tag{3.5}$$

where

$R =$ a material parameter that controls the shape of the cap

The swelling property of the soil is modelled in Abaqus using the Moisture Swelling model in conjugate with the Sorption model by considering coupled pore fluid diffusion (stress) analysis.

The moisture swelling model defines the saturation-driven volumetric swelling of the solid skeleton of a porous medium in partially saturated flow conditions. The moisture swelling model assumes that the volumetric swelling of the porous medium's solid skeleton is a function of the saturation of the wetting liquid in partially saturated flow conditions. The porous medium is partially saturated in Abaqus when the pore pressure is negative. The swelling behavior is assumed to be reversible. The logarithmic measure of swelling strain is calculated with reference to the initial saturation so that: (Abaqus documentation 2014)

$$\varepsilon_{ii}^{ms} = \frac{1}{3}\left(\varepsilon^{ms}\,(s) - \varepsilon^{ms}\left(s^I\right)\right),\ (no\ sum\ on\ i) \tag{3.6}$$

where

$\varepsilon^{ms}(s) =$ volumetric swelling strain at the current saturation

$\varepsilon^{ms}(s^I) =$ volumetric swelling strain at the initial saturation

The Sorption model represents the suction-saturation relationship of the soil and defines a porous material's absorption/exsorption behavior under partially saturated flow conditions. A porous medium becomes partially saturated when the total pore pressure becomes negative. Negative values of pore pressure represent capillary effects in the medium. The transition between absorption and exsorption and vice versa takes place along "scanning" curves. Only adsorption behavior is considered for the modelling of the swelling property.

3.4.3 Belled Pier-Soil Contact

The belled pier-soil contact was modelled in Abaqus using Coulomb frictional model in conjugate with "hard" contact model by considering contact pairs algorithm, finite sliding and node to surface contact. Pier-soil slip is allowed. As per the recommendations of Zhan et al. (2012), and by considering the soil to be a clay soil, the tangential behavior is modelled in the Coulomb frictional model by providing a very high value of the frictional coefficient, μ, but the interface shear stress was limited by providing a limit shear stress value. The limit shear stress value is dependent on the cohesion in the non-swelling zone and on the swelling pressure in the swelling zone. See Section 4.4.

An extended version of the classical isotropic Coulomb friction model is provided in Abaqus for use with all contact analysis capabilities. The extensions include an additional limit on the allowable shear stress, anisotropy, and the definition of a "secant" friction coefficient. The standard Coulomb friction model assumes that no relative motion occurs if the equivalent frictional stress, $\tau_{eq} = \sqrt{\tau_1^2 + \tau_2^2}$, is less than the critical stress, τ_{crit}, which is proportional to the contact pressure, p, in the form $\tau_{crit} = \mu p$ where μ is the friction coefficient. In Abaqus it is possible to put a limit on the critical stress: $\tau_{crit} = \min(\mu p, \tau_{max})$ where τ_{max} is user-specified. If the equivalent stress is at the critical stress ($\tau_{eq} = \tau_{crit}$), slip can occur. (Abaqus documentation 2014). **Therefore, this particular way of contact modeling in Abaqus allows for pier-soil slip.**

The "hard" contact relationship minimizes the penetration of the slave surface (soil) into the master surface (pier) at constraint locations and does not allow the transfer of tensile stress across the interface. When surfaces are in contact, any contact pressure can be transmitted between them. The surfaces separate if the contact pressure reduces to zero. Separated surfaces come into contact when the clearance between them reduces to zero. See Figure 3.5. (Abaqus documentation 2014).

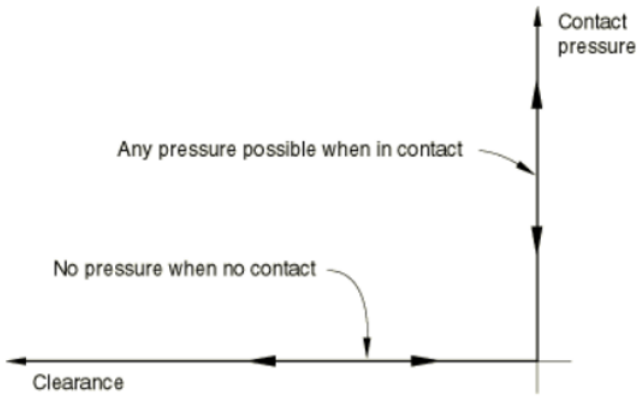

Figure 3.5: Default pressure-overclosure relationship (Abaqus documentation 2014)

3.4.4 Boundary Conditions

The boundary conditions for modelling in Abaqus are presented in Figure 3.6. These boundary conditions represent the field conditions in regards to restrained movement and water flow. The base of the model is restrained in the horizontal and vertical directions. The vertical boundary on the left side is a symmetry line, and the vertical boundary on the right side is restrained in the horizontal direction but free in the vertical direction. The base of the swelling zone is restrained in the horizontal and vertical directions.

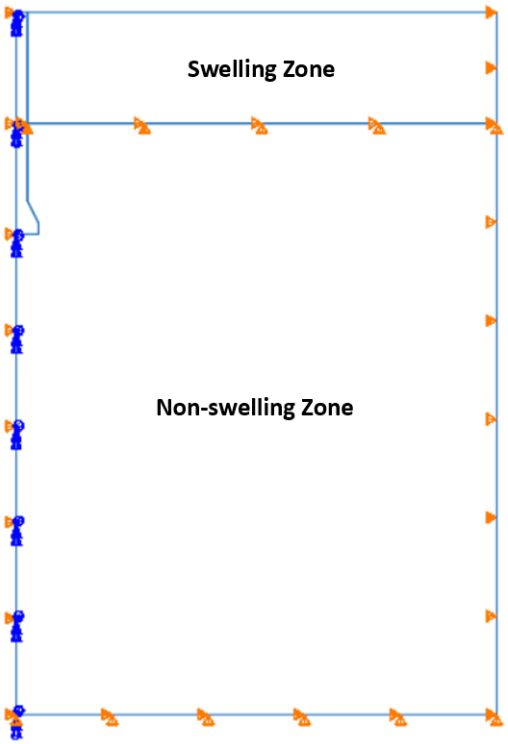

Figure 3.6: Boundary Conditions

3.4.5 Mesh and Mesh Elements

Four-node axisymmetric quadrilateral, bilinear displacement, bilinear pore pressure (CAX4P) mesh elements are used for the soil (both swelling and non-swelling zone) by considering Zhan et al.'s (2012) recommendations. The mesh elements used for the belled pier are four-node bilinear axisymmetric quadrilateral (CAX4). The meshing is presented in Figure 3.7. No mesh convergence studies have been performed.

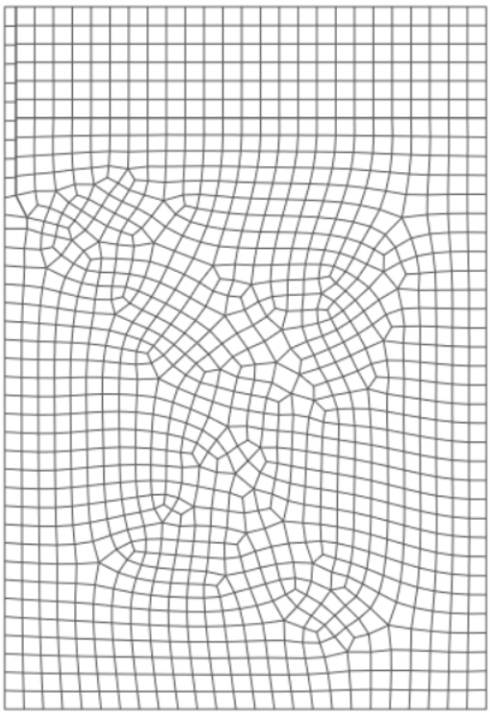

Figure 3.7: Meshing

3.4.6 Analysis Steps

The finite element analysis in Abaqus is run in two steps. In the first step, a geostatic stress field procedure is invoked. In the second step, a coupled pore fluid diffusion/stress analysis is invoked. Geometric nonlinearity is considered in both steps to account for large displacements.

A geostatic stress field procedure is used in Abaqus to verify that the initial geostatic stress field is in equilibrium with gravity loads and boundary conditions and to iterate, if necessary, to obtain equilibrium. The geostatic stress field procedure makes sure that the initial stress condition in any element within the clay layer falls within the initial yield surface of the cap model.

The geostatic stress field procedure is normally used as the first step of a geotechnical analysis; in such cases gravity loads are applied during this step. Ideally, the gravity loads and initial stresses should exactly equilibrate and produce zero deformations. Abaqus provides two procedures for establishing this initial equilibrium. The first procedure is applicable to problems for which the initial stress state is known at least approximately. The second, enhanced procedure is applicable for cases in which the initial stresses are not known. To obtain equilibrium in cases when the initial stress state is unknown, an enhanced procedure is invoked. Abaqus automatically computes the equilibrium corresponding to the initial gravity loads and the initial configuration, allowing only small displacements within user-specified tolerances. (The default tolerance is 10^{-5}). (Abaqus documentation 2014).

In the geostatic stress field procedure step, the self-weight (gravity loads) are applied by using the body force option in Abaqus. In this option, the unit weight is specified for every point on the model and the self-weight (gravity load) is calculated by multiplying the specified unit weight by the depth of every point as measured from the top of the model; i.e. the self-weight (gravity load) will be the overburden pressure. Considering the complexity of the problem, equilibrium is established by making Abaqus compute the initial stress state itself by invoking the enhanced procedure; where the tolerable displacements are taken to be $10^{-5}m$ (default value).

Figure 3.8 shows an example of stresses computed by Abaqus in units of kPa for a belled pier in expansive soil in the geostatic stress field procedure. Considering the height of the model ($19m$) and the heights of the swelling and non-swelling zones of $3m$ and $16m$ respectively, and considering the saturated unit weight ($17.6kN/m^3$) for the swelling zone and the submerged unit weight ($7.79kN/m^3$) for the non-swelling zone, the stress computed by Abaqus at the bottom of the model is $175kPa$ which closely agrees with the actual overburden at this point of $177kPa$ ($17.6kN/m^3 * 3m + 7.79kN/m^3 * 16m$).

Figure 3.9 shows an example of deformations computed by Abaqus in units of meter for a belled pier in expansive soil in the geostatic stress field procedure. As it is observed the deformations are very small and can be approximated to be equal to zero. **This proves that equilibrium was established.**

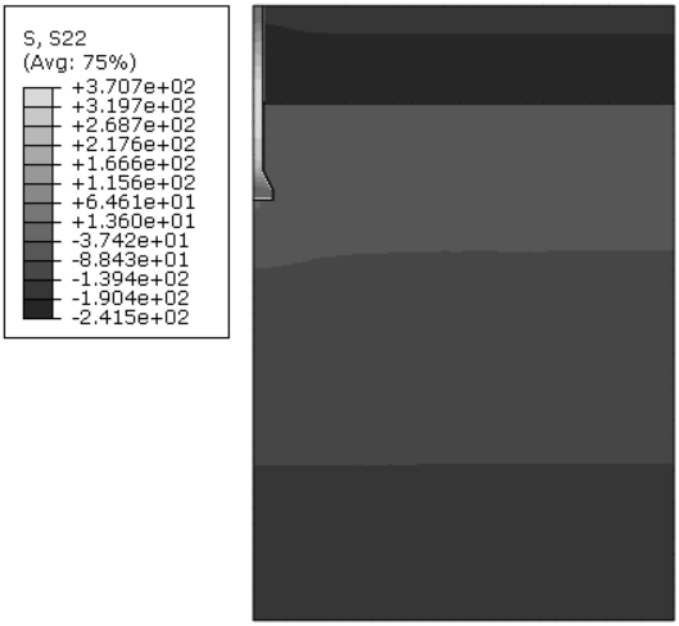

Figure 3.8: Initial Stress State as computed by Abaqus in the geostatic stress field procedure

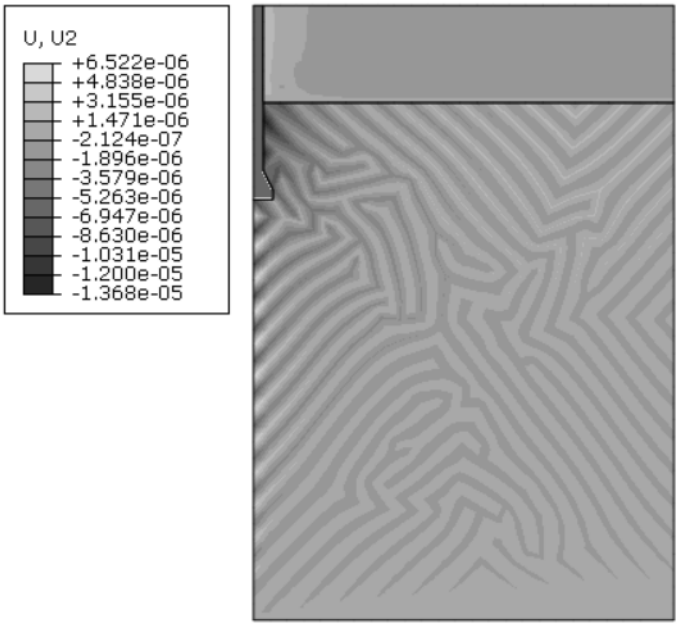

Figure 3.9: Deformations as computed by Abaqus in the geostatic stress field procedure

A coupled pore fluid diffusion/stress analysis is used in Abaqus to model single phase, partially or fully saturated fluid flow through porous media. A porous medium is modeled in Abaqus by a conventional approach that considers the medium as a multiphase material and adopts an effective stress principle to describe its behavior. The porous medium modeling provided considers the presence of two fluids in the medium. One is the "wetting liquid," which is assumed to be relatively (but not entirely) incompressible. Often the other is a gas, which is relatively compressible. An example of such a system is soil containing ground water. When the medium is partially saturated, both fluids exist at a point; when it is fully saturated, the voids are completely filled with the wetting liquid.

The coupled pore fluid diffusion/stress analysis can be transient or steady-state. Steady-state coupled pore pressure/effective stress analysis assumes that there are no transient effects in the wetting liquid continuity equation; that is, the steady-state solution corresponds to constant wetting liquid velocities and constant volume of wetting liquid per unit volume in the continuum. In a transient coupled pore pressure/effective stress analysis the backward difference operator is used to integrate the continuity equation, this operator provides unconditional stability so that the only concern with respect to time integration is accuracy.

In the coupled pore fluid diffusion/stress analysis step the horizontal boundary at the top of the swelling zone is **made permeable to allow for the saturation of the swelling zone. This will initiate the swelling process** in the swelling zone since the soil in the swelling zone has a swelling behavior defined by the Moisture Swelling model in conjugate with the Sorption model. The swelling process continues until the entire depth of the swelling zone is at a saturation level of 100%; a sufficient step time is specified to allow for this. The step considers the transient analysis. Loads on the belled pier, if any, are also applied in this

step.

3.5 Model Validation

The credibility and accuracy of the formulated finite element model in Abaqus is evaluated in this Section. Different mechanisms have been used for the evaluation and validation which include, comparison of FEM results to field measurements, comparison of FEM results to other FEM results, comparison of FEM results to the elastic pier approach and additional mechanisms that involve comparison of the swelling pressure obtained by FEM to the swelling pressure obtained from laboratory testing and comparison of the failure plane observed near the bells in the FEM to the failure plane assumed by Chen (1988).

3.5.1 Comparison to field measurements and other FEMs

Published data concerning field measurements related to behaviors of belled piers in expansive soils are not available. Therefore, comparison with field measurement data of straight shaft piers are considered instead by modeling straight shaft piers using the Finite Element software. This approach is assumed to give a close enough validation. The field measurements are taken form a site in Sudan, designated as Site-1, and established by the Building and Road Institute of the University of Khartoum (Mohamedzein et al. 1999). Straight-shaft concrete test piers were constructed at the site prior to the rainy season of 1985. The piers were $250mm$ in diameter with lengths ranging from 1 to $4m$. The test site was flooded during the rainy season, and the pier and ground heave were measured for a period of $3.5months$. The relevant properties of the site are presented in Table 3.1. Considering these conditions and using the site properties presented in Table 3.1, a representative model was created using the finite element software. Figure 3.10 shows the pier heave computed by the finite element software for the site as compared to the field measurements mentioned before. Figure 3.10 also shows pier heave computed using finite element codes proposed by Mohamedzein et al. (1999) and Nelson et al. (2012) for the specific site.

Table 3.1: Geotechnical Properties for Sudan Site-1

Property	**Value**
Initial Moisture Content (%)	10
Dry Density (kN/m^3)	15.11
Maximum Swelling Pressure (kPa)	337
Percentage Swell (%)	5.65

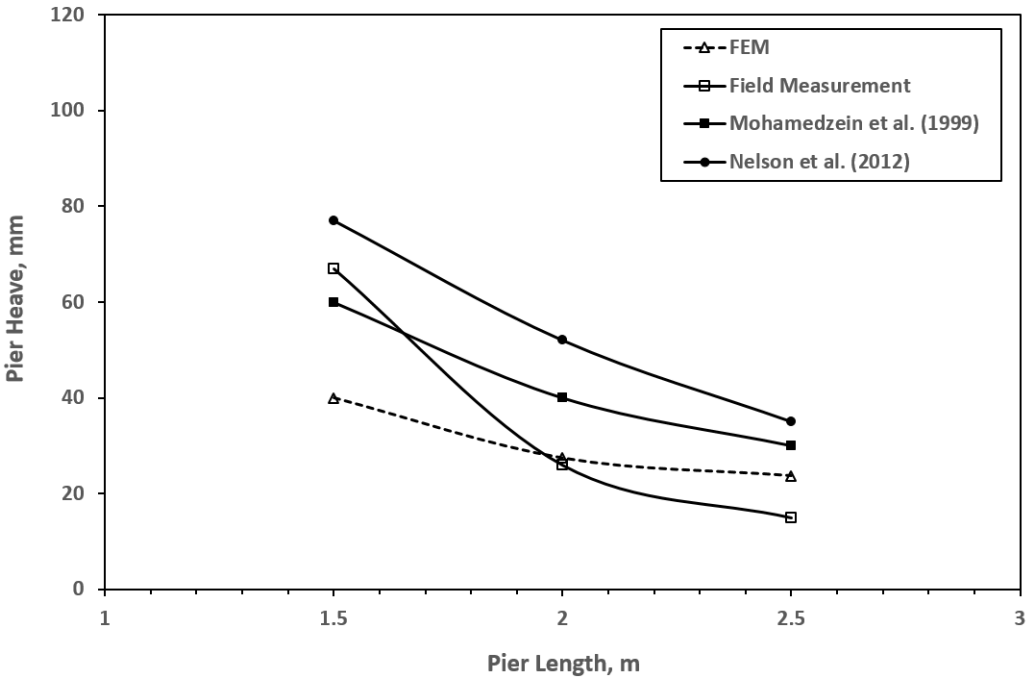

Figure 3.10: Comparison to field measurements and other FEMs

It is observed from Figure 3.10 that the pier heave computed by the finite element analysis agrees closely with field measured pier heave. Furthermore, the pier heave computed by the finite element analysis agrees closely with the field measured pier heave as compared to the pier heave computed by Mohamedzein et al. (1999) or the one computed by Nelson et al. (2012).

3.5.2 Comparison to the Elastic Pier Approach

Poulos and Davis (1980) have presented solutions for belled pier movement in an elastic medium considering soil-pier slip for belled piers with bell sizes $db/d = 2$ (base to shaft ratio). This is known as the elastic pier approach. This was somewhat modified by Nelson and Miller (1992) and Nelson et al. (2007) to make it more easily usable by the design engineer. The finite element solutions for belled piers are compared with the ones presented by Nelson and Miller (1992) in Figures 3.11 and 3.12. The parameters considered in the comparison are presented in Table 3.2. Material and contact properties considered in the comparison are presented in Chapter 4. Concerning bell proportioning, Chen's (1988) recommendations are considered. The pier heave, soil heave and maximum tensile force developed in the piers have been normalized as can be seen in Figure 3.11 and 3.12, the variables are defined as follows (Nelson and Miller 1992):

$\rho_o =$ field heave

$\rho_p =$ pier heave

$P_{max} =$ maximum tensile force in the belled pier

$F_{um} = 0.01Es$

$Es =$ modulus of elasticity of the soil

$d =$ shaft diameter

$Cu =$ undrained cohesion

Table 3.2: Parameters considered in the comparison to the Elastic Pier Approach

Parameter	**Value**
Belled Pier length, $L(m)$	10
Belled Pier shaft diameter, $d(m)$	1
Belled Pier base diameter, $db(m)$	2

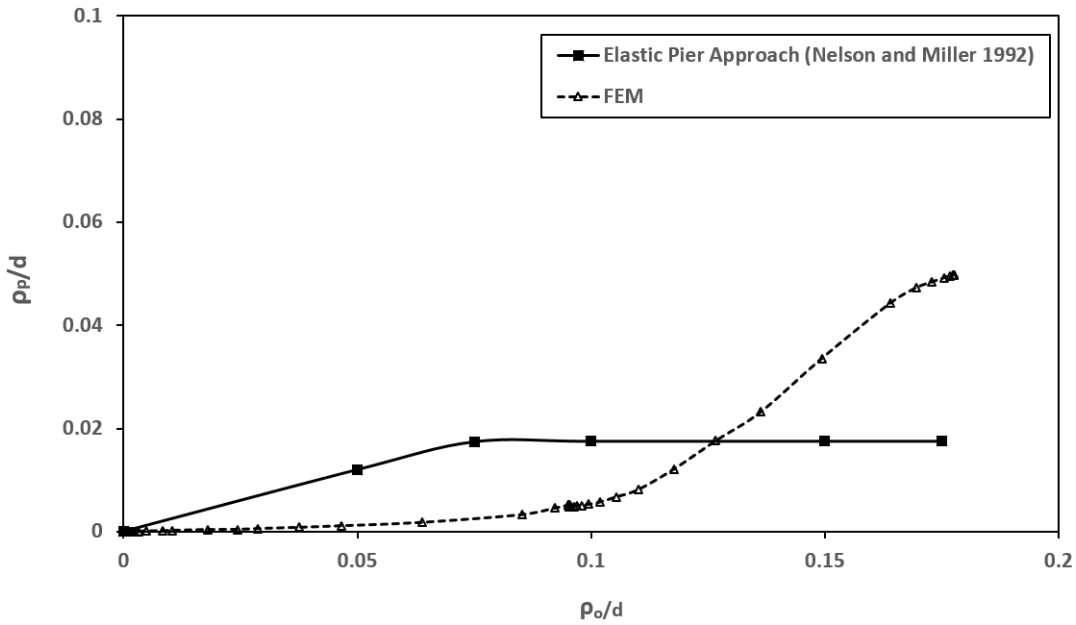

Figure 3.11: Comparison to the Elastic Pier Approach considering Pier Heave

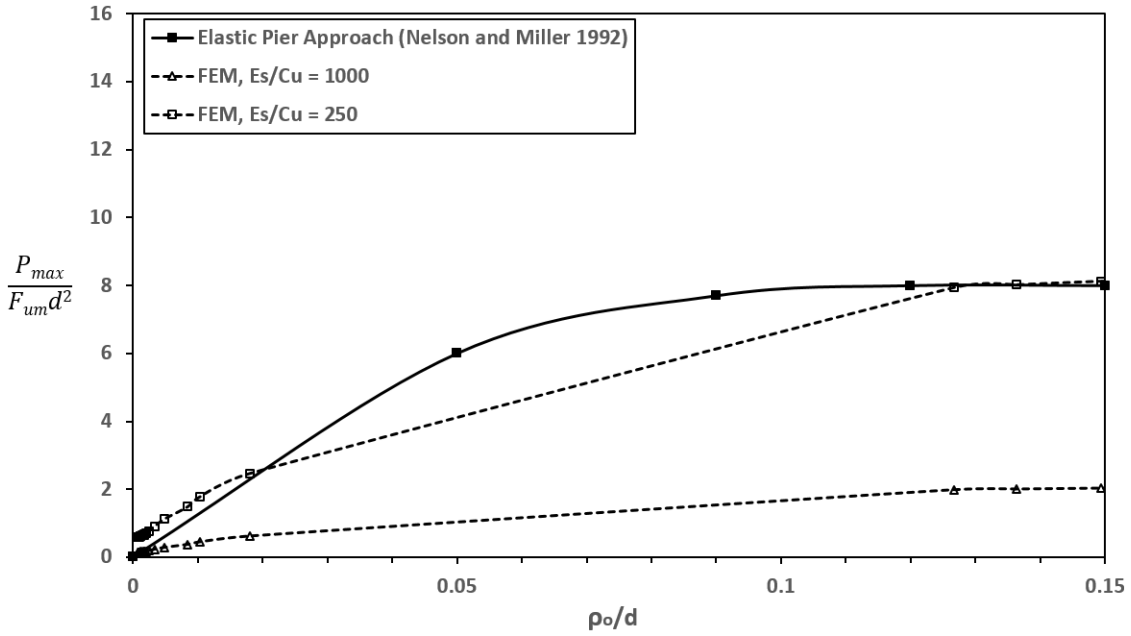

Figure 3.12: Comparison to the Elastic Pier Approach considering Maximum Tensile Force developed in the piers

It is observed from Figure 3.11 that the solutions form the finite element analysis closely match the solutions from the elastic pier approach (Nelson and Miller 1992) when pier heave is considered. Small differences seem to arise because the elastic pier approach doesn't consider the plastic behavior of the soil. The differences suggest that the finite element analysis gives conservative values as compared to the elastic pier approach. In Figure 3.12 it is observed, when considering maximum tensile force developed in the piers, the solutions presented by the finite element analysis closely match the solutions from the elastic pier approach (Nelson and Miller 1992) especially when smaller values of the ratio Es/Cu are considered. The effect of the ratio Es/Cu on belled pier behavior in expansive soils is investigated in Section 5.2.8.

3.5.3 Additional Validation Mechanisms

Besides the two main validation mechanisms mentioned, two additional indirect validation mechanisms are considered. The first considers the swelling pressure of the expansive soil at natural conditions (Saturation level of 87%). The expansive soil was modeled in the finite element software at this natural condition and a swelling pressure of $151kPa$ was observed. This closely matches the swelling pressure of $155kPa$ obtained from laboratory testing (see Section 4.2.6). The second considers failure plane observed in the vicinity of the bells. The concentration of strains, which indicates the failure plane, observed in the finite element model closely resembles the failure plane assumed by Chen (1988). See Figures 3.13 and 3.14.

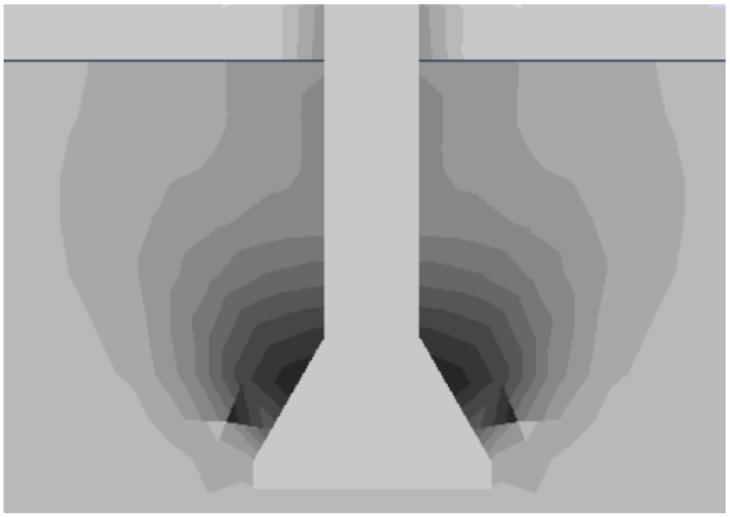

Figure 3.13: Failure Plane observed in the Finite Element Software Abaqus

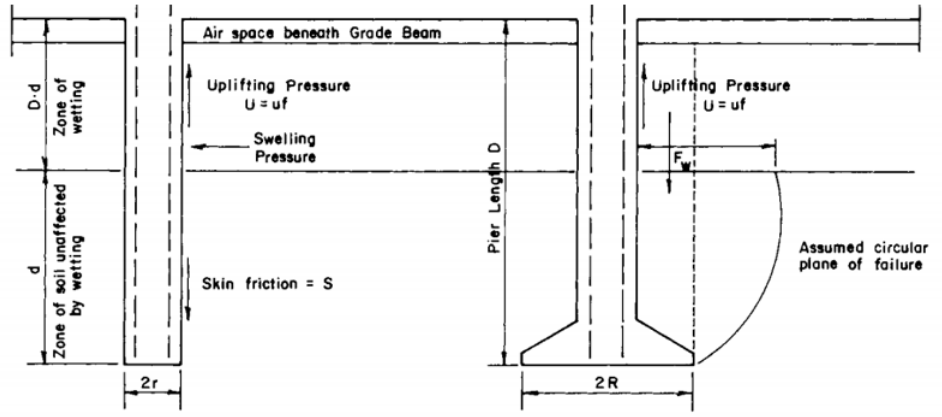

Figure 3.14: Failure Plane Assumed by Chen (1988)

Chapter 4

Material and Contact Properties

4.1 Chapter Introduction

In this chapter, material and contact properties used in the formulation of the finite element modelling in Abaqus are presented. Details of the laboratory testing, literatures, assumptions and equations employed to determine these properties are presented in chapter 3.

4.2 Soil Properties

4.2.1 Basic Index Properties

The basic index properties of the soil used for this research work are presented in this Section. These index properties are determined from laboratory tests and corresponding calculations. The index properties presented in this Section are moisture contents, degree of saturations, void ratios, unit weights and specific gravities. These index properties are presented in Table 4.1.

Table 4.1: Basic Index Properties

Index Property	Designation	Value	Unit
Natural Moisture Content	w_N	0.371	
Natural Void Ratio	e_N, e_O	1.15	
Natural Saturation	S_N	0.87	
Initial Moisture Content	w_i	0.153	
Initial Saturation	S_i	0.52	
Initial Void Ratio	e_i	0.82	
Specific Gravity	G_S	2.71	
Bulk Unit Weight	γ_b	16.95	kN/m^3
Saturated Unit Weight	γ_{sat}	17.6	kN/m^3
Submerged Unit Weight	γ_{sub}	7.79	kN/m^3
Dry Unit Weight	γ_d	12.36	kN/m^3
Unit Weight of Water	γ_w	9.81	kN/m^3

As can be observed from Table 4.1, the soil used for the work has a specific gravity of 2.71 which is within the proposed values by Bowles (2001) for inorganic clay. A natural saturation of 87% is observed for the soil used for the work (Table 4.1). The initial saturation level is taken by assuming the moisture content at the beginning of the dry season. This value is assumed to be moisture content of the air dried sample plus 5% moisture, i.e. 15.3. It is customary to consider soils with saturation above 85% as fully saturated soils (Murray and Sivakumar 2010). However, for this study, full saturation is assumed to occur at 100%. Therefore, the soil used for the work is considered to be under unsaturated conditions. This assumption is taken because the soil exhibits swelling properties until its saturation reaches 100%.

4.2.2 Grain Size and Distribution

The grain size and distribution of the particular soil used for the work is presented in Table 4.5:

Table 4.2: Grain Size and Distribution

Sieve Number	**Grain Size/Sieve Opening** (mm)	**Percentage Passing** (%)
$3''$	75	100.0
$2''$	50	100.0
$1.5''$	37.5	100.0
$1''$	25	100.0
$3/4''$	19	100.0
$1/2''$	12.5	100.0
$0.38''$	9.5	99.8
$No.4$	4.75	99.8
$No.8$	2.36	99.8
$No.10$	2	99.8
$No.16$	1.18	99.8
$No.30$	0.6	99.7
$No.50$	0.3	99.6
$No.100$	0.15	99.3
$No.200$	0.075	99.3
	0.038	86.0
	0.027	86.0
	0.019	82.8
	0.014	79.7
	0.010	78.1
	0.007	76.5
	0.005	74.9
	0.005	71.8
	0.004	70.2
	0.003	68.6
	0.002	67.1
	0.001	65.5

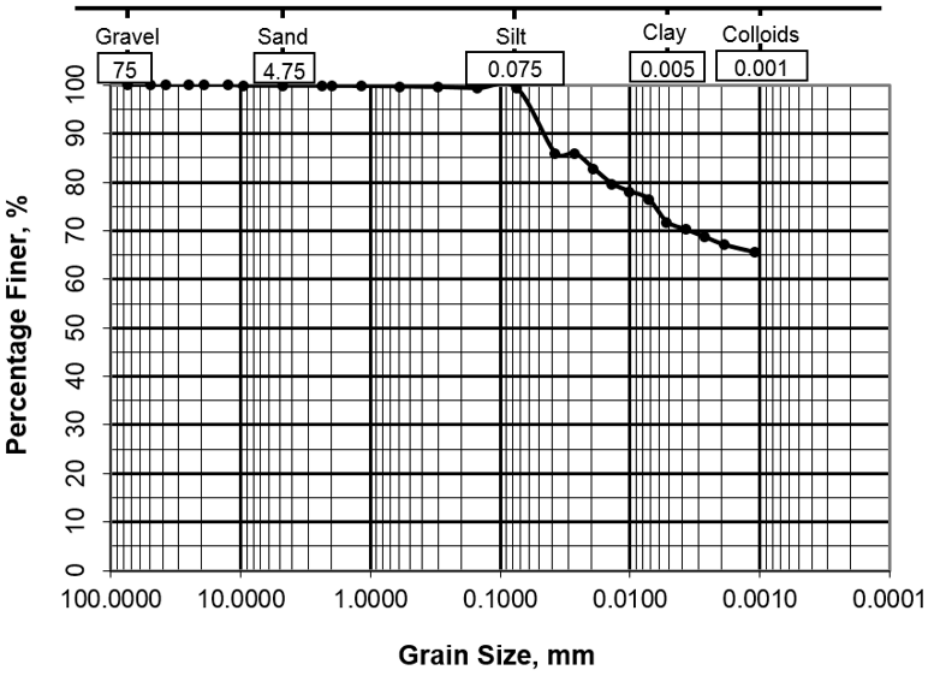

Figure 4.1: Grain Size Distribution Curve

It can be easily observed from Figure 4.1, or the grain size distribution curve of the soil, that the soil under consideration is a fine-grained soil type. The soil is properly classified in Section 4.2.5.

4.2.3 Atterberg Limits

The Atterberg limits and indices as determined from laboratory testing and related calculations are presented as follows. Additionally, the liquid limit flow curve is also presented.

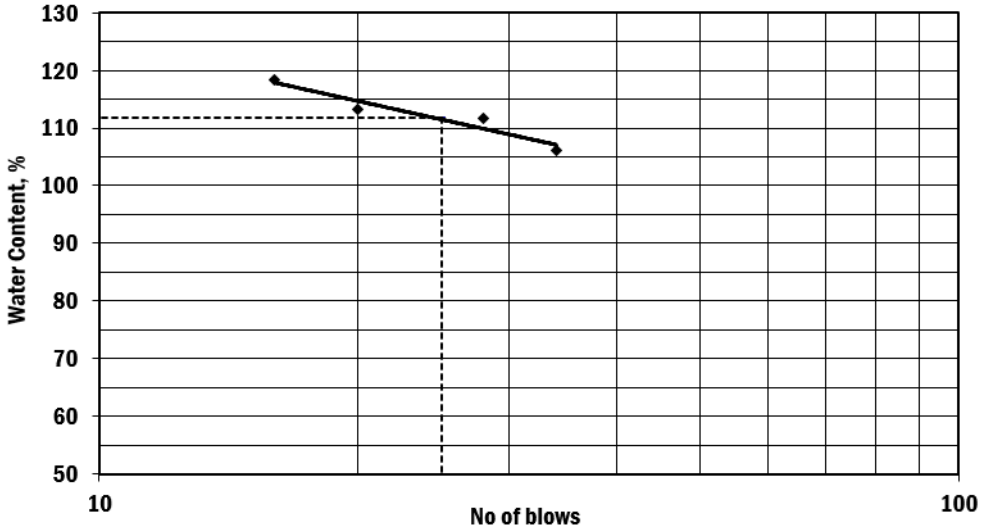

Figure 4.2: Liquid Limit Flow Curve

Table 4.3: Atterberg Limits and Indices

Atterberg Limit/Index	Designation	Value	Value (%)
Liquid Limit	LL, w_L	1.12	112
Plastic Limit	PL, w_P	0.39	39
Plastic Index	P_I, I_P	0.73	73

From the high liquid limit and plastic index presented in Table 4.3, on can deduce that the particular soil in consideration has high plasticity nature. The soil is properly classified in Section 4.2.5.

4.2.4 Free Swell

The free swell of the soil in consideration as determined from the free swell test is presented as follows:

Table 4.4: Free Swell Test Result

Initial	Final Volume		Average	Free
	Sample	Sample		
Volume (cc)	No.1 (cc)	No.2 (cc)	Final Volume (cc)	Swell Index (%)
10.0	22.0	21.5	21.8	**118**

The free swell value of 118% as observed from Table 4.4 indicates that the soil under investigation has a very high expansive potential.

4.2.5 Classification of the Soil

As stated in the above Sections, specific gravity, grain size distribution and Atterberg limits, the soil under consideration shows indications of fine grained inorganic clay soil with high plasticity and expansive nature. In this Section, the soil is properly classified considering international systems of soil classification.

4.2.5.1 Unified Soil Classification System (USCS)

The values of the grain size distributions and Atterberg limits and indices used to classify the soil used in the work according to the unified soil classification system (Murthy 2002) are presented as follows as determined from laboratory testing and as stated in the above Sections. The plot of the soil used for the work on the A-chart (Murthy 2002) is also presented as this is also important to classify the soil using the unified soil classification system.

Table 4.5: Grain Size Distribution and Atterberg values used in the USCS

Percentage Passing No. 200 Sieve	**Liquid Limit (%)**	**Plastic Index (%)**
99.3	112	73

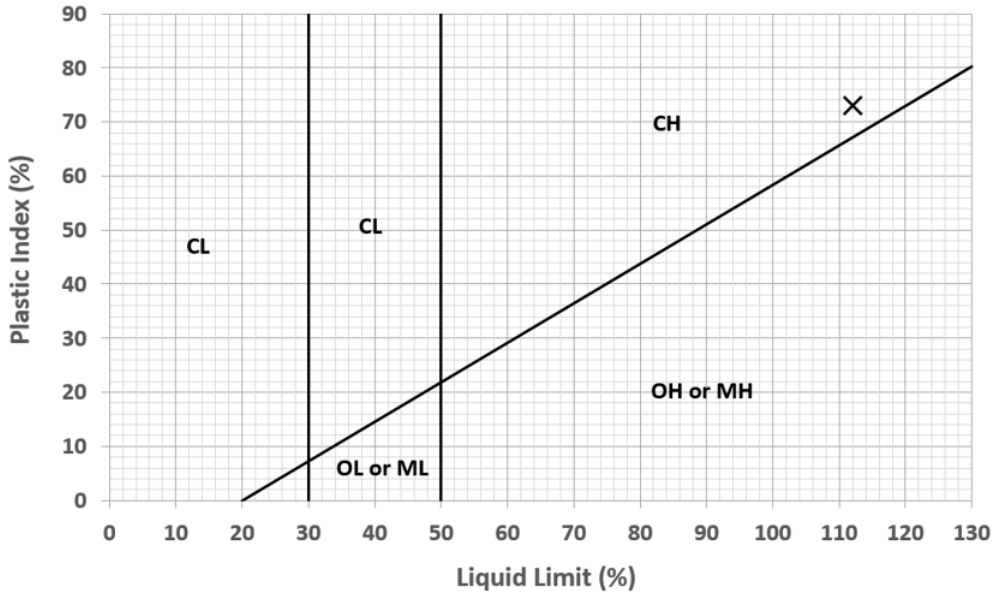

Figure 4.3: Soil Plot on the A-Chart (Murthy 2002)

Considering grain size distribution, liquid limit, plastic index and plot on the A-Chart, the soil is classified as CH (inorganic clay of high plasticity, fat clay) by the unified soil classification system. This falls in accordance with the observations made in the previous Sections. Considering the soil plot on the A-Chart (Figure), it is observed that the soil plot falls in the region on the A-Chart for expansive soils of Addis Ababa presented by Sisay and Haile (2004).

4.2.5.2 Activity

The activity of the soil (Skempton 1953), which is related to expansive potential, is determined in this Section. Clay fraction finer than 0.002mm and plastic index values used to determine the activity of the soil together with the determined activity value are presented as follows. The plot of the soil on the activity chart (Skempton 1953) is also presented.

Table 4.6: Activity and data used to determine its value (Skempton 1953)

Plastic Index (%)	**Clay fraction finer than 0.002mm (%)**	**Activity, Ac**
73	67.1	1.09

Table 4.7: Relationship between Activity values and Skempton's Category (Skempton 1953)

Activity	Skempton's category
Ac < 0.75	Inactive
0.75< Ac<1.25	Normal
Ac> 1.25	**Active**

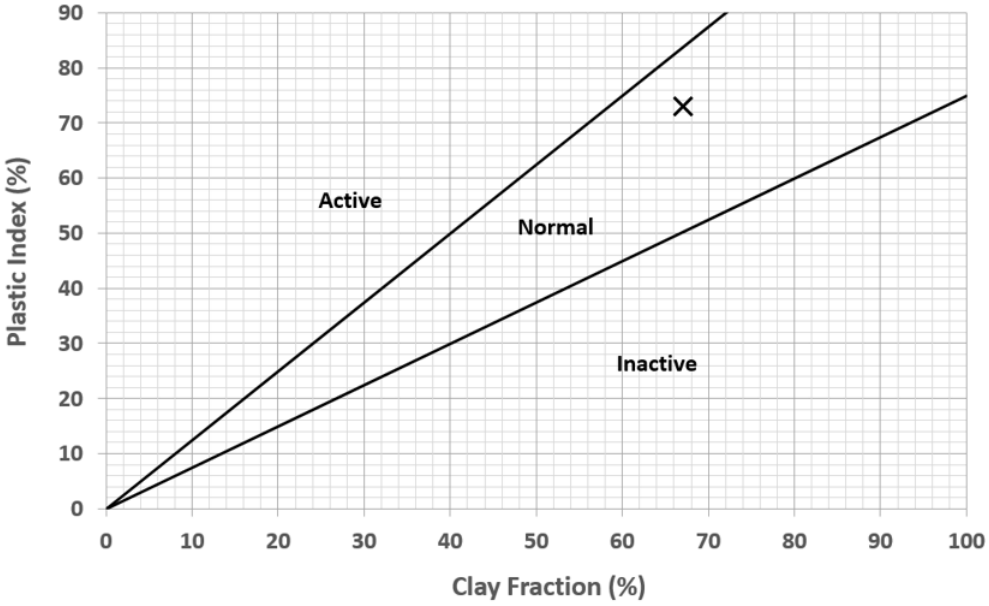

Figure 4.4: Soil Plot on the Activity Chart

As observed from the plot of the soil on the activity chart proposed by Skempton (Figure 4.4), the soil activity is classified as normal. It is argued that this classification underestimates the swelling potential of the soil used for the work. This argument is valid considering the high free swell obtained in Section 4.2.4 and high swelling pressure obtained in Section 4.2.6. (Note that the swelling pressure obtained in Section 4.2.6 is at 87% saturation. Much higher values are expected at lower saturation levels). Considering this situation, an attempt was made to classify the activity of the soil by considering an activity chart proposed by a different author (De Bruyn et al. 1956), see Figure 4.5. As expected, this time, the soil falls into category 'Bad' implying high swelling potential of the soil. The soil also falls in the category of 'most expansive soils located in Addis Ababa as proposed by Sisay and Haile (2004).

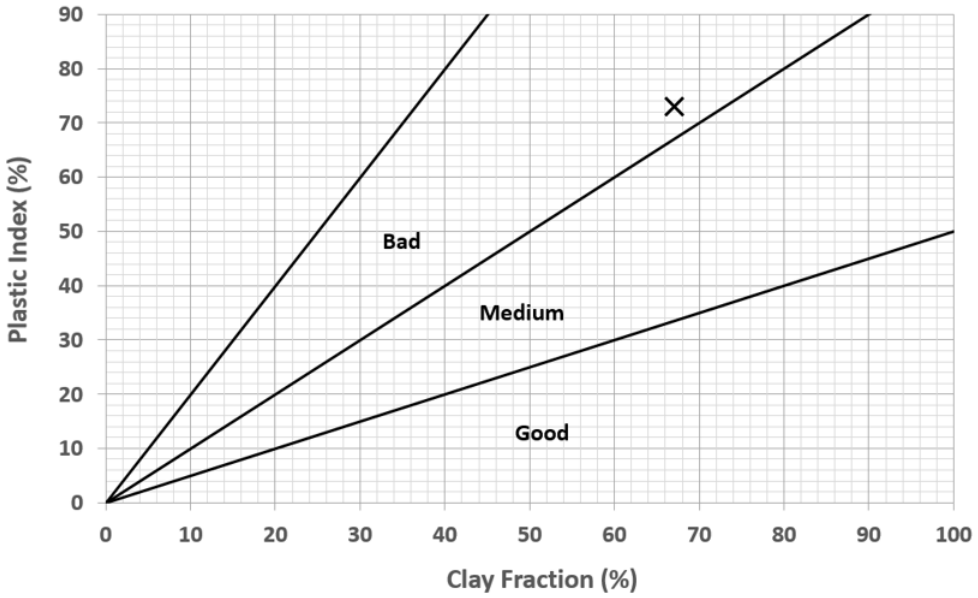

Figure 4.5: Soil Plot on the Activity Chart (De Bruyn et al. 1956)

4.2.6 One Dimensional Consolidation Test related Properties

A one dimensional consolidation test was conducted on the soil used for the work and important soil parameters were obtained. These soil parameters are presented in this Section. Figures, specifically, the void ratio versus pressure plots (e-P plots), and other necessary parameters used to determine these specific parameters are also presented here.

Table 4.8: One Dimensional Consolidation test results and related values

Parameter	**Designation**	**Value**	**Unit**	**Mechanism used to obtain**
Liquid Limit	LL, w_L	112	%	Liquid Limit Test
Specific Gravity	G_s	2.71		Specific Gravity Test
Natural Void Ratio	$e_{N,}e_O$	1.15		Soil Parameter Relationships
Natural Saturation	S_N	87	%	Soil Parameter Relationships
Submerged Unit Weight	γ_{sub}	7.79	kN/m^3	Soil Parameter Relationships
Sampling Depth	h	9	m	Field measurements
Compression Index	C_c	0.34		e-log P plot (Figure 4.7)
Recompression Index	C_r	0.017		Literature (Bowles 2001)
Coefficient of Compressibility	a_v	0.000273	kPa^{-1}	e-P plot (Figure 4.8)
Coefficient of volume Compressibility	m_v	0.000127	kPa^{-1}	Soil Parameter Relationships
Effective Overburden Pressure	p'_o, σ'_o	70.11	kPa	Submerged unit weight multiplied by sampling depth
Preconsolidation Pressure	Pc, σ_c	192	kPa	e-log P plot (Figure 4.9)
Swelling Pressure	Ps, σ_s	155	kPa	e-log P plot (Figure 4.10)
Over Consolidation Ratio	OCR	2.74		Ratio of the preconsolidation pressure to effective overburden

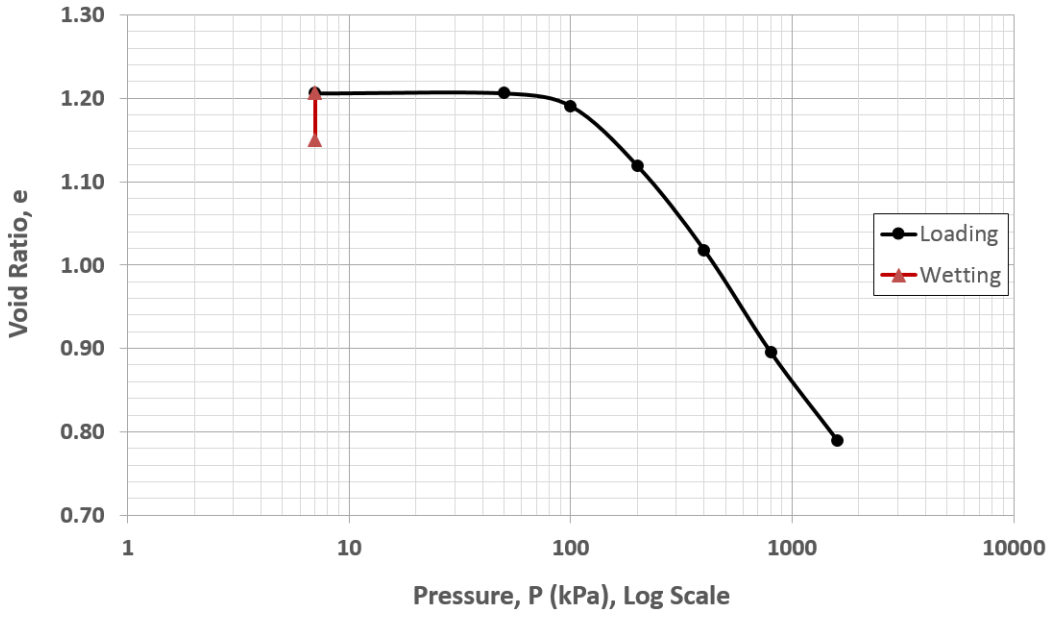

Figure 4.6: Void Ratio versus Logarithm of Pressure Plot

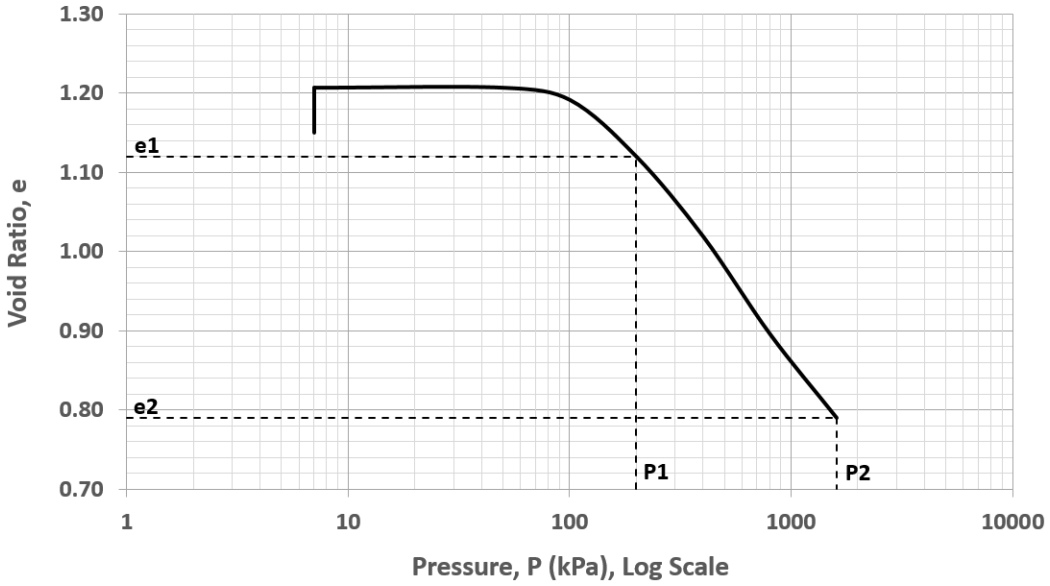

Figure 4.7: Determination of Compression Index from void ratio versus logarithm of pressure plot

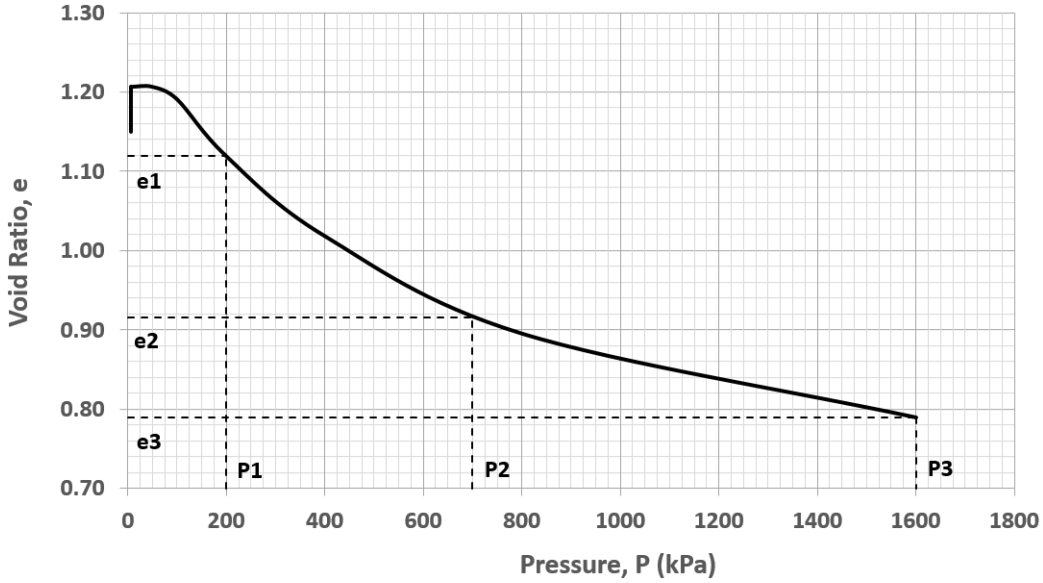

Figure 4.8: Determination of Coefficient of Compressibility from void ratio versus pressure plot

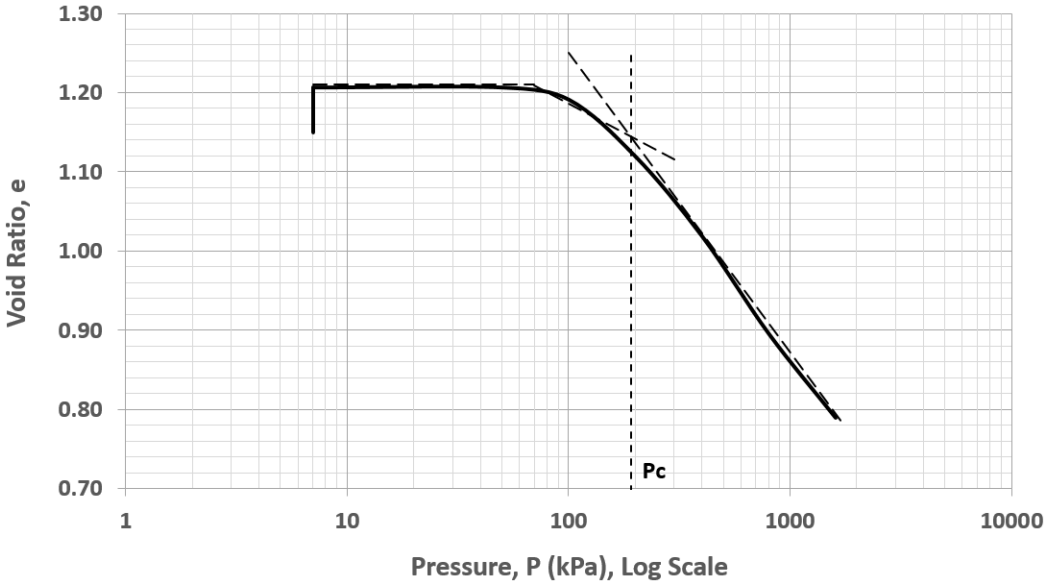

Figure 4.9: Determination of Preconsolidation Pressure from void ratio versus logarithm of pressure plot

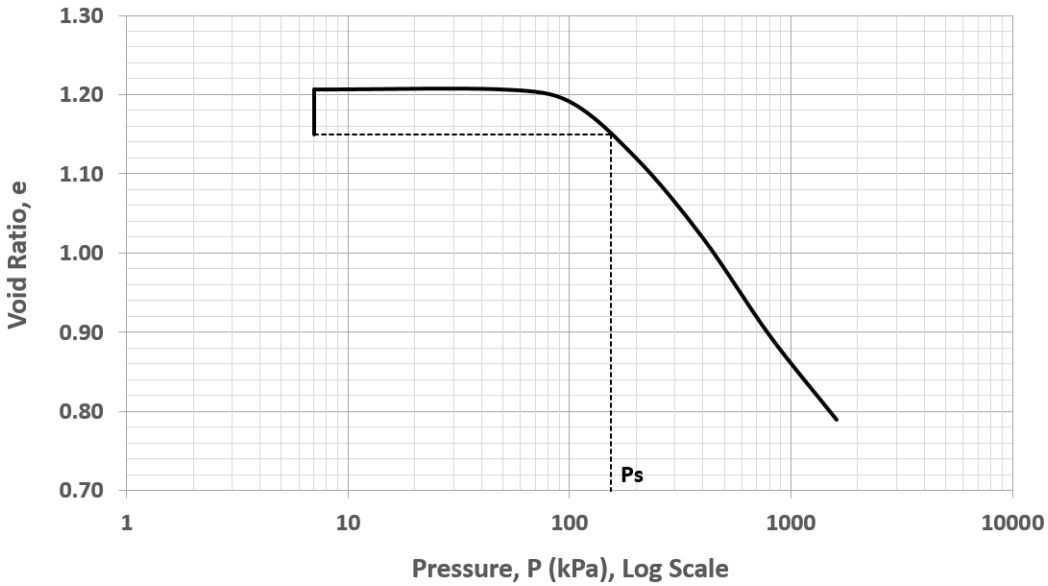

Figure 4.10: Determination of Swelling Pressure from void ratio versus logarithm of pressure plot

As can be observed from Table 4.8, the soil used for the work has an over consolidation ratio, OCR value of 2.74. This indicates that the soil is an overconsolidated soil. Again, referring Table 4.8 and Figure 4.10, the swelling pressure of the soil used for the work is $155kPa$. This value of swelling pressure is obtained at a saturation level of 87% , which is the natural saturation level.

4.2.7 Elastic Properties

In this Section, soil parameters related to the elastic nature of the soil used for the work are presented. The elastic properties presented are, modulus of elasticity, Poisson's ratio and coefficient of lateral earth pressure.

Table 4.9: Elastic Property Parameters

Property	Designation	Value	Unit	Mechanism used to obtain
Modulus of Elasticity/ Young's Modulus	Es	77	MPa	Literature (Zhan et al. 2012; Bowles 2001)
Poisson's Ratio	ν	0.45		Literature (Bowles 2001)
Coefficient of Earth Pressure at Rest	k_o	0.82		Literature (Bowles 2001)

4.2.8 Plastic Properties

Parameters related to the plastic nature of the soil used for the work are presented in this Section. Furthermore, parameters used in the cap plasticity model (modified Drucker–Prager model) used to model the plastic nature of the soil in the finite element modelling are also presented here. The cap hardening curve related to the cap plasticity model is also presented.

Table 4.10: Plastic Property Parameters

Property	Designation	Value	Unit	Mechanism used to obtain
Undrained Cohesion	Cu	77	kPa	Literature (Bowles 2001)
Undrained Angle of Friction	ϕ_u	0		

Table 4.11: Cap Plasticity Model Parameters (Abaqus documentation 2014)

Parameter	Designation	Value	Unit
Material Cohesion	d	133.4	kPa
Angle of Friction	β	0.1	$Degrees$
Cap Eccentricity	R	0.1	
Initial Yield Surface Position	$\varepsilon_{vol}^{pl}\|_0$	0	
Transition Surface Radius	α	0.05	
Flow Stress Ratio	K	1	

Cap Hardening Curve

In this sub-Section, parameters related to the cap hardening curve of the soil used for the work are presented. The equation (the relationship between mean effective yield stress p_b'

and plastic volumetric strain ε_{vol}^{pl} or ε_{vp}) used to determine the cap hardening curve is also presented here (equation 4.1). Equation 4.1 is obtained from equation 3.4 using the values presented in Table 4.12. Finally, the cap hardening curve itself is presented. Note that the initial mean effective yield stress, p'_o, is taken to be equal to the preconsolidation pressure, Pc, because the soil is an over consolidated soil.

Table 4.12: Parameters related to the cap hardening curve

Parameter	Designation	Value	Unit
Compression Index	C_c	0.342	
Swelling Index	C_s	0.017	
Natural Void Ratio	e_o	1.15	
Preconsolidation Pressure	Pc	192	kPa

$$p'_b = 192 \exp^{15.2\varepsilon_{vol}^{pl}} \tag{4.1}$$

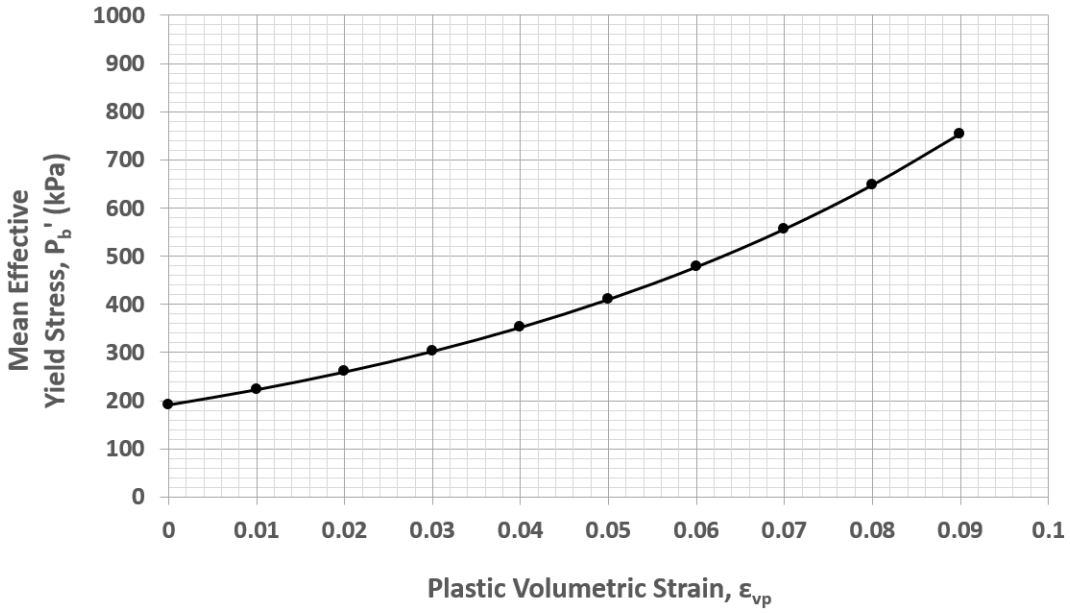

Figure 4.11: Cap Hardening Curve

4.2.9 Swelling Property, Unsaturated Property and Permeability

The swelling behavior of the soil used for the work is modelled in the finite element software by defining both unsaturated soil behavior properties and swelling behavior properties. The unsaturated soil behavior is defined by the unsaturated soil's soil water characteristic curve, SWCC curve (relationship between the soil's saturation level and the soil's negative pore pressure level). The soil water characteristic curve is predicted by the program SEEP/W and both the curve and values used to predict the curve are presented here. The swelling

behavior property is defined by defining a relationship between the soil's saturation level and the soil's volumetric swelling strain level. Laboratory test was conducted to find this relationship and the results of this testing are presented here. The volumetric swelling strain is taken to be equal to twice that of the vertical swelling strain (Puppala et al. 2013). Also, presented in this Section is, the saturated permeability value of the soil. It's been observed form the finite element analysis that variations in the SWCC curve don't result in much variations in the finite element results. The primary purpose of the SWCC curve is to set the initial saturation level of the soil.

Table 4.13: Values used to predict the soil water characteristic curve

Void Ratio, e	1.15
Porosity, n	0.535
Saturated Volumetric Water Content, Θ_w (m^3/m^3)	0.535
Liquid Limit (%)	112
Diameter at 10% passing (mm)	0
Diameter at 60% passing (mm)	0
Coefficient of volume compressibility, m_v (kPa^{-1})	0.000127

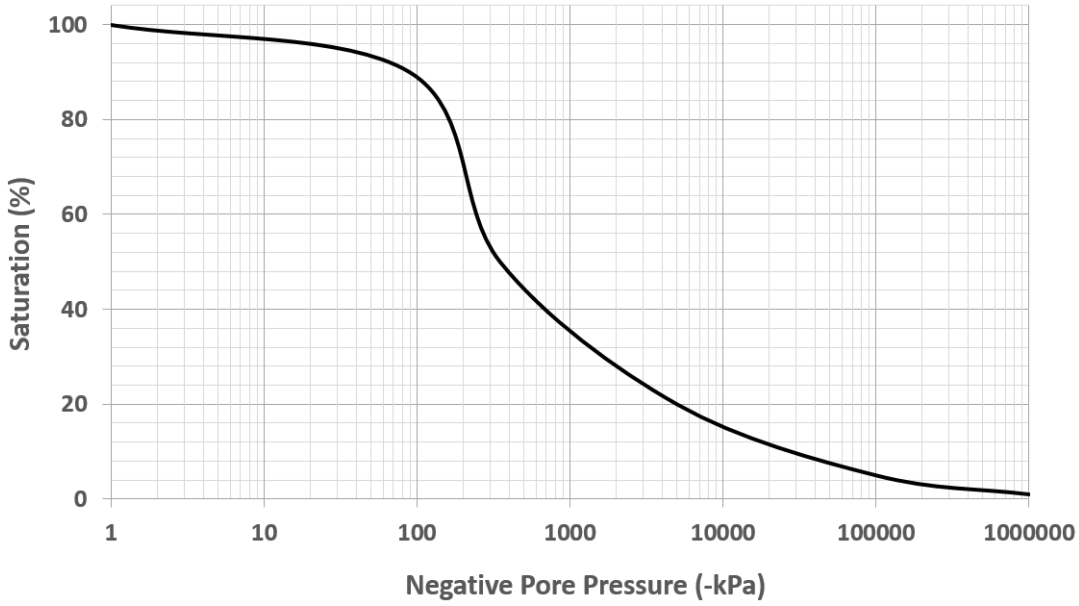

Figure 4.12: Soil Water Characteristic Curve/SWCC (SEEP/W 2007)

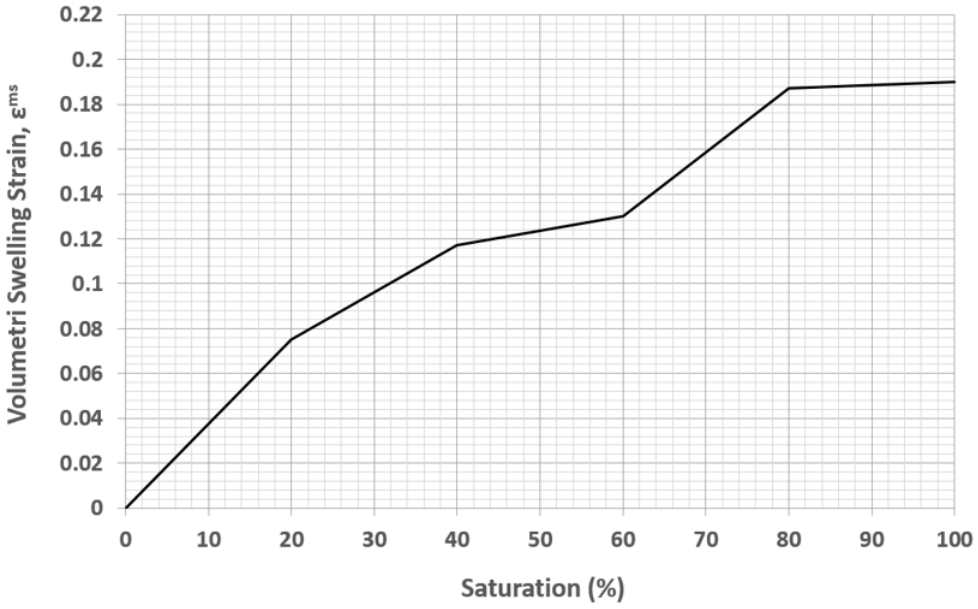

Figure 4.13: Saturation-Volumetric Swelling Strain Relationship

Table 4.14: Permeability value of the soil

Parameter	Designation	Value	Unit
Permeability (saturated)	K_{sat}	$2.5 * 10^{-9}$	m/s

4.3 Pier Properties

The pier properties used to model the belled pier in the finite element model are presented here. The pier has elastic properties only; furthermore, the material presenting the pier is concrete, so the properties presented in Table 4.15 are that of typical of concrete.

Table 4.15: Pier Properties

Property	Designation	Value	Unit
Unit Weight	γ	25	kN/m^3
Young's Modulus	E	25	GPa
Poisson's Ratio	υ	0.2	

4.4 Contact Properties

In this Section, properties related to the interaction or contact between the belled piers and the soil are presented.

Table 4.16: Contact/Interaction properties and related values

Property	**Designation**	**Value**	**Unit**	**Mechanism used to obtain**
Adhesion Factor	α	0.5		Literature (Chen 1988)
Cohesion	Cu	77	kPa	
Interface Shear Stress limit for Non-Swelling Zone	f_s	38.5	kPa	
Coefficient of Uplift	α_s	0.15		Literature (Chen 1988)
Maximum Swelling Pressure at natural saturation	$\sigma_{s,n}$	151	kPa	Finite Element Analysis
Interface Shear Stress limit for the Swelling Zone considering natural Saturation	$f_{u,n}$	23	kPa	

Chapter 5

Results and Discussions

5.1 Chapter Introduction

As mentioned in the objectives Section of the work, the major objective of the work is to model belled piers in expansive soils using the FEM software Abaqus and investigate the effects of parameters that can affect belled pier behaviors in expansive soils, conduct a cost comparison of belled piers in expansive soils and produce trend lines that can be used to design belled piers in expansive soils. These investigations of parameters, cost comparison and the proposed trend lines are presented in this chapter. Furthermore, discussions are made by considering comparisons to previous works related to the specific topic under consideration.

For most of the parametric investigations, the **depth of the swelling zone is taken to be 3m** as per the recommendations of Sisay and Haile (2004). Different values of the swelling pressure are considered, namely, $250kPa$, $500kPa$ and $750kPa$. $250kPa$ and $500kPa$ swelling pressures represent the usual case of expansive soils in Ethiopia (Sisay and Haile 2004). $750kPa$ swelling pressure is considered to clearly observe the effect of some of the parameters in the parametric study which may not have been possible considering $250kPa$ and $500kPa$ swelling pressures. Concerning bell proportioning, Chen's (1988) recommendations are considered.

Note that when considering pier movements, upward movements are defined as positive and downward movements are defined as negative, when considering axial stresses developed inside the piers, tensile stresses are defined as positive and compressive stresses are defined as negative and when considering interface shear stresses developed between the shaft of the piers and the swelling zone, downward interface shear stresses on the pier shaft (interface shear stresses that resist pier heave) are defined as positive and upward interface shear stresses on the pier shaft (interface shear stresses that cause heave) are defined as negative.

5.2 Parametric Investigation of Belled Piers in Expansive Soils

5.2.1 Effect of Length on Belled Pier Behaviour

The behavior of a belled pier embedded in an expansive soil can be affected by the length of the belled pier, i.e. different lengths could result in different behaviours. This is investigated by assuming different lengths of the belled pier and considering the consequent effects on the belled pier heave (upward displacement) and the development of the axial stresses (tensile stresses) in the belled pier. The results of the investigation are presented in Figures 5.1 to 5.9. The belled pier for this length investigation has a shaft diameter (d) of $0.6m$ and a bell to shaft ratio (db/d) of 2. Also, a straight shaft pier with a shaft diameter (d) of $0.6m$ was considered to investigate relations to straight shaft piers.

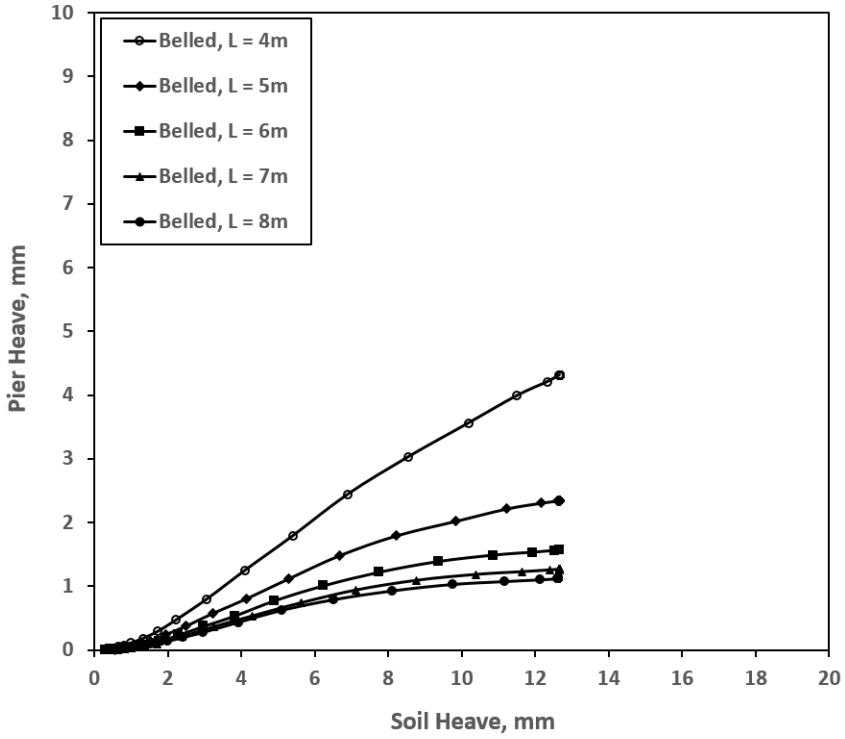

Figure 5.1: Effect of Length on Belled Pier Heave for $250kPa$ Swelling Pressure

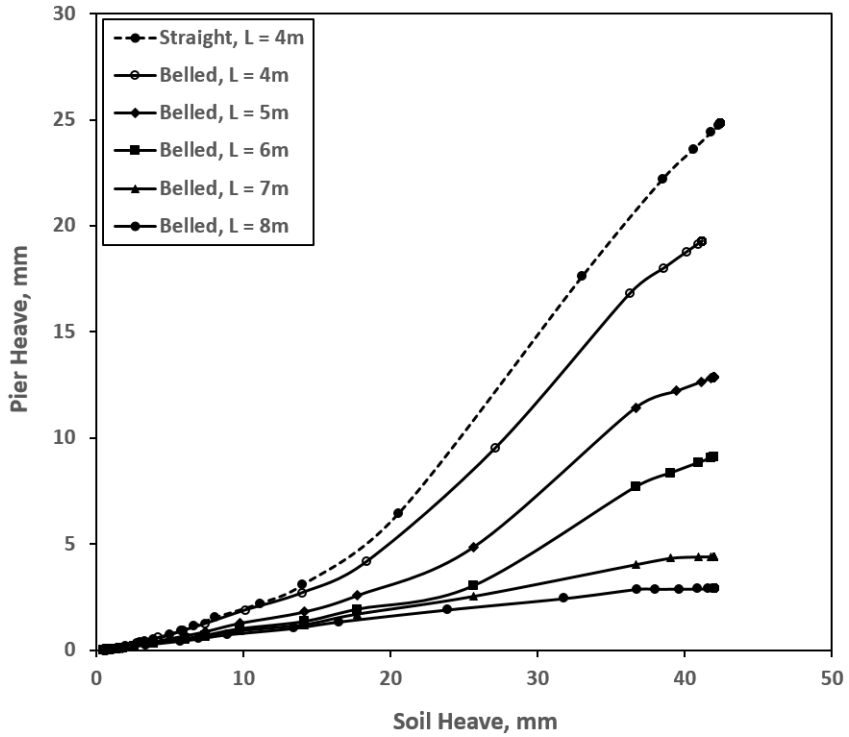

Figure 5.2: Effect of Length on Belled Pier Heave for $500kPa$ Swelling Pressure

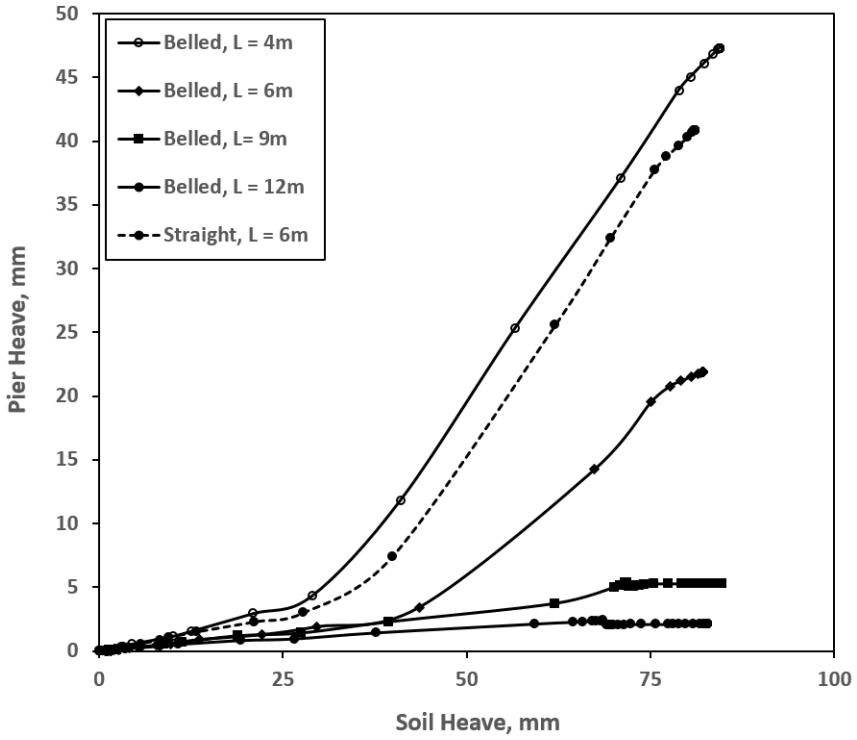

Figure 5.3: Effect of Length on Belled Pier Heave for $750kPa$ Swelling Pressure

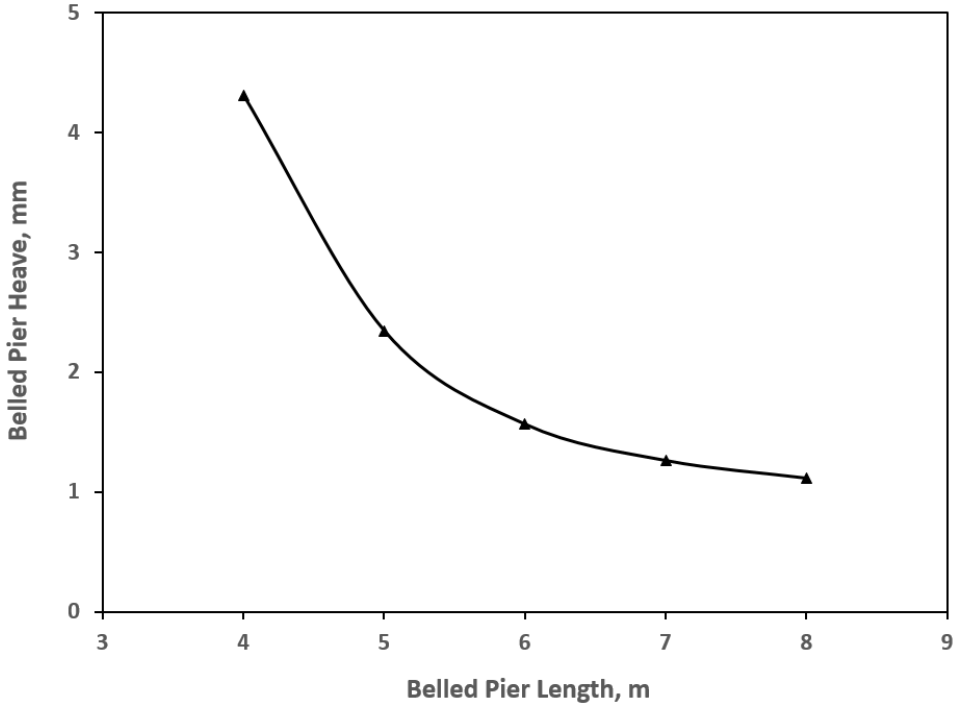

Figure 5.4: Relation between Belled Pier Heave and Belled Pier length for $250kPa$ Swelling Pressure

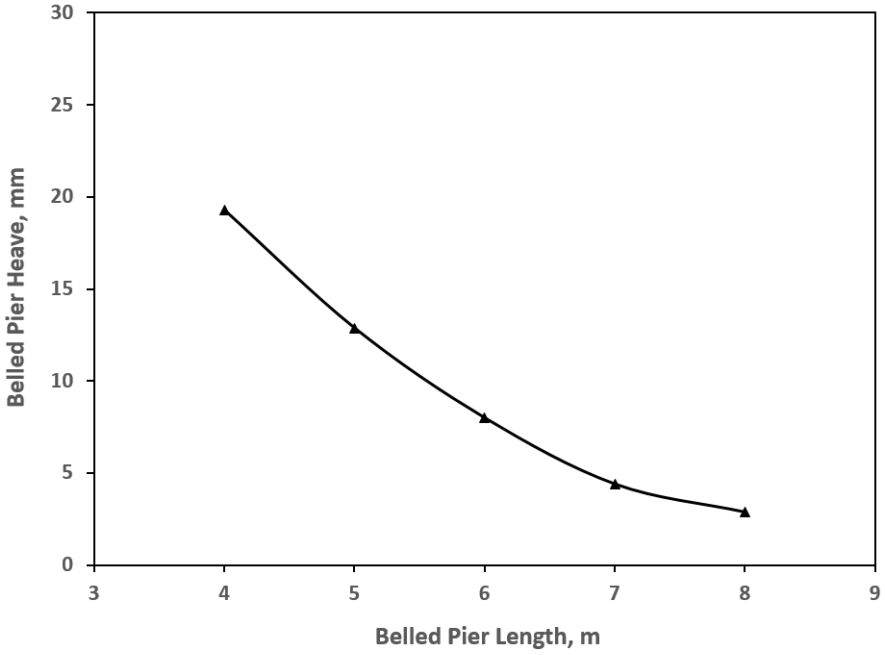

Figure 5.5: Relation between Belled Pier Heave and Belled Pier length for $500kPa$ Swelling Pressure

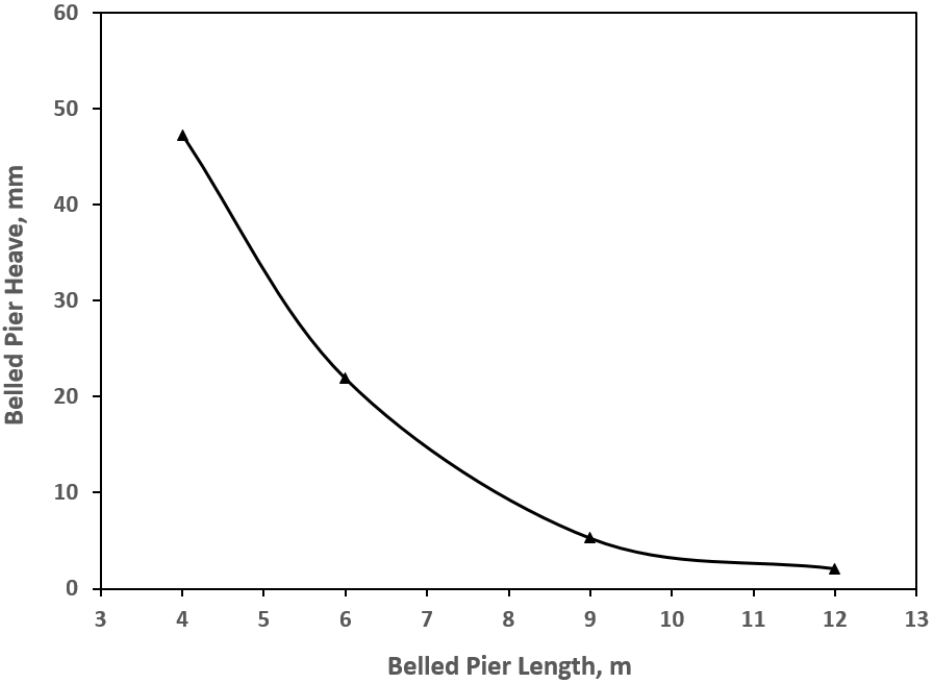

Figure 5.6: Relation between Belled Pier Heave and Belled Pier length for $750kPa$ Swelling Pressure

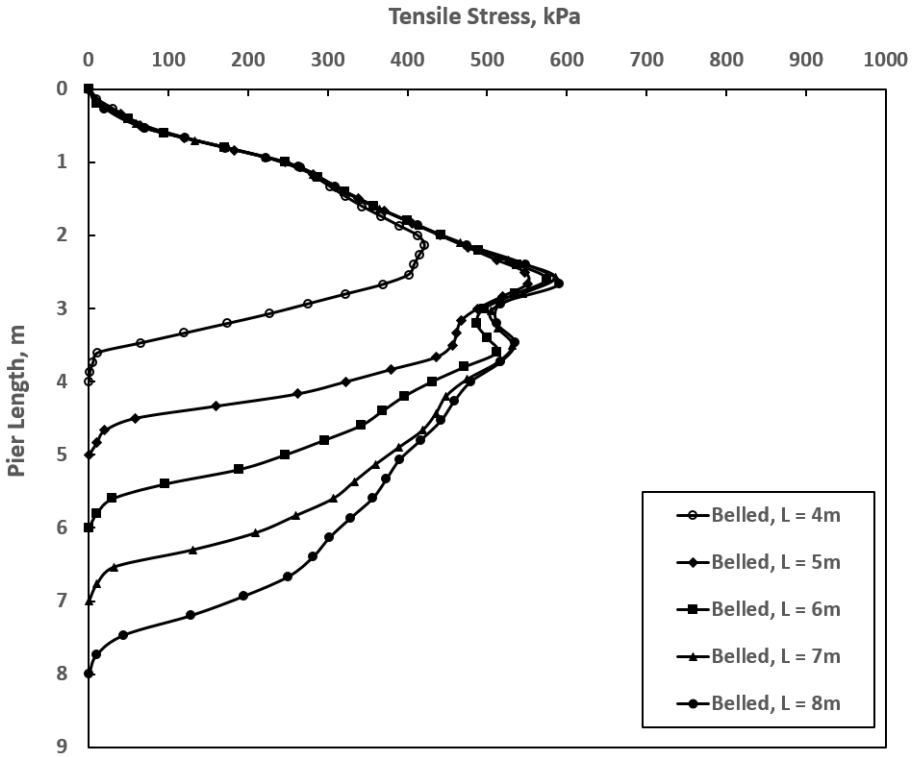

Figure 5.7: Effect of Length on Tensile Stresses developed in Belled Piers for $250kPa$ Swelling Pressure

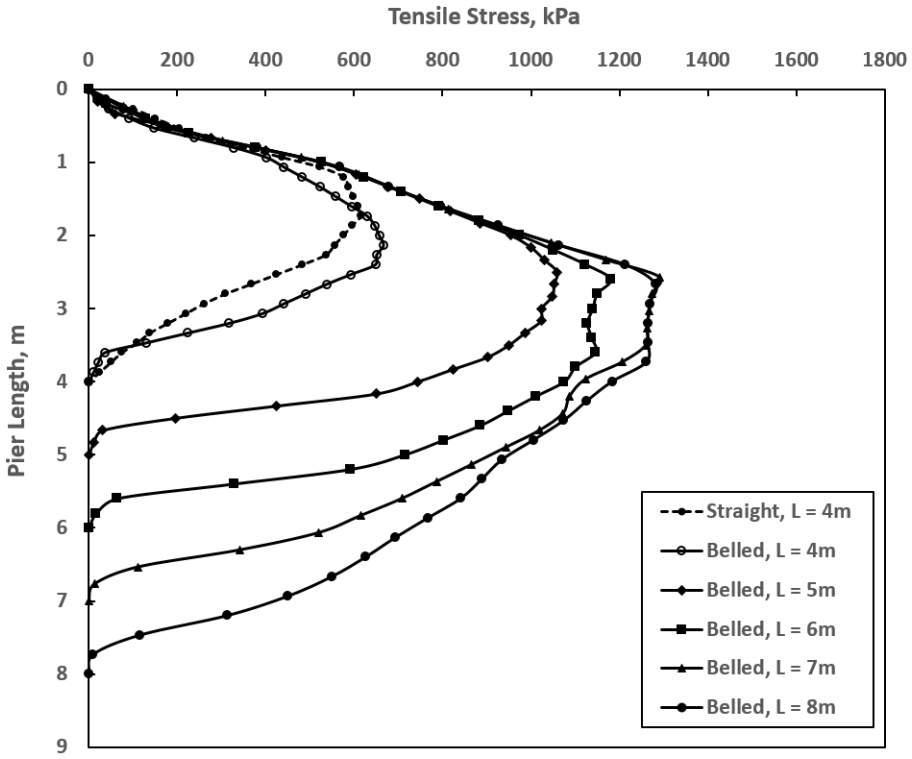

Figure 5.8: Effect of Length on Tensile Stresses developed in Belled Piers for $500kPa$ Swelling Pressure

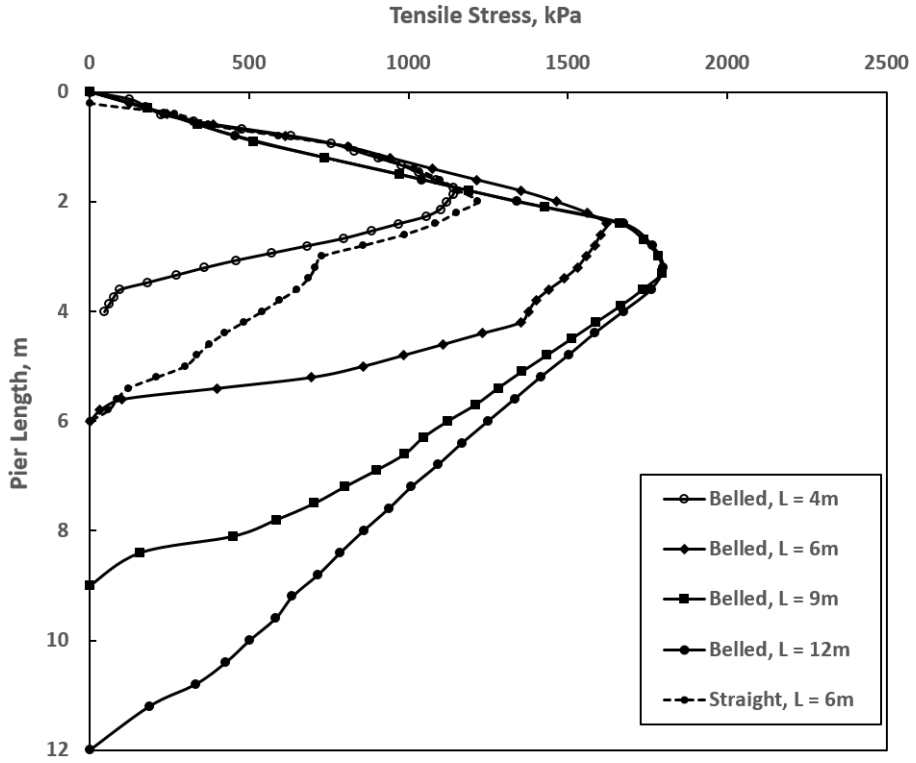

Figure 5.9: Effect of Length on Tensile Stresses developed in Belled Piers for $750kPa$ Swelling Pressure

Considering Figures 5.1 to 5.9, the following observations can be made. When the belled pier length increases, which also means the length of embedment of the belled pier in the non-swelling zone increases, the belled pier heave decreases. This demonstrates the importance of providing adequate anchorage length. However, increasing the belled pier length also increases the tensile stresses developed inside the belled pier. This means more cost to provide tensile reinforcement. This should be noted when designing belled piers and selecting the appropriate lengths for a safe design.

The decrease in belled pier heave mentioned above is observed to be less and less sensitive to the increase in belled pier length. For example, considering $750kPa$ swelling pressure, when length increased from $6m$ to $9m$, which is an increment of $3m$, the heave decreased from $22mm$ to $5mm$, which is a decrement of $17mm$. However, when the length increased from $9m$ to $12m$, which is again an increase of $3m$, the heave decreased from $5mm$ to $2mm$. That's just a decrement of $3mm$. The same observation can be made about the increase in tensile stress and its sensitivity to the increase in length, i.e. sensitivity becomes less and less as length increases.

The location of the maximum tensile stress along the length of the belled piers is another observation that can be made. For the shorter belled piers, this location is around $L/2$, while for the longer belled piers, it's around $L/3$ from the pier top. This means, as the length of the belled pier increases, the location of the maximum tensile force shifts upward from the center.

The value of this maximum tensile stress can also be observed. Again considering $750kPa$ swelling pressure, for $L = 4m$, the maximum tensile stress is $1140kPa$. For $L = 6m$, it is $1622kPa$. For$L = 9m$, it is $1795kPa$. For $L = 12m$, it is $1800kPa$. Considering concrete with cylindrical strength (f_{ck}) of $30MPa$, the tensile strength (f_{ctk}) will be $2027kPa$ (Mosley et al. 2007). This means none of the belled piers considered will need tensile reinforcement; although, reinforcement for shrinkage and temperature may still be necessary.

Based on observations of the above mentioned Figures, relationships between straight shaft piers and belled piers can be established. The pier heave to soil heave relationship is similar, but, for the same length, belled piers exhibit much smaller heave than straight shaft piers. The tensile stress to length relationship (tensile stress distribution) is also similar, but, for the same length, more tensile stresses develops in belled piers than in straight shaft piers.

Belled pier heave decreases as length increases because increasing the length increases the resisting skin friction force on the shaft in the non-swelling zone; see Figure 2.2. The resisting skin friction force on the shaft (F_s) is given by equation 5.1. Therefore, as F_s increases, pier heave decreases, and if F_s is large enough, pier heave will not occur.

$$F_s = f_s \pi d L' \tag{5.1}$$

where:

$f_s =$ resisting interface shear stress (skin friction) on the shaft

$d =$ shaft diameter

$L' =$ shaft length on which resisting interface shear stresses act upon

The interface shear stress distribution on the shaft of the belled piers (f_u and f_s; the negative values are f_u or uplift interface shear stress and the positive values are f_s or resisting interface shear stress) is presented in Figure 5.10 as outputted by Abaqus.

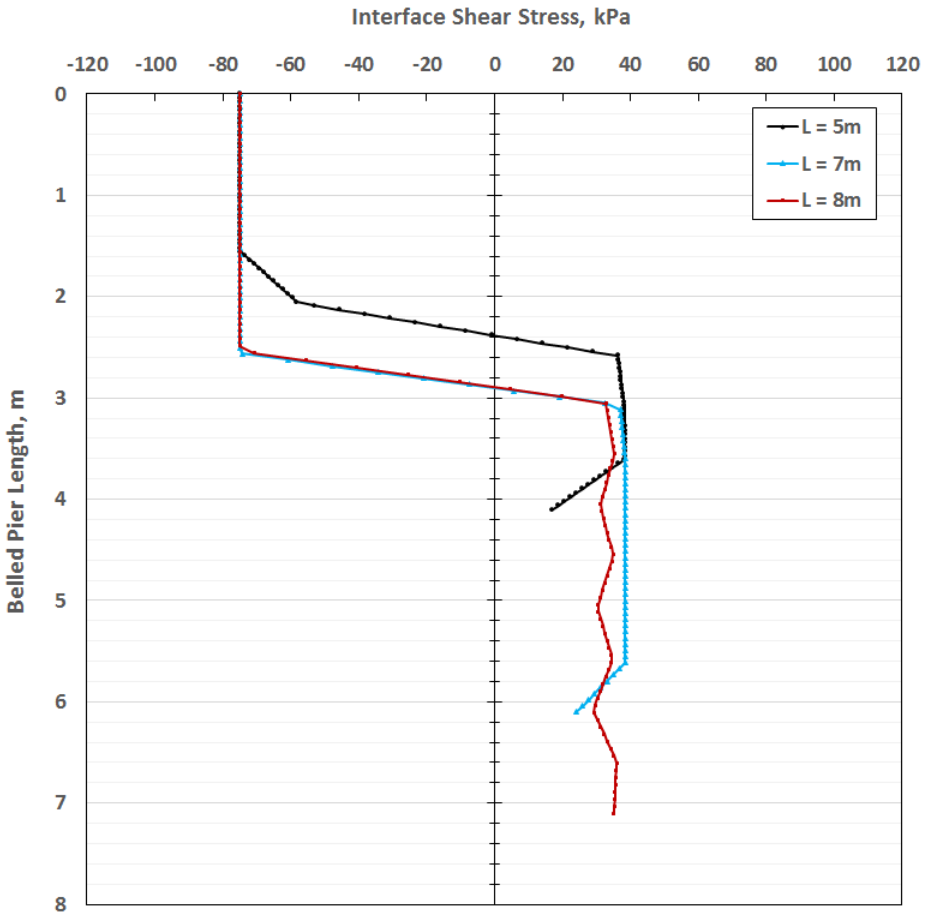

Figure 5.10: Interface Shear Stress Distribution considering variations in Belled Pier Length for $500kPa$ swelling Pressure

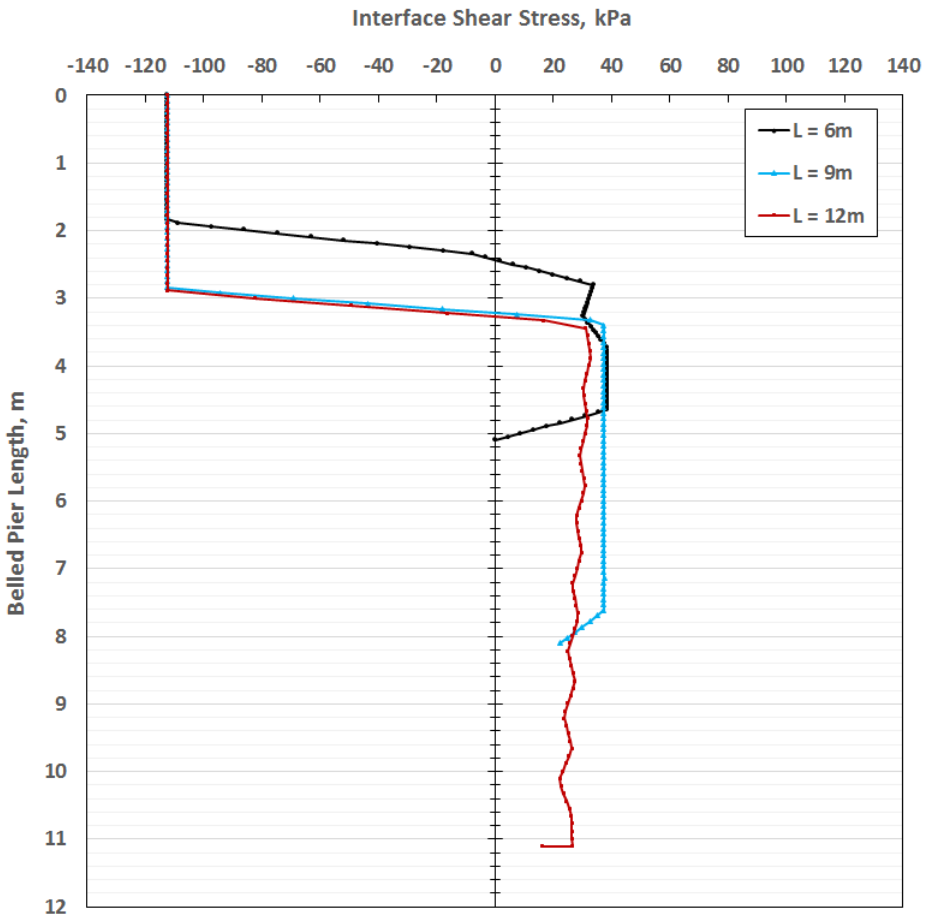

Figure 5.11: Interface Shear Stress Distribution considering variations in Belled Pier Length for $750kPa$ Swelling Pressure

Considering equation 5.1, increasing the total length of the belled pier (L) increases the shaft length in the non-swelling zone (L') which in-turn increases the resisting force (F_s). The resisting force (F_s) resists against the uplift force (the uplift force causes pier heave); see Figure 2.2. The uplift force or the uplift skin friction force (F_u) is given by equation 5.2.

$$F_u = f_u \pi d L'' \tag{5.2}$$

where:

$f_u =$ uplift interface shear stress (skin friction) on the shaft

$d =$ shaft diameter

$L'' =$ shaft length on which uplift interface shear stresses act upon

In addition to F_s, resistance to the uplift force (F_u) is also provided by the weight of the pier (W_p), skin friction resistance force on the bell (F_{sb}) and bearing resistance force on the bell (F_b). W_p, F_{sb} and F_b are given by equations 5.3, 5.4 and 5.5 respectively.

$$W_p = \gamma_c \left(A_s L_s + A_F L_F + A_B L_B \right) \tag{5.3}$$

where:

$\gamma_c =$ unit weight of concrete

$A_s,\ A_F,\ A_B =$ cross sectional areas of the shaft, frustum and base respectively; see Figure 5.12

$L_s,\ L_F,\ L_B =$ lengths of the shaft, frustum and base respectively; see Figure 5.12

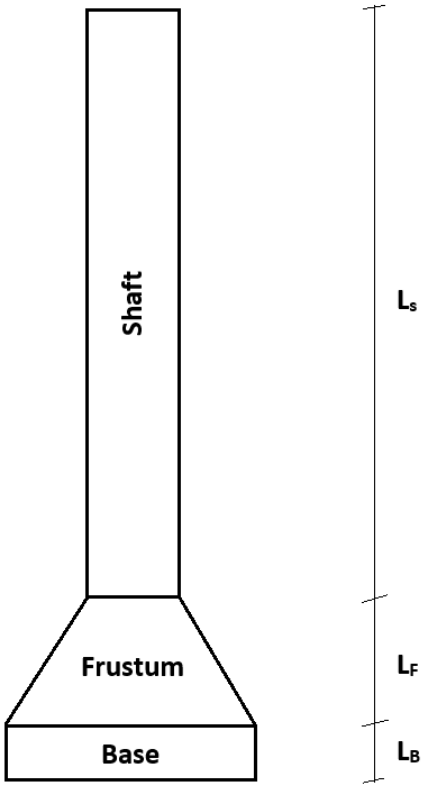

Figure 5.12: Belled Pier Description

When the length of the belled pier (L) is increased, W_p (weight of the pier) also increases because cross sectional area of the shaft (A_s) increases. This is another reason why the belled pier heave decreases when L is increased.

$$F_{sb} = f_{sb} A_{sur} \tag{5.4}$$

where:

$f_{sb} =$ interface shear stress (skin friction) on the bell

$A_{sur} =$ surface area of the bell

$$F_b = f_b \pi \left(\frac{db^2}{4} - \frac{d^2}{4} \right) \tag{5.5}$$

where:

$f_b =$ bearing stress on the bell

The value of the bearing stress on the bell (f_b) depends on the weight of the soil above the bell and the movement (heave) of the belled pier. The biggest advantage of belled piers is that if there is a sudden rise of the GWT, there could be loss of all the frictional resistance forces (F_s and F_{sb}), but resistance to heave can still be provided by the bearing resistance force, F_b, which depends on the weight of the soil, and this weight is not lost due to the rise of the GWT. The same doesn't hold true for straight shaft piers, i.e., if there is a sudden rise of the GWT, there could be a loss of all the resistance forces and the pier would fail.

The decrease in belled pier heave gets less and less sensitive to the increase in belled pier length because **smaller pier movements** at larger values of length (L) do not allow for the full development of the interface shear stress (f_s) as can be observed for the $12m$ length belled pier in Figure 5.10. This will result in lesser and lesser values of f_s and consequently F_s (frictional resistance force) at larger values of L, thus resulting in lesser and lesser decrements in the pier heave.

Tensile stresses develop in the belled piers because the uplift force (F_u) and the resisting forces (F_s, W_p, F_{sb} and F_b) act in opposite directions (see Figure 2.2) causing tensile stresses to develop in the belled piers. The tensile stresses developed will have a maximum value at interface of the uplift force (F_u) and resisting force (F_s) and eventually decrease to a value of zero at the top and tips of the belled pier where 'tensioning' of the pier ceases; see Figure 5.44. The maximum tensile stress usually occurs near the bottom of the swelling zone at the interface of the uplift force (F_u) and the resisting force (F_s). The maximum tensile stress can also occur within the swelling zone as observed for the $4m$ belled pier in Figure 5.9. This is due to the relatively high movement (heave) of the $4m$ belled pier and the soil heave profile (see Section 5.2.5) which allows for resisting interface shear stresses to develop in the swelling zone as seen in Figure 5.10.

Tensile stresses developed in the belled piers increase as length (L) increases because increasing the length increases the resisting force F_s(as mentioned previously). When F_s increases, the belled pier will be under more 'tensioning' resulting in more tensile stresses to develop. But this increment of the tensile stresses developed in the belled piers becomes less and less at higher values of length (L) as the value of F_s becomes less and less as mentioned previously.

5.2.2 Effect of shaft diameter on Belled Pier Behaviour

Another parameter that can affect the behavior of belled piers embedded in expansive soils is the shaft diameter. This investigation of the effect of shaft diameter is discussed in this Section. Different shaft diameters are considered and the consequent effects are investigated by considering pier head heave and tensile stresses developed along the lengths of the piers. For the investigation, belled piers of bell to shaft ratio (db/d) of 2 and length (L) of $5m$ for $250kPa$ and $500kPa$ swelling pressures and $6m$ for $750kPa$ swelling pressure are considered. Results of the investigation are presented in Figures 5.13 to 5.20.

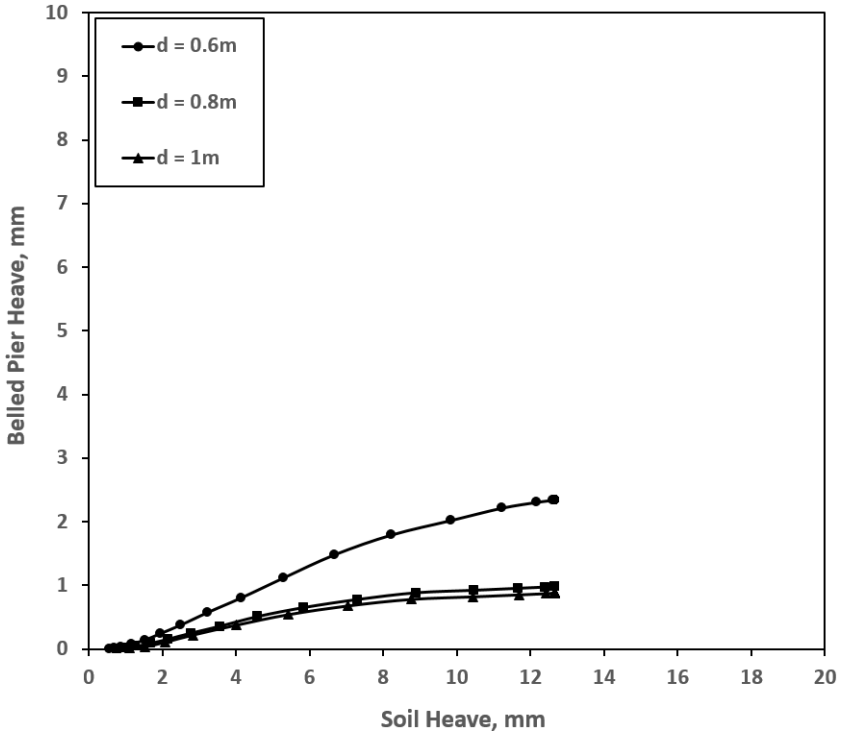

Figure 5.13: Effect of Shaft Diameter on Belled Pier Heave for $250kPa$ Swelling Pressure

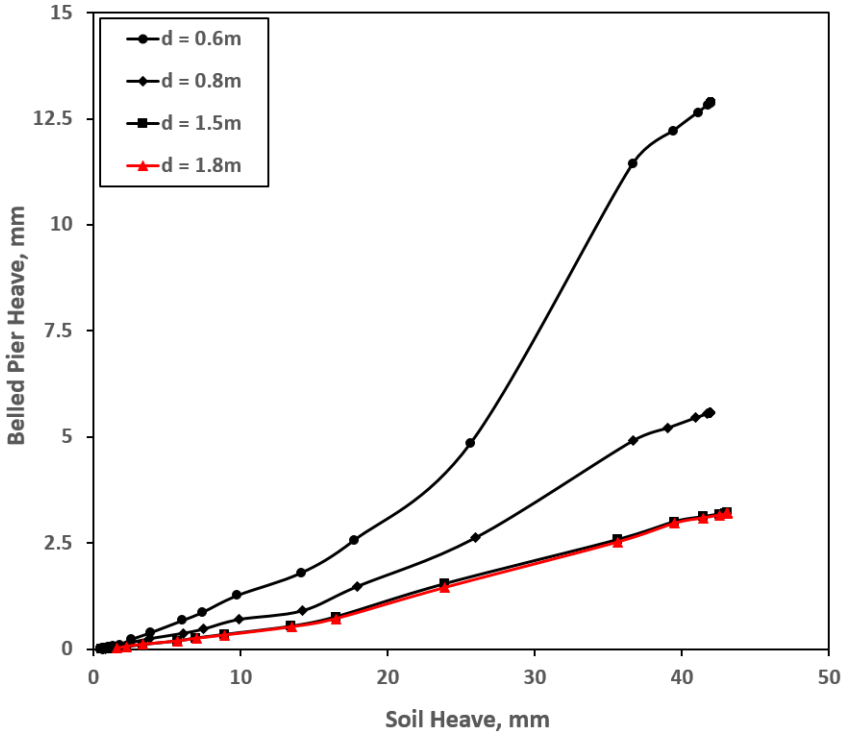

Figure 5.14: Effect of Shaft Diameter on Belled Pier Heave for $500kPa$ Swelling Pressure

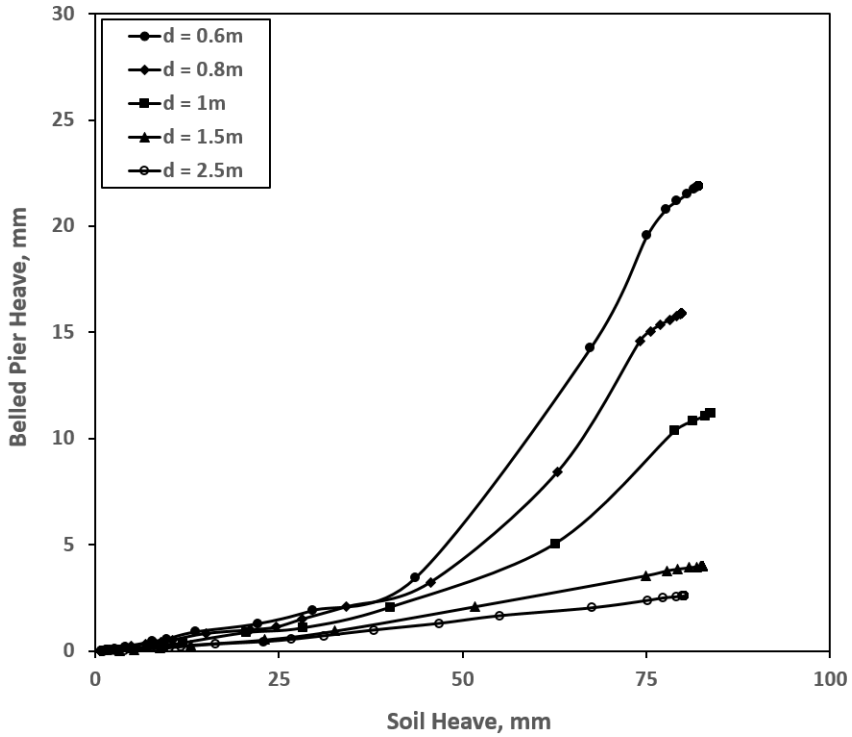

Figure 5.15: Effect of Shaft Diameter on Belled Pier Heave for $750kPa$ Swelling Pressure

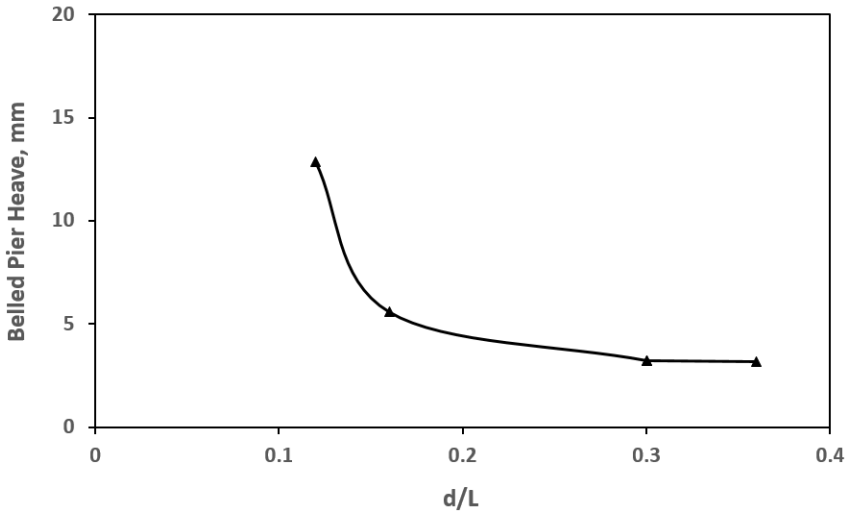

Figure 5.16: Limiting Diameter for $500kPa$ Swelling Pressure

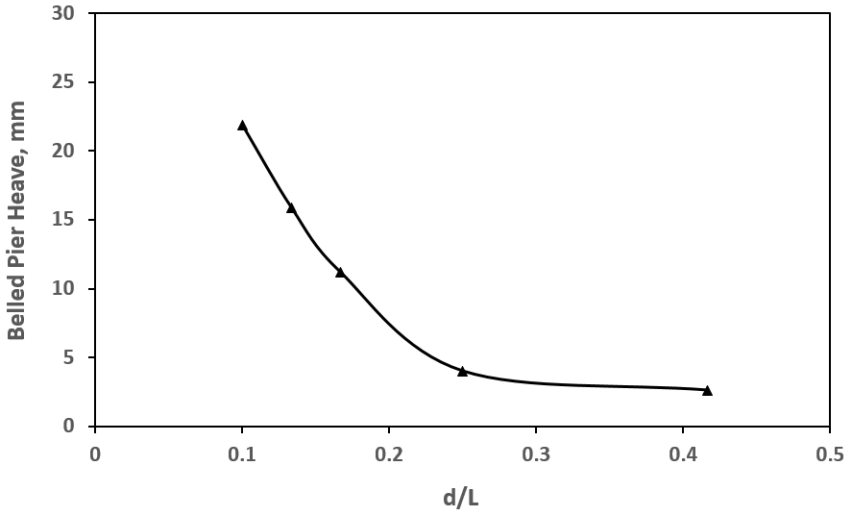

Figure 5.17: Limiting Diameter for $750kPa$ Swelling Pressure

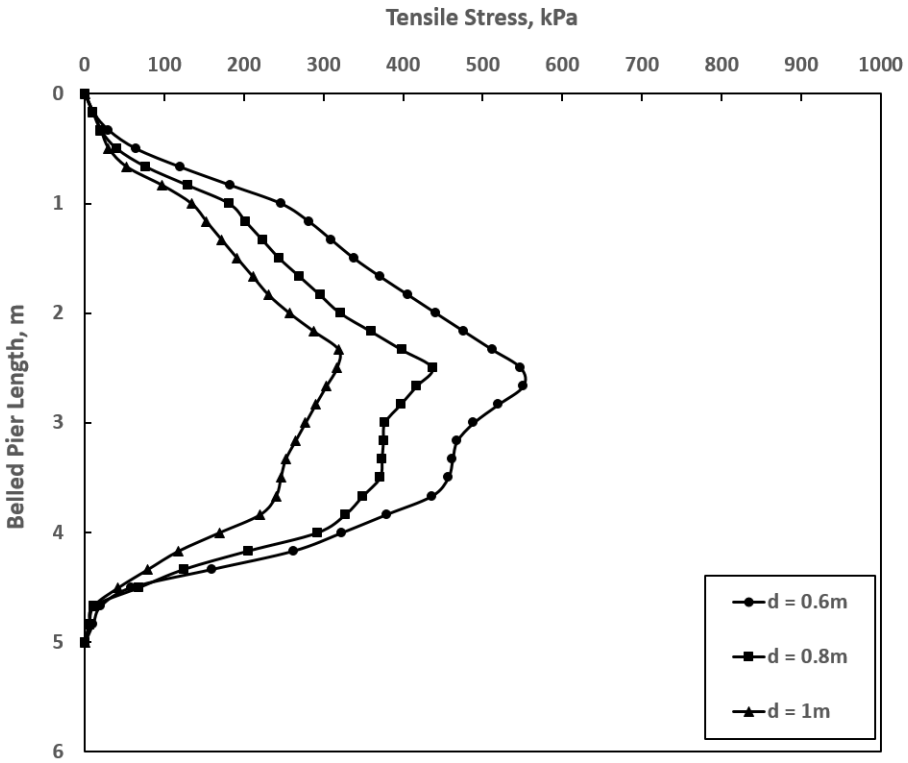

Figure 5.18: Effect of Shaft Diameter on Tensile Stresses developed in Belled Piers for $200kPa$ Swelling Pressure

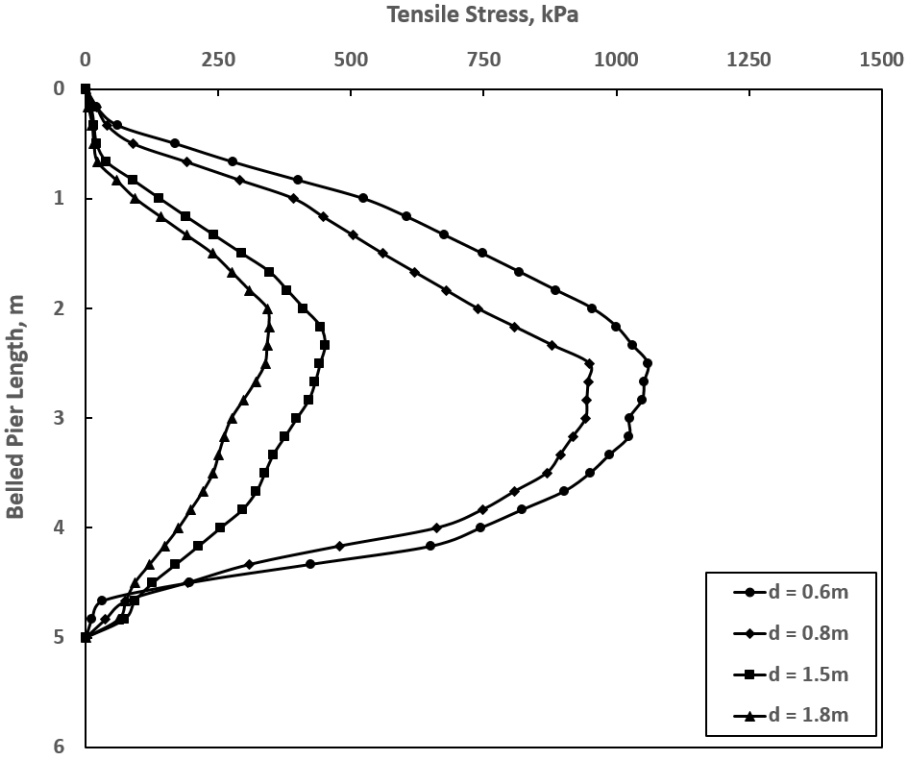

Figure 5.19: Effect of Shaft Diameter on Tensile Stresses developed in Belled Piers for $500kPa$ Swelling Pressure

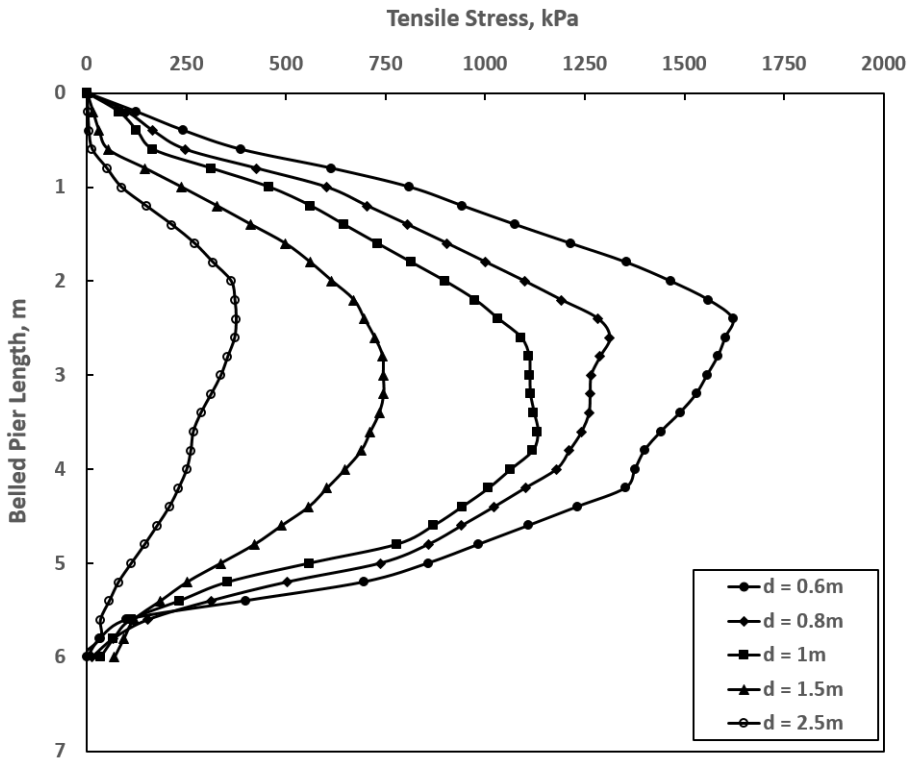

Figure 5.20: Effect of Shaft Diameter on Tensile Stresses developed in Belled Piers for $750kPa$ Swelling Pressure

Considering Figures 5.13 to 5.20, it is observed that as the shaft diameter increases both the belled pier heave and the tensile stresses developed inside the belled piers decrease. This is different from the effect of length observed in Section 5.2.1, where increasing length decreased pier heave but increased tensile stresses developed. **Therefore, it may be better to increase the shaft diameter rather than the length to obtain safe designs when designing belled piers in expansive soils.**

The decreases in heave and tensile stresses mentioned above get less and less sensitive to the increase in shaft diameter. The same observation was made for the effect of length. For example, considering $750kPa$ swelling pressure, as the shaft diameter increased from $0.6m$ to $1.5m$ (an increase of $0.9m$), the pier heave decreased by about $18mm$ and the maximum tensile stress decreased by about $877KPa$, while, as the shaft diameter increased from $1.5m$ to $2.5m$ (an increase of $1m$), the pier heave decreased by just about $1.4mm$ and the maximum tensile stress decreased by just about $370KPa$.

This sensitivity concept was investigated for straight shaft piers by Xiao et al. (2011) and Nelson and Miller (1992). Both concluded that there is a limiting value of the diameter after which its increase will have no effect on pier heave reduction. For Xiao et al. (2011) this value was found to be $d/L = 0.04$. For Nelson and Miller (1992) this value was found to be $d/L = 0.03$. An attempt was made to investigate if there is such a limiting value for belled piers. The results are presented in Figures 5.16 and 5.17. It can be observed from

Figures 5.16 and 5.17 that the limiting diameter for belled piers is $d/L = 0.3$ which is much higher value than the ones observed for straight shaft piers. **This means increasing the shaft diameter to obtain safe designs is more effective in belled piers than in straight shaft piers.**

Considering Figures 5.18 to 5.20, the following additional observations were made. The maximum tensile stress tends to be distributed over a wider length on the belled piers as the shaft diameter increases. This will avoid stress concentrations. The value of this maximum tensile stress for $750kPa$ swelling pressure is as follows. For $d = 0.6m$, it is $1622kPa$. For $d = 0.8m$, it is $1312kPa$. For $d = 1m$, it is $1131kPa$. For $d = 1.5m$, it is $746kPa$. For $d = 2.5m$, it is $374kPa$. Again, considering concrete with tensile strength (f_{ctk}) of $2027kPa$ (Mosley et al. 2007), it can be observed that none of the belled piers considered need tensile reinforcement, however, reinforcement for shrinkage and temperature may need to be provided.

Belled pier heave decreases as shaft diameter (d) increases because increasing the shaft diameter increases the resisting force W_p (weight of the belled pier). Considering equation 5.3, as d increases, all A_s, A_F and A_B (cross sectional areas of the shaft, frustum and base respectively) increase, thus, W_p will also increase. A_F and A_B increase because the frustum and the base have to be proportioned relative to the shaft (Chen 1988). Further more, increasing d also increases the resisting forces F_{sb} and F_b. Considering equations 5.4 and 5.5, as d increases, A_{sur} (surface area of the bell) and $\pi\left(\frac{db^2}{4} - \frac{d^2}{4}\right)$ increase, resulting in increments in F_{sb} and F_b respectively. Increasing d also increases the resisting force F_s; but this increment is canceled out by the equal amount of increment in the uplift force F_u; see equations 5.1 and 5.2. Thus, increase in F_s is not the reason why belled pier heave decreases as d increases.

The decrease in belled pier heave gets less and less sensitive to the increase in shaft diameter (d) because **smaller pier movements** at larger values of d do not allow for the full development of the interface shear stress (f_s) as can be observed for the $1.5m$ diameter belled pier in Figure 5.22. This will result in lesser and lesser values of f_s and consequently F_s at larger values of d, thus resulting in lesser and lesser decrements in the pier heave.

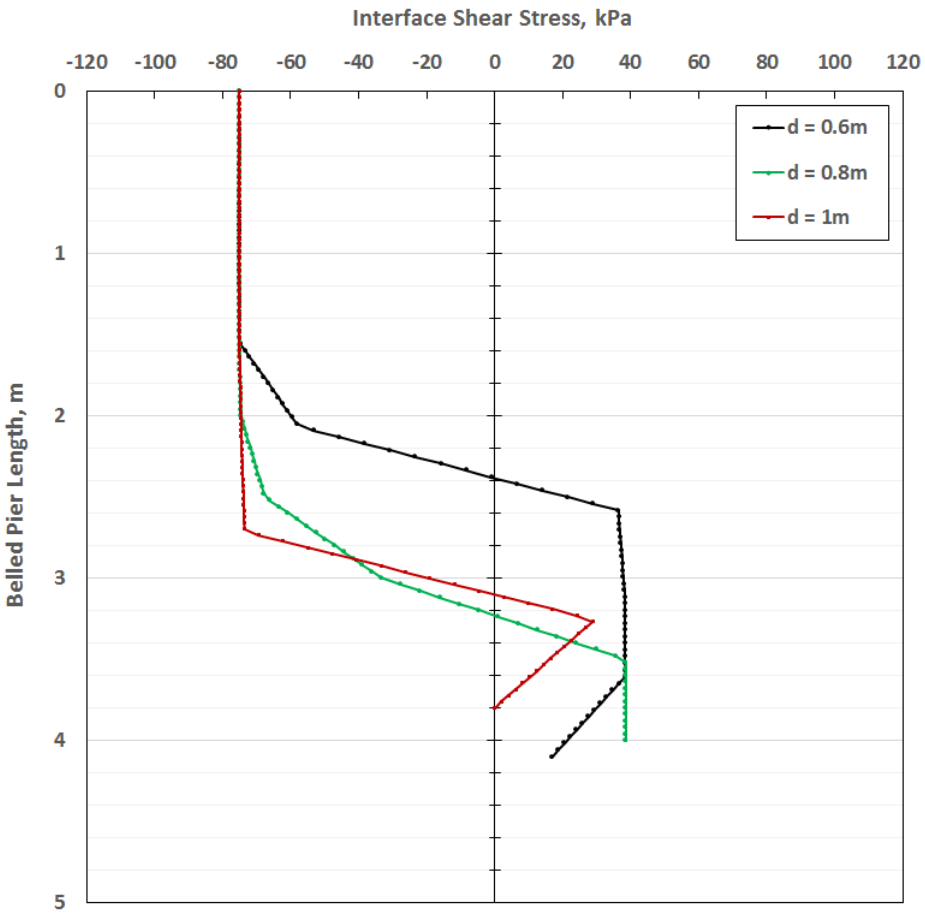

Figure 5.21: Interface Shear Stress distribution considering variations in Shaft Diameter for $500kPa$ Swelling Pressure

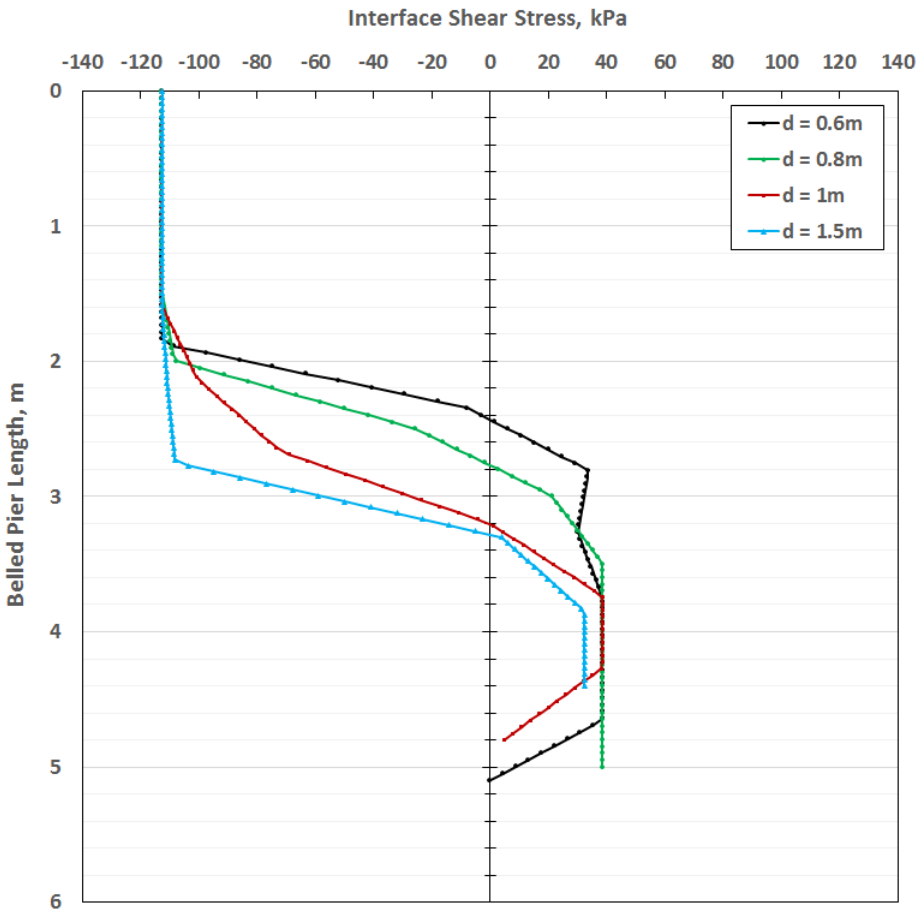

Figure 5.22: Interface Shear Stress distribution considering variations in Shaft Diameter for $750kPa$ Swelling Pressure

Tensile stresses developed in the belled piers **decrease** as the shaft diameter (d) increases because increasing d increases the 'tensioning' resistance of the belled pier. This is because as d increases, the cross-section of the belled pier increases and the uplift and resisting forces will be acting over a larger cross-sectional area resulting in decrements of the tensile stresses developed ($Stress = Force/Area$). This phenomena also helps avoid stress concentrations.

The decrement of the tensile stresses developed in the belled piers becomes less and less at higher values of d (shaft diameter) because the value of F_s (resisting frictional force) becomes less and less as mentioned previously.

5.2.3 Effect of Bell Size on Belled Pier Behaviour

The bell size can affect the behavior of belled piers embedded in expansive soils. This is investigated by considering different bell sizes and observing the effect on the pier heave and the tensile stress distribution. The results of this investigation are presented in Figures 5.23 to 5.28. For the investigation, belled piers of shaft diameter (d) of $0.6m$ and length (L) of $4.5m$ for $250kPa$ and $500kPa$ swelling pressures and $5.5m$ for $750kPa$ swelling pressure are

considered. The bell size is expressed in terms of the ratio of the bell diameter to shaft diameter (d_b/d or db/d).

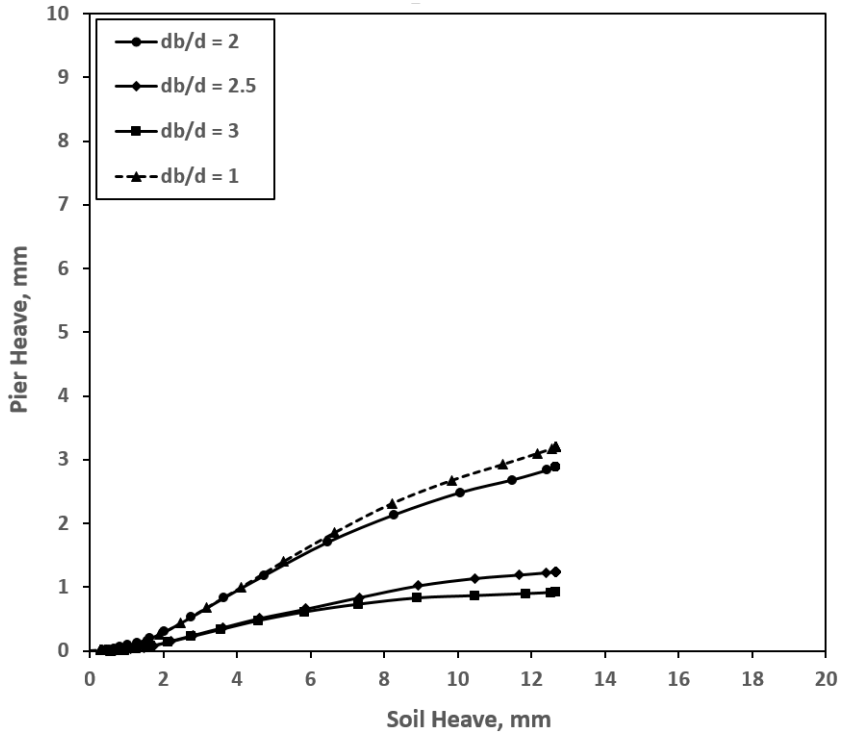

Figure 5.23: Effect of Bell Size on Belled Pier Heave for $250kPa$ Swelling Pressure

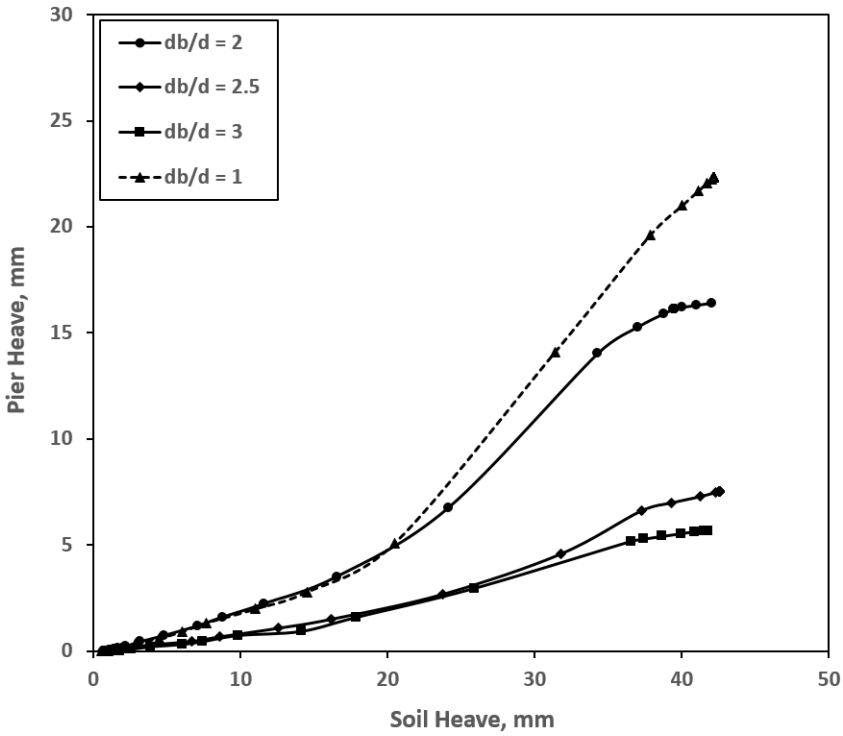

Figure 5.24: Effect of Bell Size on Belled Pier Heave for $500kPa$ Swelling Pressure

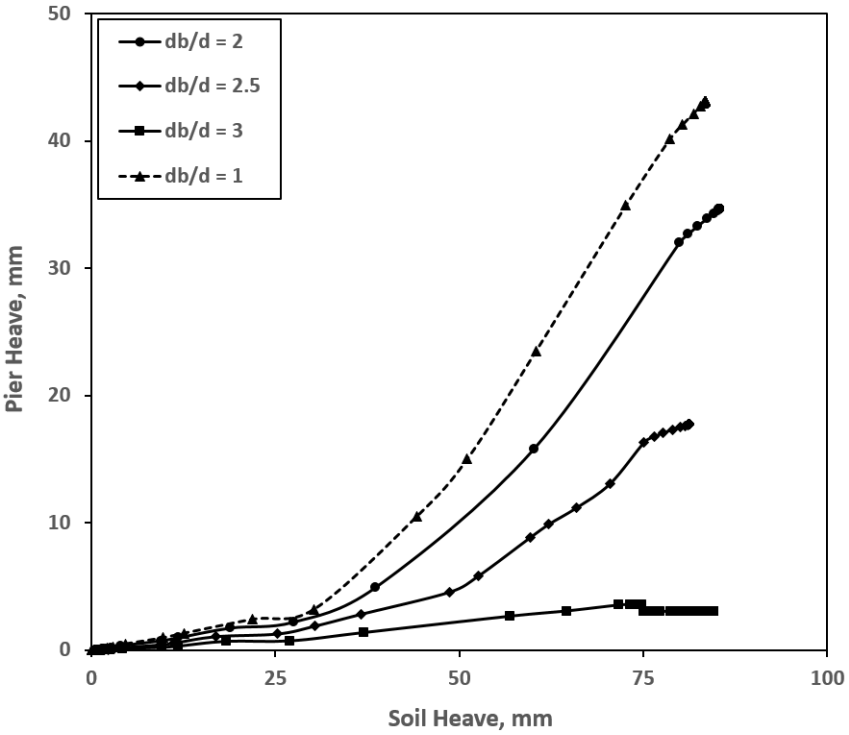

Figure 5.25: Effect of Bell Size on Belled Pier Heave for $750kPa$ Swelling Pressure

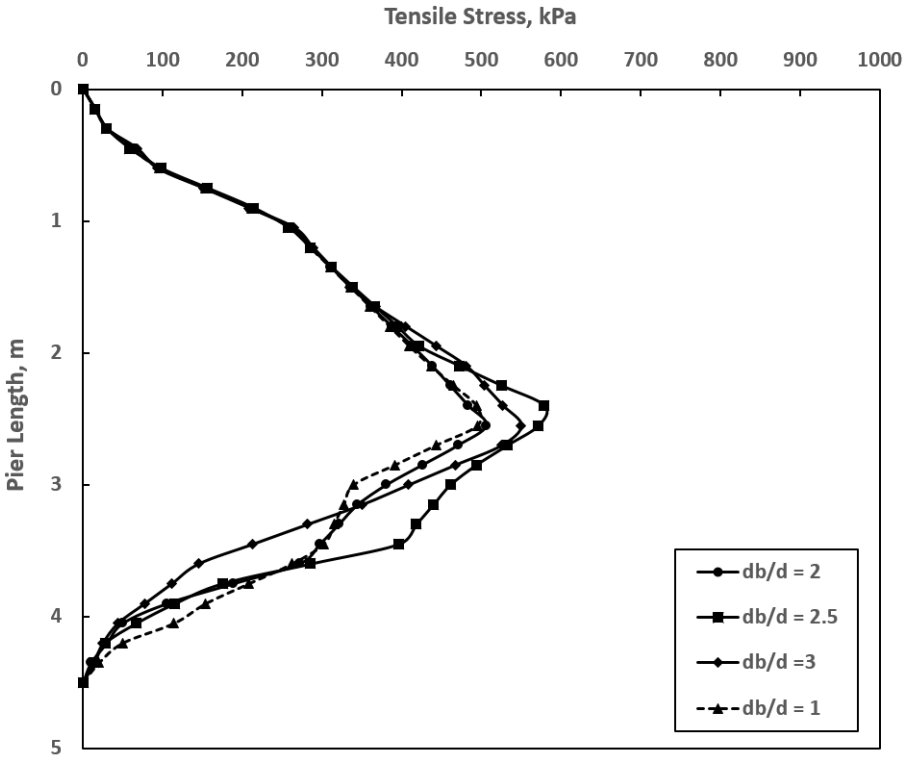

Figure 5.26: Effect of Bell Size on Tensile Stresses developed in Belled Piers for $250kPa$ Swelling Pressure

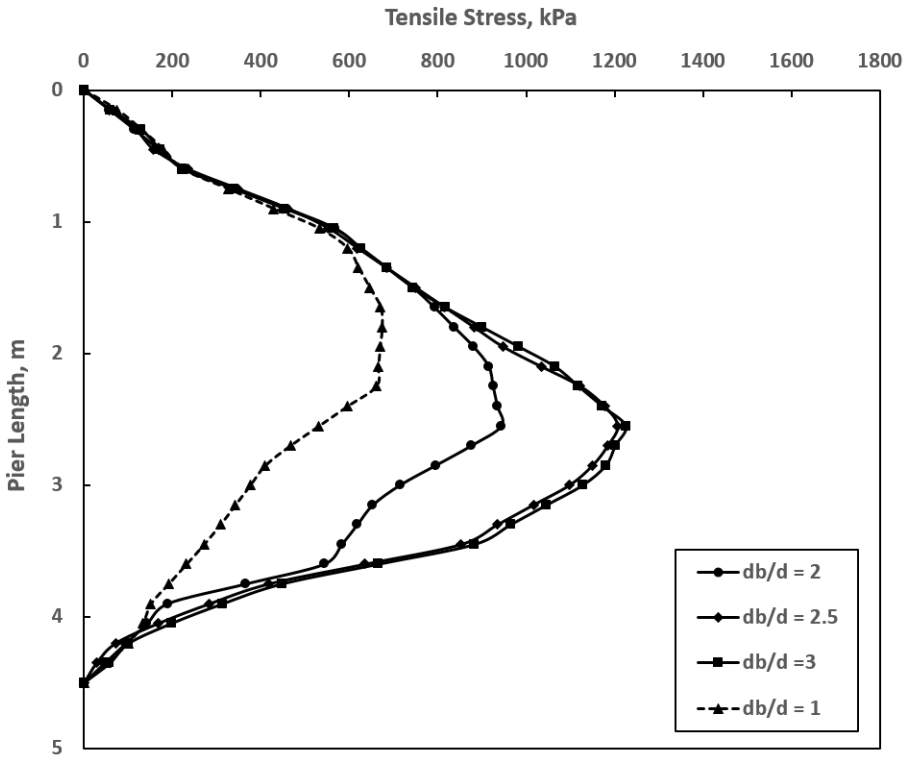

Figure 5.27: Effect of Bell Size on Tensile Stresses developed in Belled Piers for $500kPa$ Swelling Pressure

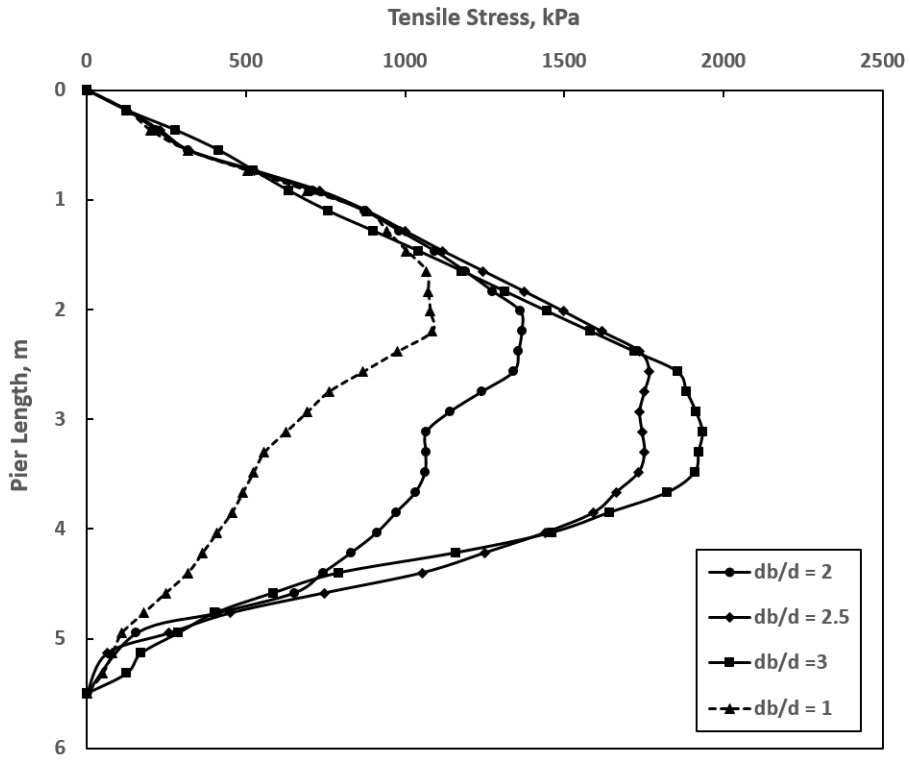

Figure 5.28: Effect of Bell Size on Tensile Stresses developed in Belled Piers for $750kPa$ Swelling Pressure

Considering Figures 5.23 to 5.28, as the bell size increases, it can be observed that the pier heave decreases but the tensile stress developed in the piers increases. The same was observed for the effects of length. However, considering $750kPa$ swelling pressure, when the bell size increased from db/d of 2 to db/d of 3, pier heave decreased by $32mm$. The volume of concrete needed to increase the bell size by this amount is $1.376m^3$. To bring about the same reduction in heave, the length needed to increase from $5.3m$ to $10m$. The volume of concrete needed to increase the length by this amount is $1.33m^3$. For both cases, the tensile stress increased by about $570KPa$. Therefore, it can be concluded that, in-order to obtain safe designs, **increasing bell size and increasing length has about the same effect**. Note that volumes are calculated as per Chen's (1988) recommendations.

Due to limitations to bell sizes (Chen 1988), it's difficult to conduct sensitivity investigations for the effect of bell sizes as was done for the effects of lengths and diameters. But some additional observations can be made. As the bell size increases, the maximum tensile stress tends to be distributed over a wider length on the belled piers. This will avoid stress concentrations. The location of the maximum tensile stress seems to shift downward as the bell size increases.

Belled pier heave decreases as bell size (db/d) increases because increasing the bell size increases the resisting forces F_{sb} and F_b. Considering equation 5.4 and 5.5, increasing the bell size (db/d) increases A_{sur} (surface area of the bell) and $\pi\left(\frac{db^2}{4} - \frac{d^2}{4}\right)$ and thus also increasing F_{sb} and F_b respectively. The same phenomenon is responsible for the increment of tensile stresses developed in belled piers as the bell size increases; i.e. as F_{sb} and F_b increase, the belled pier will be under more and more 'tensioning' resulting in increments of the tensile stresses developed.

Again, considering equations 5.4 and 5.5, the interface shear stress distribution on the bell (f_{sb}) and the bearing stress distribution on the bell (f_b) are given for different bell sizes in Figures 5.29 to 5.32 as outputted by Abaqus.

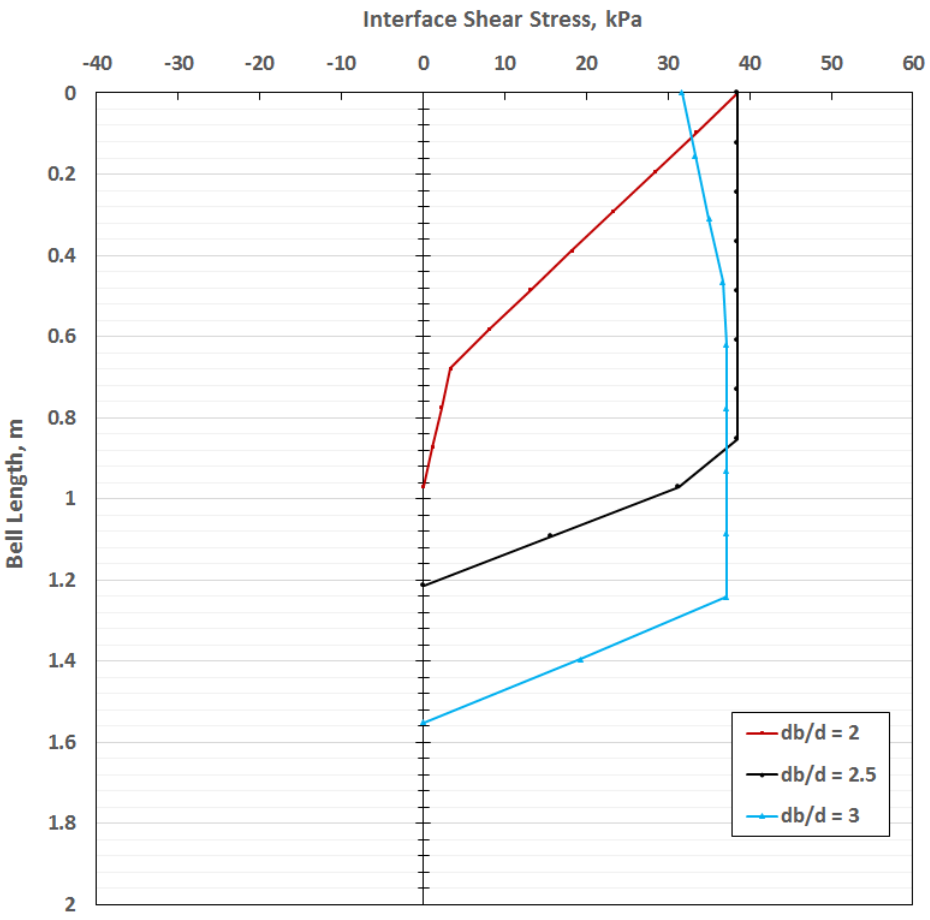

Figure 5.29: Interface Shear Stress distribution on the Bell (Frustum and Base) for $500kPa$ Swelling Pressure

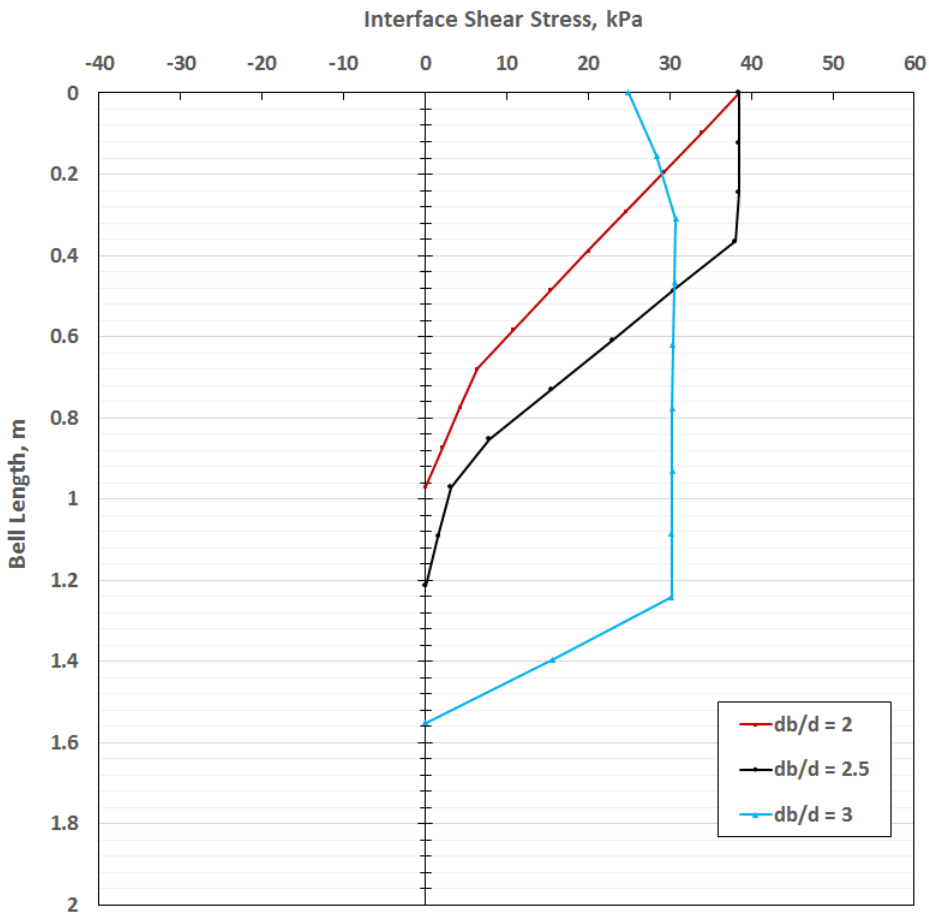

Figure 5.30: Interface Shear Stress distribution on the Bell (Frustum and Base) for $750kPa$ Swelling Pressure

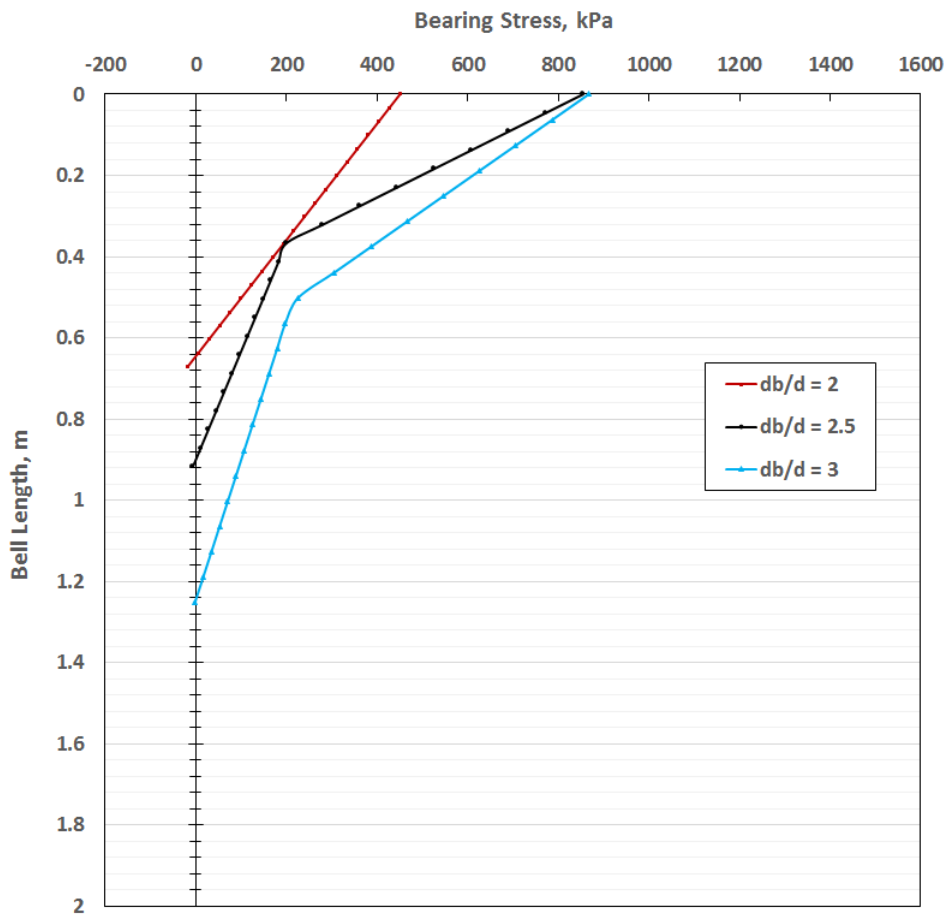

Figure 5.31: Bearing Stress Distribution on the Bell (Frustum only) for $500kPa$ Swelling Pressure

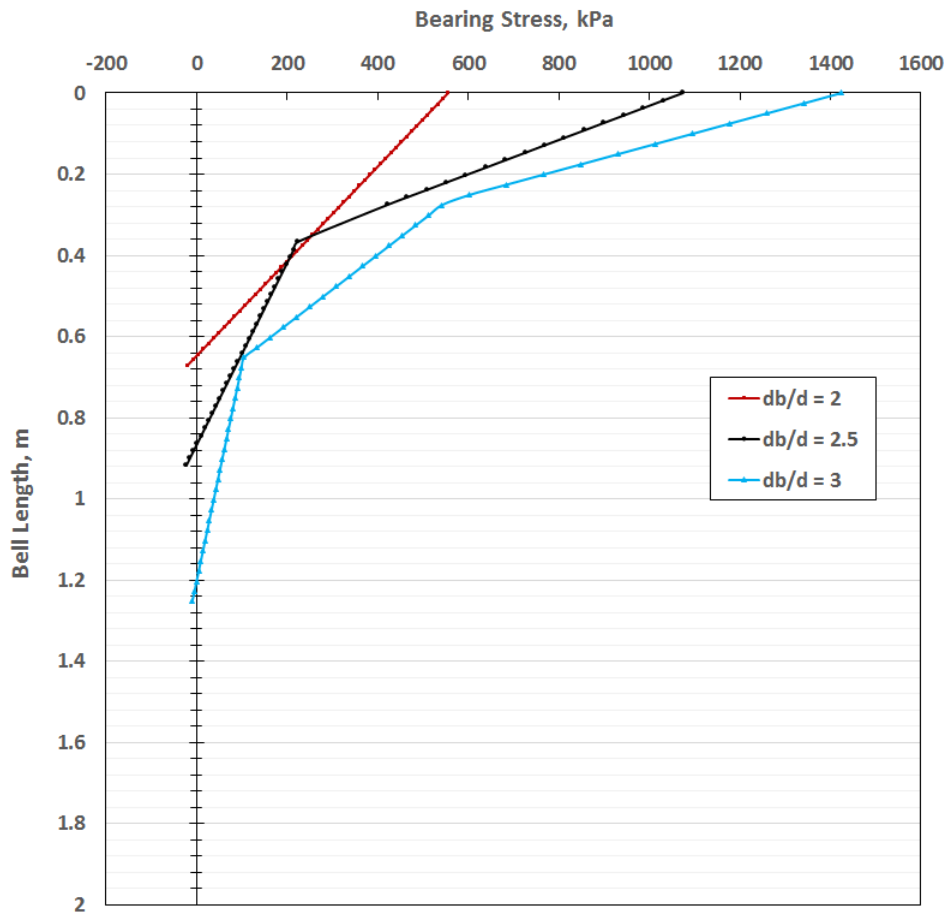

Figure 5.32: Bearing Stress Distribution on the Bell (Frustum only) for $750kPa$ Swelling Pressure

5.2.4 Effect of Bell Friction on Belled Pier Behavior

The rigid pier method is a common method of determining uplift capacity of belled piers embedded in expansive soils. In this method, the bell resistance (capacity) is mostly determined by the equation proposed by O'Neill (1988). In this equation, the bell is assumed to have only bearing resistance. The frictional resistance (F_{sb}) is neglected. But, as the sides of the bell are inclined at a very high slope ($\geq 60degrees$) (Chen 1988), frictional resistance will develop on these surfaces. In this Section, the effect of considering or neglecting this frictional resistance is investigated. This is investigated by considering the subsequent effect on pier heave and tensile stresses developed in the belled piers. The results of this investigation are presented in Figures 5.33 to 5.38. Belled piers of length (L) of $6m$, shaft diameter (d) of $0.6m$ and bell to shaft ratios (db/d) of 2 and 3 are considered in the investigation. For the investigation, belled piers of shaft diameter (d) of $0.6m$ and length (L) of $4.5m$ for $250kPa$ and $500kPa$ swelling pressures and $5.5m$ for $750kPa$ swelling pressure are considered.

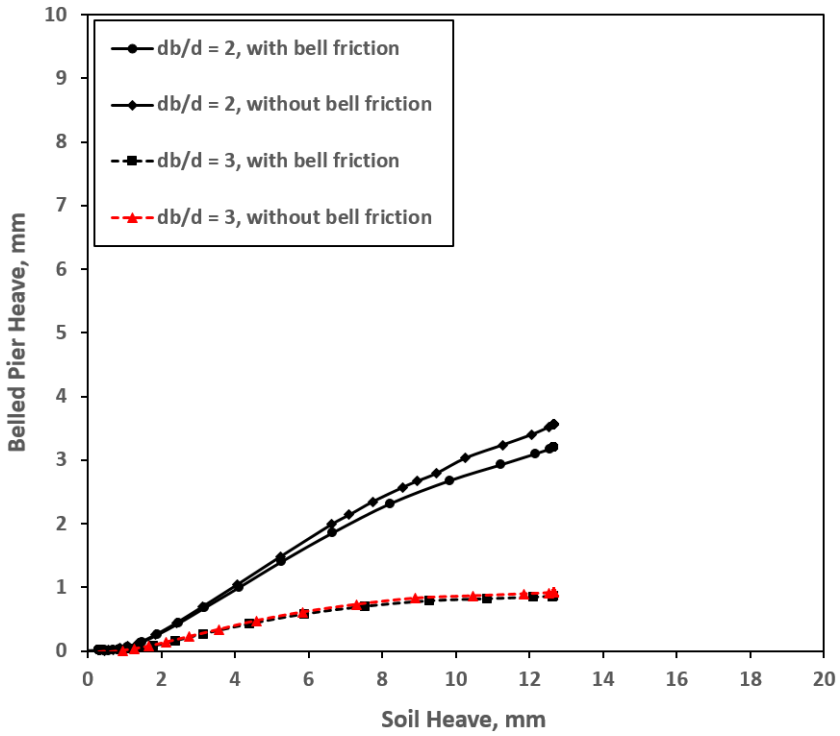

Figure 5.33: Effect of Bell Friction on Belled Pier Heave for $250kPa$ Swelling Pressure

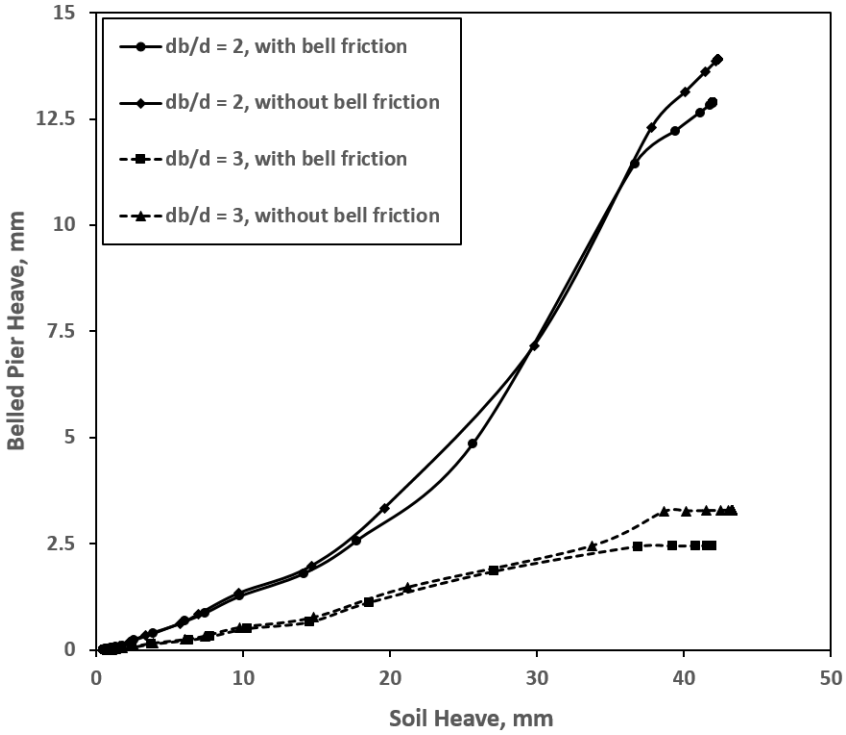

Figure 5.34: Effect of Bell Friction on Belled Pier Heave for $500kPa$ Swelling Pressure

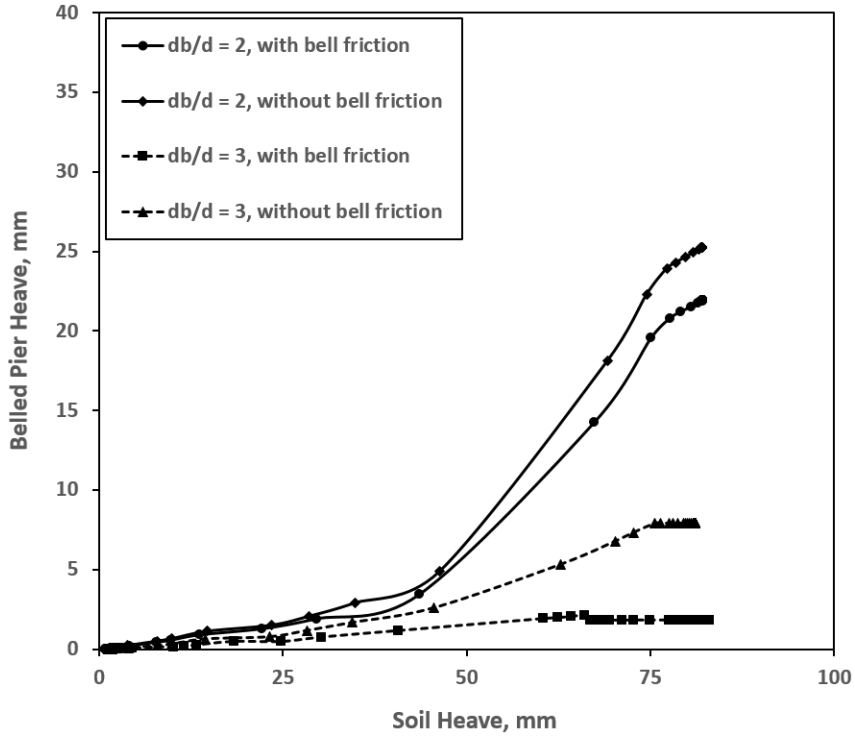

Figure 5.35: Effect of Bell Friction on Belled Pier Heave for $750kPa$ Swelling Pressure

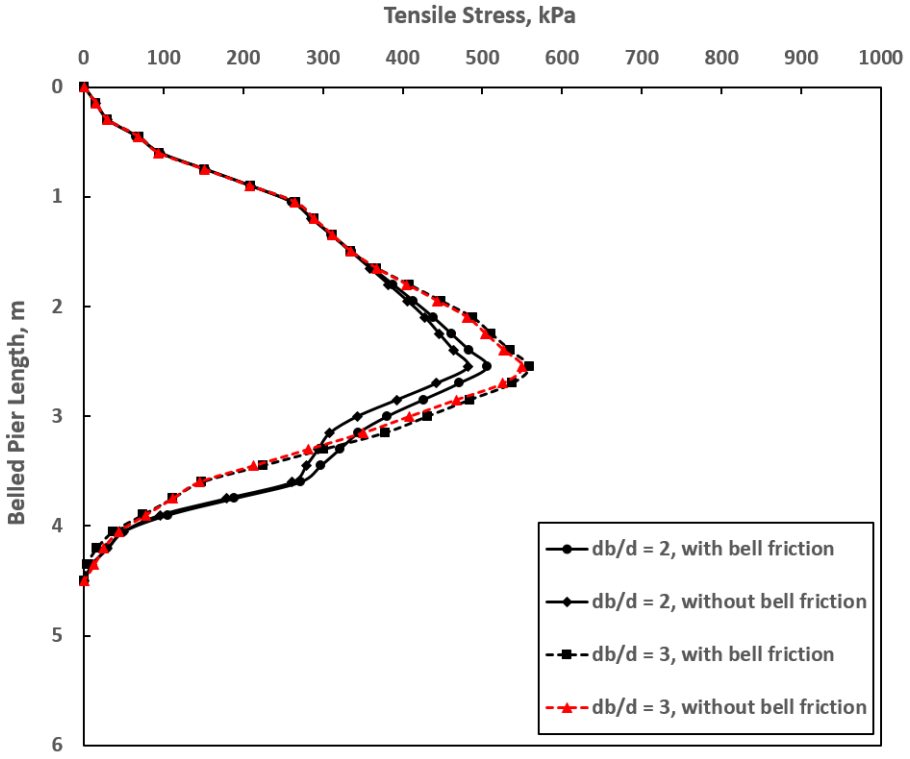

Figure 5.36: Effect of Bell Friction on Tensile Stresses developed in Belled Piers for $250kPa$ Swelling Pressure

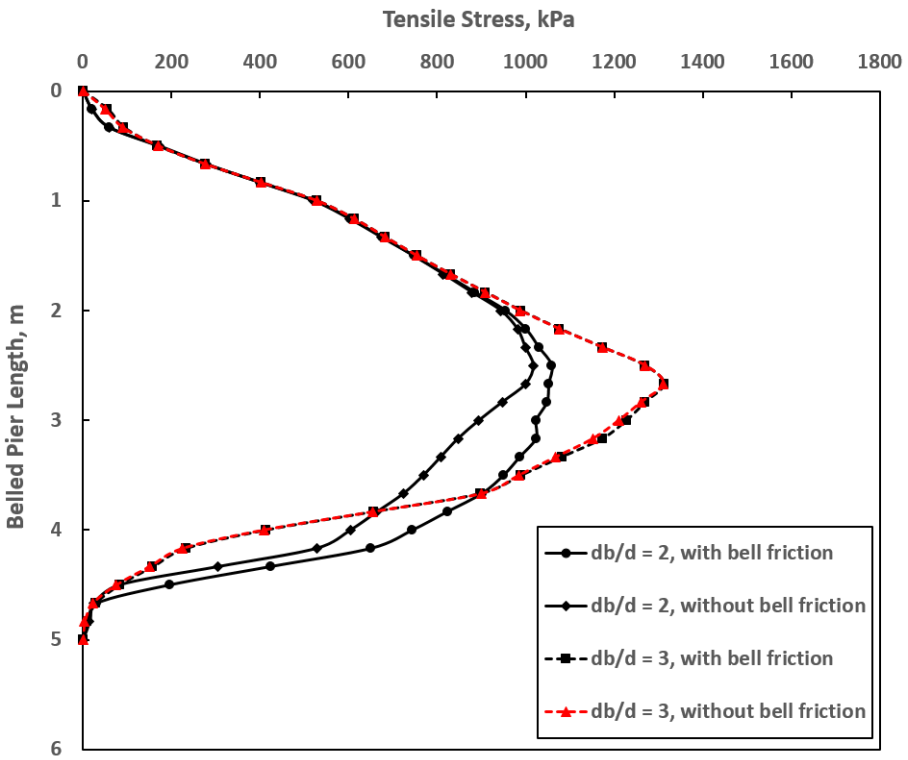

Figure 5.37: Effect of Bell Friction on Tensile Stresses developed in Belled Piers for $500kPa$ Swelling Pressure

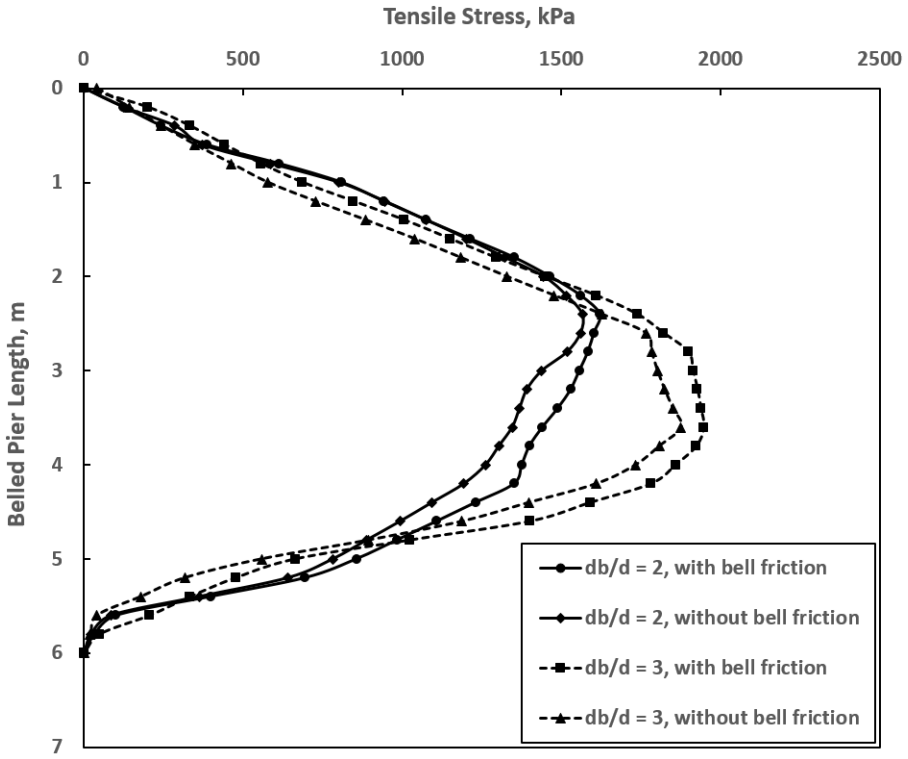

Figure 5.38: Effect of Bell Friction on Tensile Stresses developed in Belled Piers for $750kPa$ Swelling Pressure

As can be observed from Figures 5.33 to 5.38, neglecting the bell friction (F_{sb}) increases the belled pier heave (this will result in a conservative design), and decreases the tensile stresses developed in the belled pier (this will result in an unsafe design). Therefore, it is recommended caution be used when using O'Neill's (1988) equation or any other equation that does not consider the bell friction.

Belled pier heave increases when F_{sb} (bell friction) is neglected because F_{sb} is a resisting force as mentioned previously. Neglecting F_{sb} also puts the belled pier under less 'tensioning", and thus, the tensile stresses developed will also be less. Considering equation 5.4, large bell sizes have larger A_{sur} (surface area of the bell) than small bell sizes; therefore, neglecting or considering the bell friction (F_{sb}) is more significant in large bell size belled piers than in small bell size belled piers.

5.2.5 Effect of Depth of Swelling Zone on Belled Pier Behavior

It is customary to underestimate the depth of the swelling zone. This has been mentioned by several authors including, Nelson et al. (2012), Kaufmann et al. (2010), Nelson and Miller (1992). Underestimation of the swelling zone depth (Z_a or Za) in such a way can have consequences on belled pier behavior. This is investigated by considering the consequences on belled pier heave, tensile stresses developed in the belled piers and interface shear stresses developed between the shaft of the belled piers and the swelling zone. The results of this investigation are presented in Figures 5.39 to 5.46. For the investigation, for $250kPa$ and $500kPa$ swelling pressures, belled piers of length (L) of $8m$, shaft diameter (d) of $0.6m$ and bell to shaft ratio (db/d) of 2; for $750kPa$ swelling pressure, belled piers of length (L) of $12m$, shaft diameter (d) of $0.8m$ and bell to shaft ratio (db/d) of 2.5 are considered. Depths of the swelling zone up to $7m$ are considered. Large values of the depth of the swelling zone could appear when we have breakage of utility pipes and leakage from septic tanks.

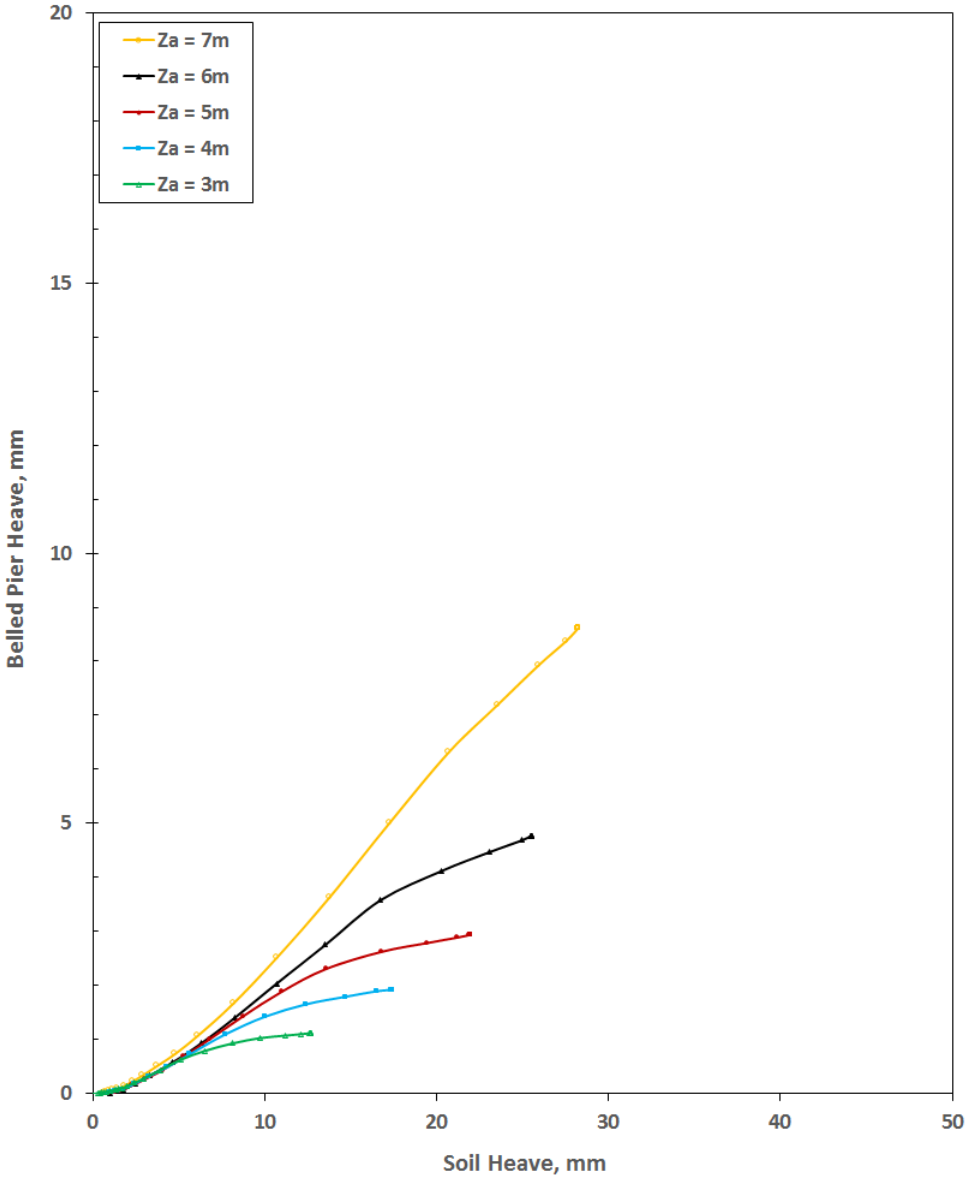

Figure 5.39: Effect of Depth of Swelling Zone on Belled Pier Heave for $250kPa$ Swelling Pressure

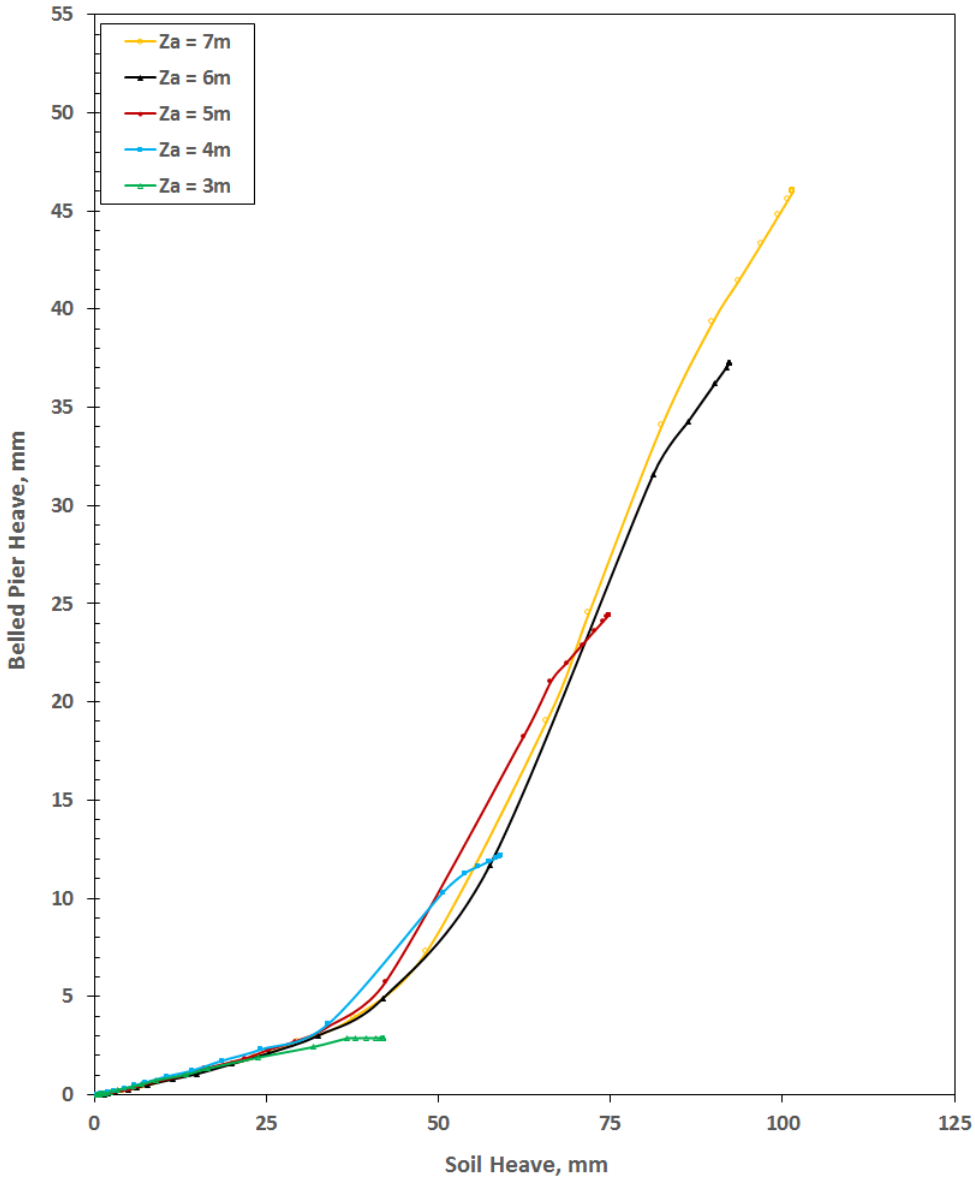

Figure 5.40: Effect of Depth of Swelling Zone on Belled Pier Heave for $500kPa$ Swelling Pressure

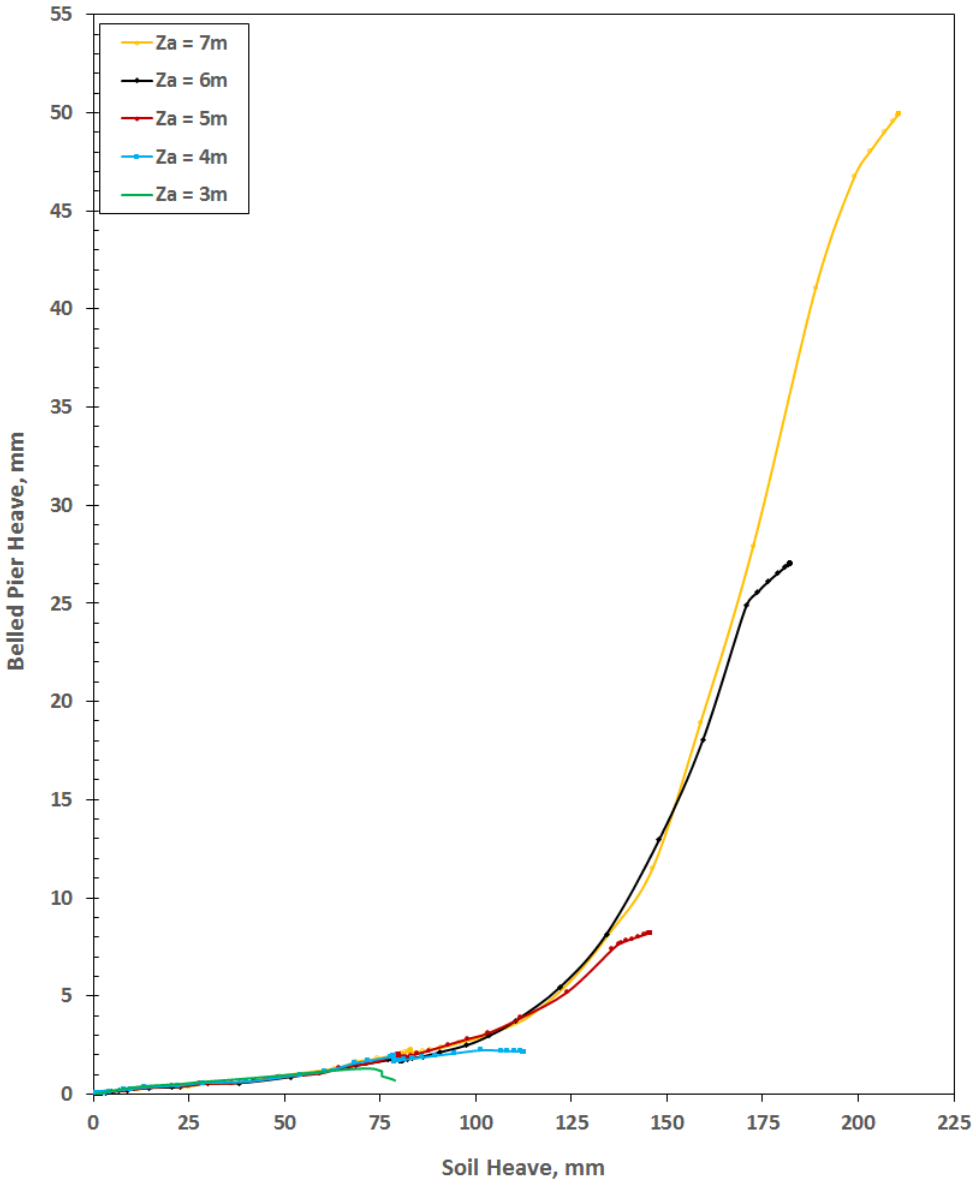

Figure 5.41: Effect of Depth of Swelling Zone on Belled Pier Heave for $750kPa$ Swelling Pressure

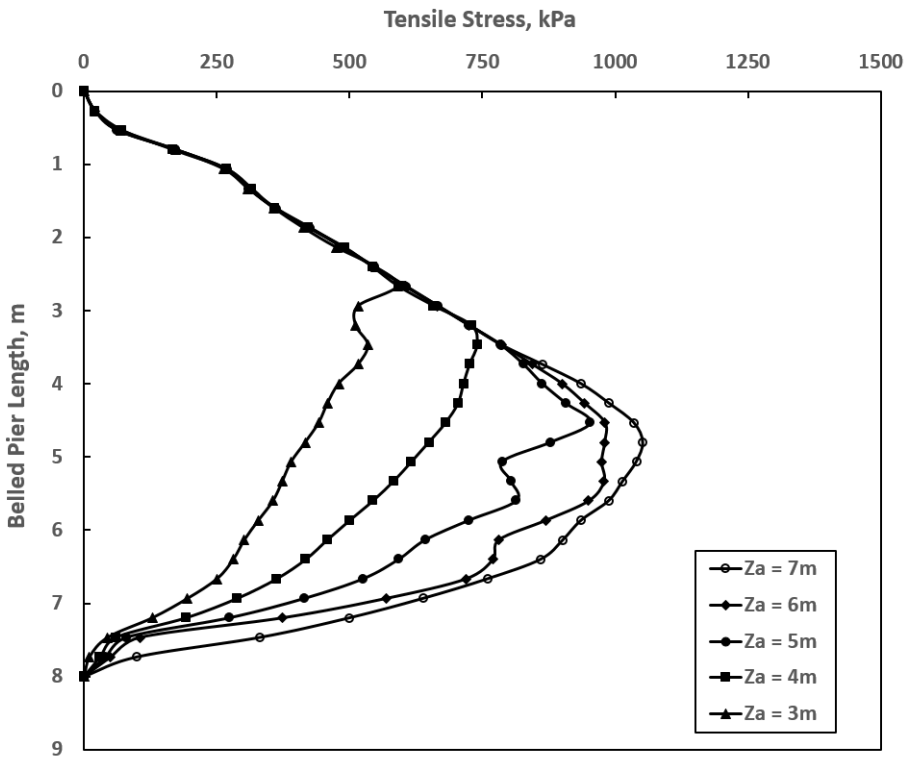

Figure 5.42: Effect of Depth of Swelling Zone on Tensile Stresses Developed in Belled Piers for $250kPa$ Swelling Pressure

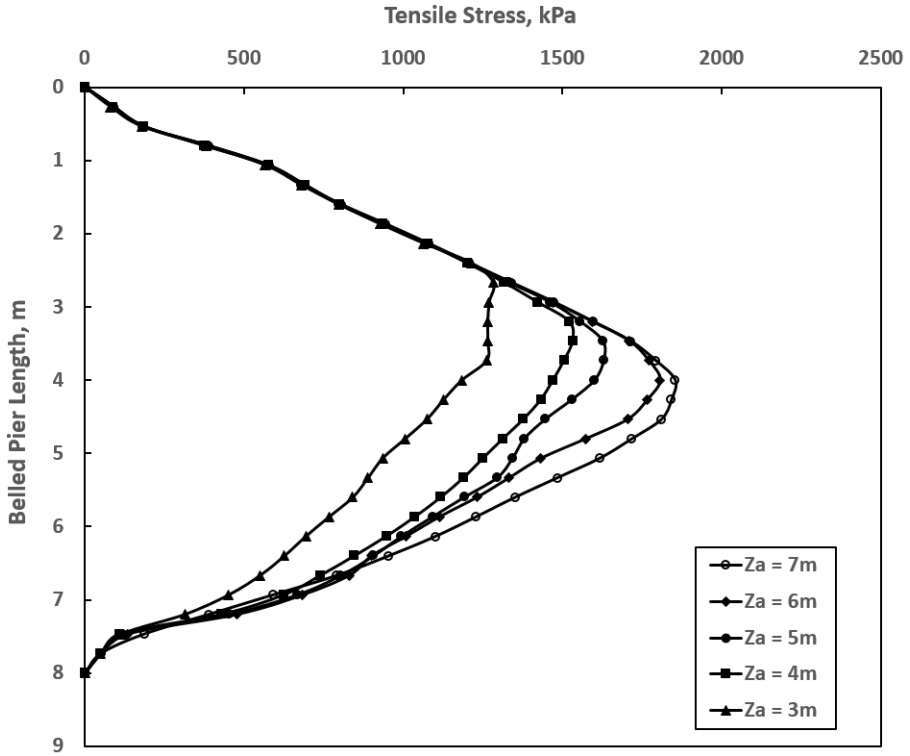

Figure 5.43: Effect of Depth of Swelling Zone on Tensile Stresses Developed in Belled Piers for $500kPa$ Swelling Pressure

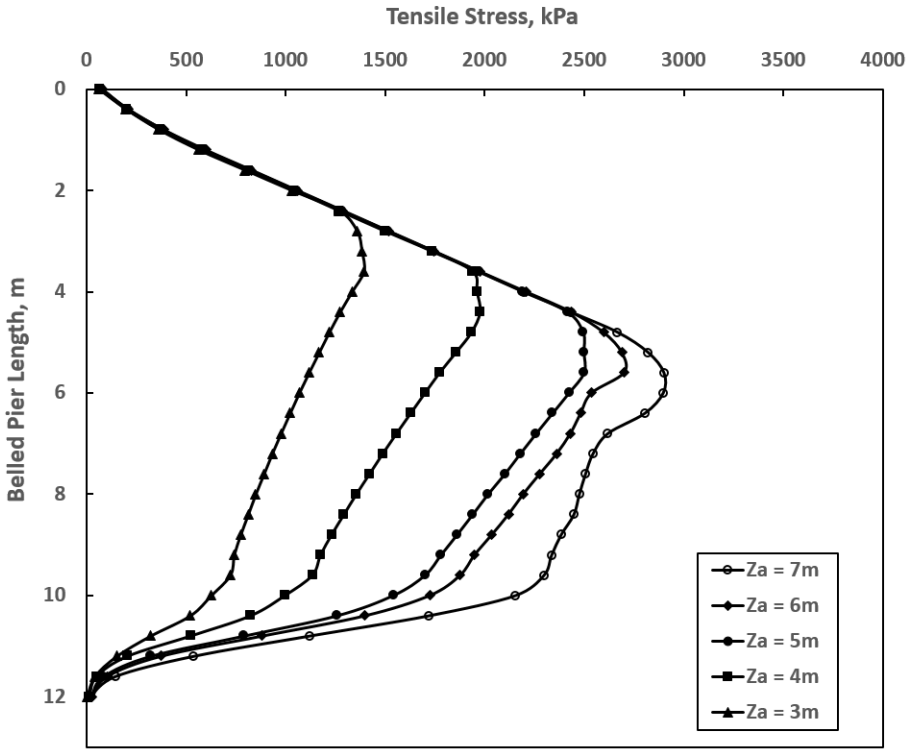

Figure 5.44: Effect of Depth of Swelling Zone on Tensile Stresses Developed in Belled Piers for $750kPa$ Swelling Pressure

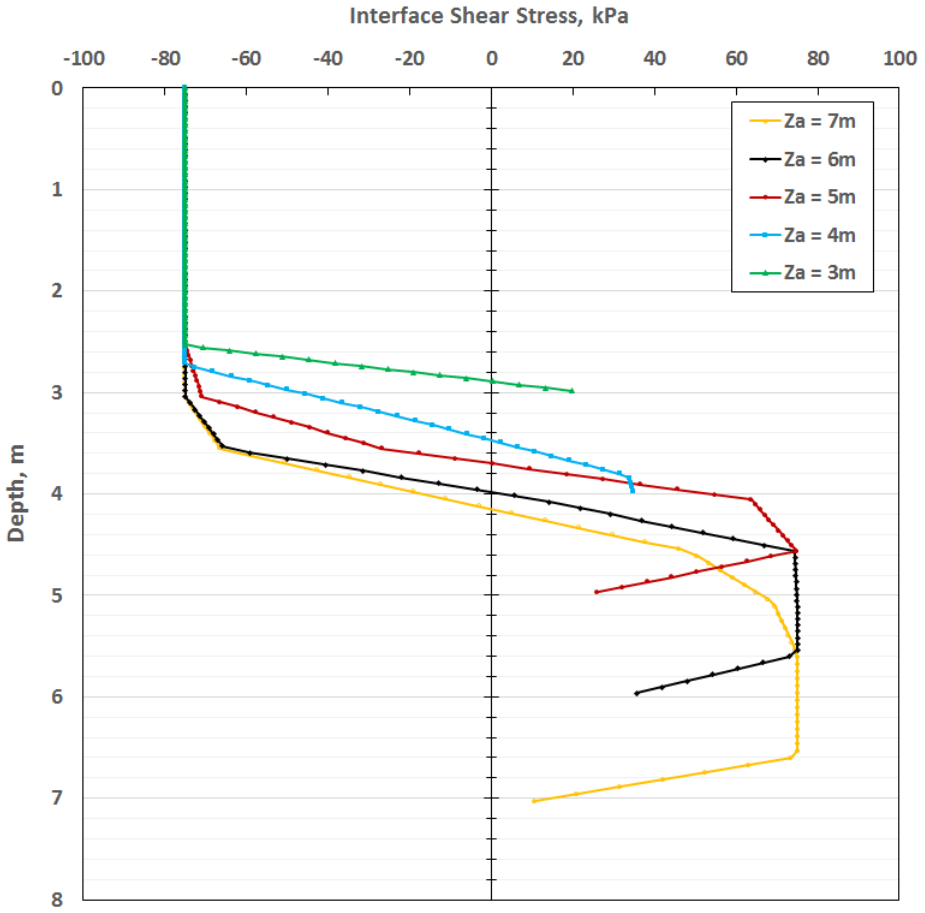

Figure 5.45: Effect of Depth of Swelling Zone on Interface Shear Stresses Developed Between the Belled Pier Shaft and the Swelling Zone for $500kPa$ Swelling Pressure

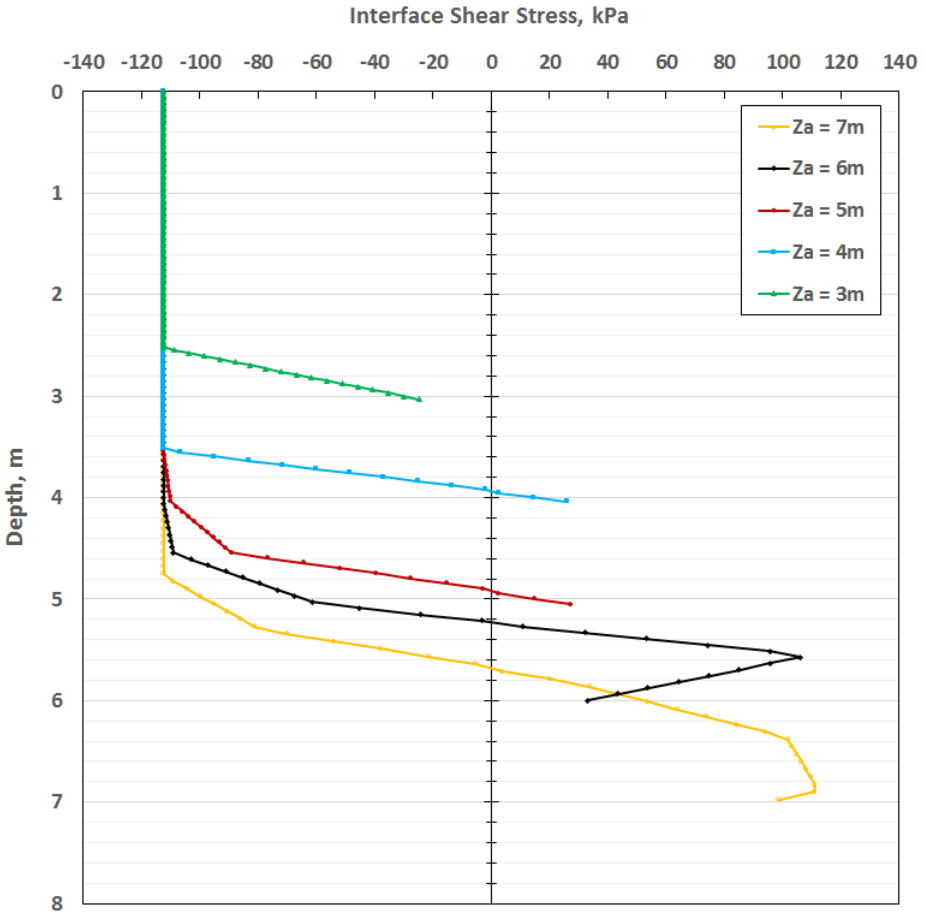

Figure 5.46: Effect of Depth of Swelling Zone on Interface Shear Stresses Developed Between the Belled Pier Shaft and the Swelling Zone for $750kPa$ Swelling Pressure

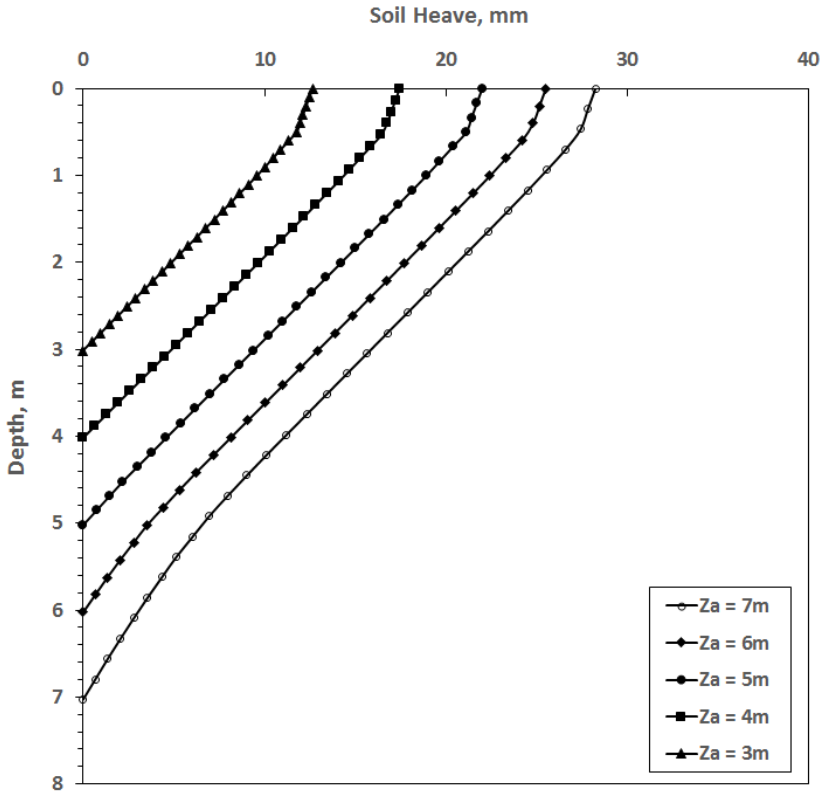

Figure 5.47: Soil Heave Profile for $250kPa$ Swelling Pressure

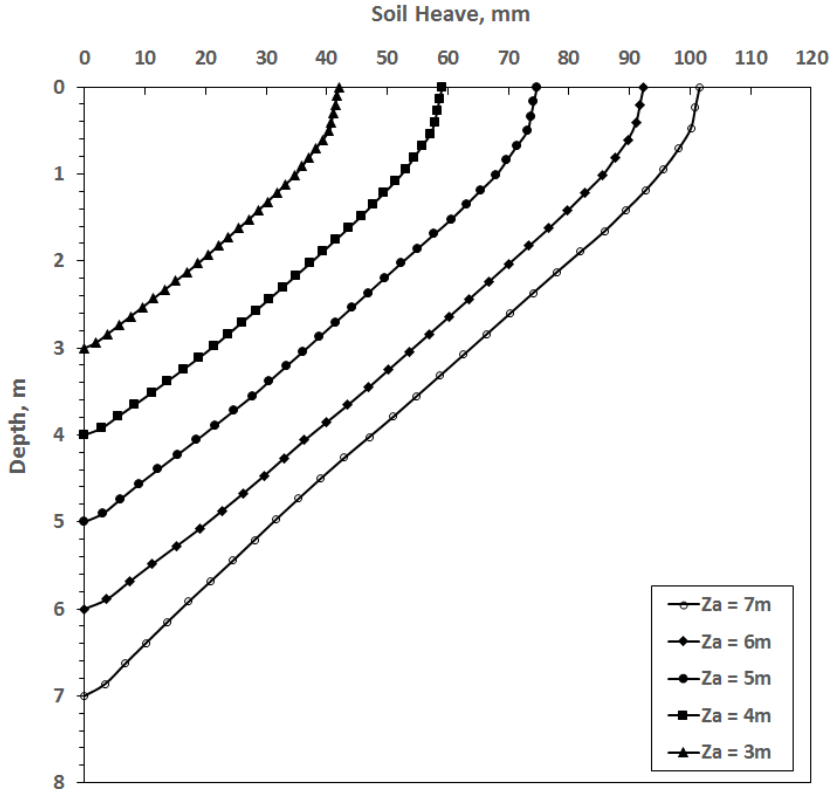

Figure 5.48: Soil Heave Profile for $500kPa$ Swelling Pressure

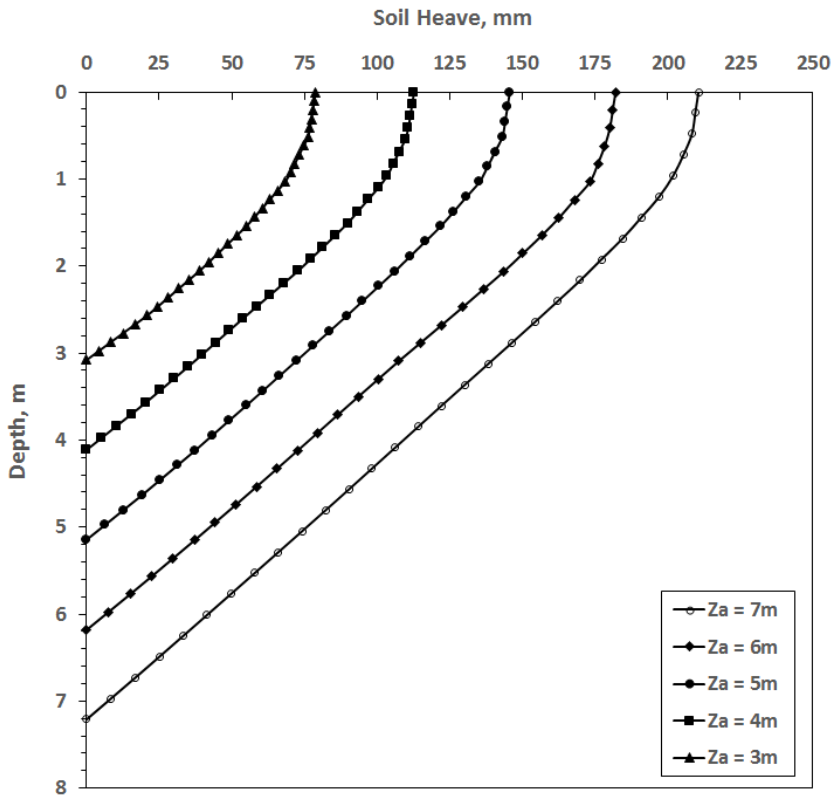

Figure 5.49: Soil Heave Profile for $750kPa$ Swelling Pressure

Considering Figures 5.39 to 5.44, it is observed that when the depth of the swelling zone increases, both the pier heave and the tensile stresses in the piers increase significantly. For example, considering $750kPa$ swelling pressure, when the swelling zone increased from a depth of $3m$ to a depth $7m$, the pier heave increased by a large value of about $50mm$ and the maximum tensile stress increased by a large value of about $1510KPa$. Therefore, underestimating the depth of swelling zone can result in excessively unsafe designs when considering belled piers in expansive soils. It can also be observed that the location of the swelling zone coincides with the location of the maximum tensile stress developed in the belled piers. But this is not always the case as discussed in Section 5.2.1.

Additional observations can be made considering $750kPa$ swelling pressure. Increasing the depth of the swelling zone increases the soil heave in addition to the pier heave. For example, when the swelling zone increased from a depth of $3m$ to a depth $7m$, the soil heave increased by a value of about $132mm$.

Interesting observations can be made when considering Figures 5.45 and 5.46. For larger depths of the swelling zone ($5m$, $6m$ and $7m$), interface shear stresses that resist pier heave develop in the swelling zone. This same phenomenon was observed by several authors for straight shaft piers (Nelson et al. 2012; Kaufmann et al. 2010; Mohamedzein et al. 1999). The reasoning lies in the relatively high movement (heave) of belled piers embedded in larger depths of the swelling zone and the heaving profiles of swelling soils; i.e. heave is maximum

at the top of the swelling zone and zero at the bottom (see Figure 5.47 to 5.49). The small amount of heave near the bottom of the swelling zone combined with the relatively high belled pier movement (heave) allows for the development of resisting interface shear stresses in the swelling zone. Furthermore, even for smaller depths of the swelling zone ($3m$ and $4m$), much smaller interface shear stresses that cause pier heave were observed near the bottom of the swelling zone (again due to the heave profile mentioned). This phenomenon was observed by O'Neill (1988) for straight shaft piers.

Most methods and equations that use the rigid method of belled pier design in expansive soils (Chen 1988; O'Neill 1988) consider a constant maximum value for the interface shear stress throughout the length of the belled pier in the swelling zone. Considering the above paragraph, doing so will result in excessively conservative designs.

Belled pier heave increases as the depth of the swelling zone (Za) increases because increasing Za increases the uplift force (F_u). Considering equation 5.2, as Za increases L'' (shaft length on which uplift interface shear stresses act upon) also increases, as can be clearly observed from Figures 5.45 and 5.46, and thus, F_u also increases. The same phenomenon is responsible for the increment of tensile stresses developed in belled piers as the depth of the active zone (Za) increases; i.e. as F_u increases, the belled pier will be under more and more 'tensioning' resulting in increments of the tensile stresses developed.

5.2.6 Effect of Time of Saturation on Belled Pier Behavior

One advantage of modelling with Abaqus is that the progression with time of various parameters can be investigated. In this Section, the progression with "time of saturation" of the belled pier heave and the maximum tensile stress developed in the belled piers is investigated. The results of this investigation are presented in Figures 5.50 and 5.51. A Belled pier of length (L) of $6m$, shaft diameter (d) of $0.6m$ and bell to shaft ratio (db/d) of 2 is considered in the investigation. The initial saturation level of the soil is considered to be 52% and the swelling pressure is considered to be $500kPa$.

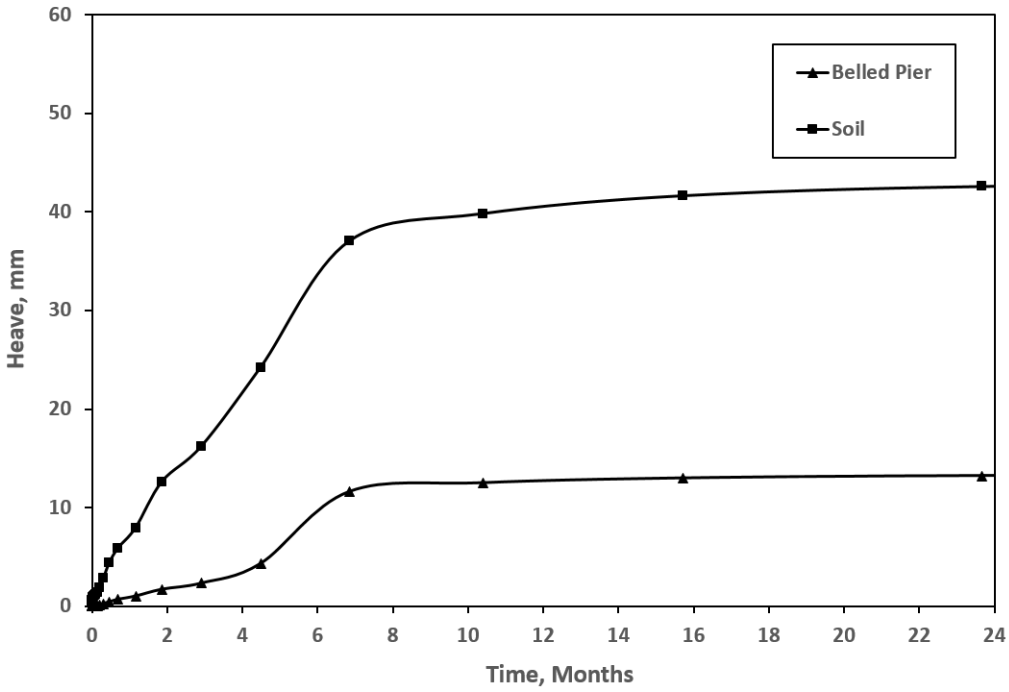

Figure 5.50: Effect of Time of Saturation on Belled Pier Heave ($3m$ depth of the swelling zone)

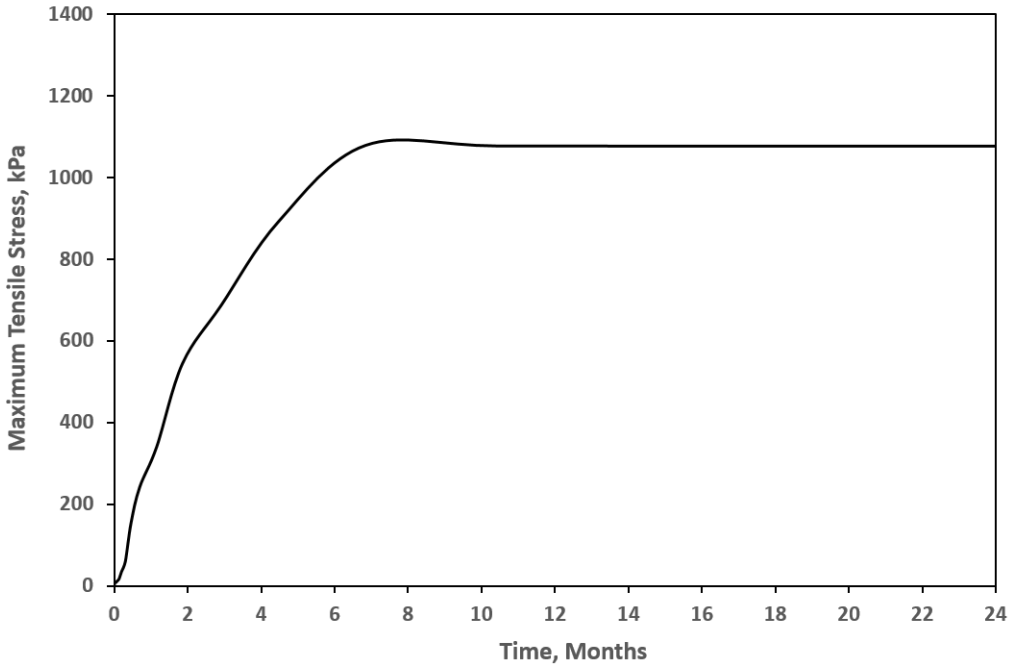

Figure 5.51: Effect of Time of Saturation on Tensile Stress Developed in Belled Pier ($3m$ depth of the swelling zone)

Considering Figures 5.50 and 5.51, soil heave, belled pier heave and tensile stress attain their maximum values in about $7months$ of continuous Saturation.

Considering Figure 5.50, it is particularly interesting to note that, whereas soil heave

begins almost immediately after the saturation process has begun, belled pier heave does not begin until some time later. This is because some amount of soil heaving needs to develop before the heaving soil is able to cause the heave of the belled pier; i.e. considering equation 5.2, f_u (uplift interface shear stress) needs to adequately develop. The same phenomenon was observed by Nelson et al. (2007) for straight shaft piers (see Section 2.6).

The effect of the depth of the swelling zone (Za) on the time of continuous saturation needed for soil heave, belled pier heave and maximum tensile stress to attain their maximum values was also studied. Results are presented in Figure 5.52.

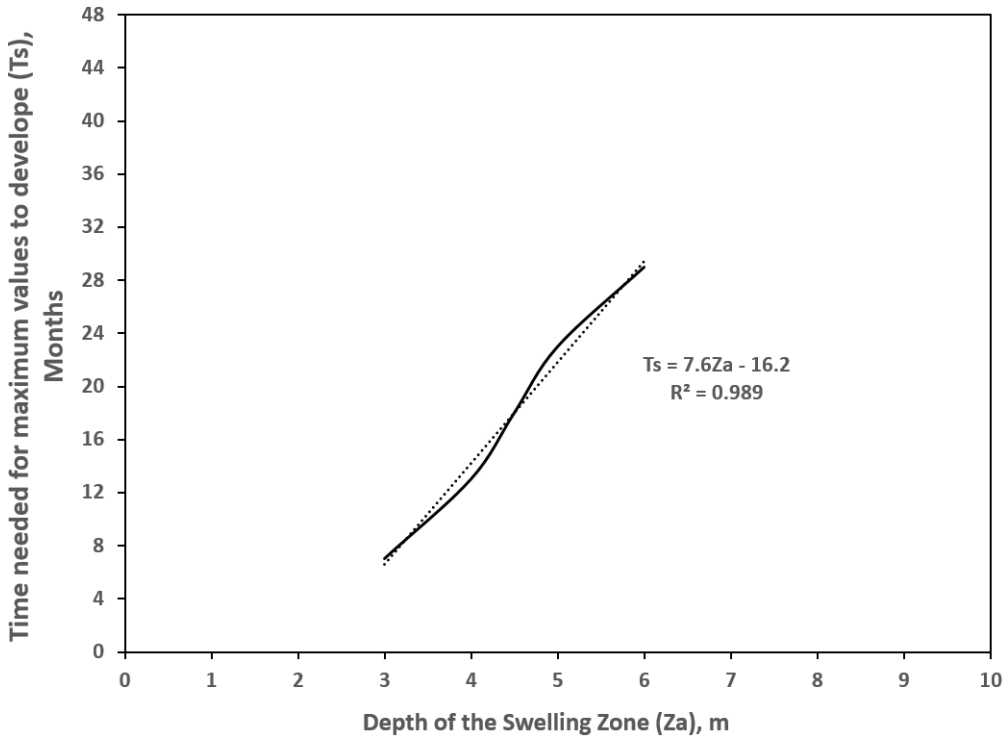

Figure 5.52: Effect of the depth of the swelling zone on the time of continuous saturation needed for soil heave, belled pier heave and maximum tensile stress to attain their maximum values

An equation was fitted to the curve obtained from Figure 5.52 and an **equation relating Za and Ts was obtained** (equation 5.6).

$$Ts = 7.6Za - 16.2 \tag{5.6}$$

where:

$Ts =$ time of continuous saturation needed for soil heave, belled pier heave and maximum tensile stress to attain their maximum values

$Za =$ depth of the swelling zone

Note that the time of saturation discussed considers the saturation level of the soil to be around 52% (see Section 4.2.1). **If higher values of the saturation level are to be considered, then smaller values of Ts will be obtained.**

5.2.7 Effect of the ratio of Young's Modulus to Undrained Cohesion on Belled Pier Behaviour

As mentioned earlier, the model considers both elastic and plastic behaviors of the soil. In this Section, the effects of the elastic behavior parameter, young's modulus (Es) and the plastic behavior parameter, undrained cohesion (Cu) are investigated. This investigation is done by considering the ratio of the young's modulus of the soil to the undrained cohesion of the soil (Es/Cu) and its effect on belled pier heave and tensile stresses developed in the belled piers. This ratio is considered because as Cu varies so does Es. The results of the investigation are presented in Figures 5.53 to 5.58. The range of the ratio (Es/Cu) used in the investigation is determined by considering the range of Young's modulus for hard clays, $50MPa$ to $100MPa$ (Bowles 2001); as this range represents expansive soils. Belled piers of length (L) of $6m$, shaft diameter (d) of $0.6m$ and bell to shaft ratio (db/d) of 2 are considered in the investigation.

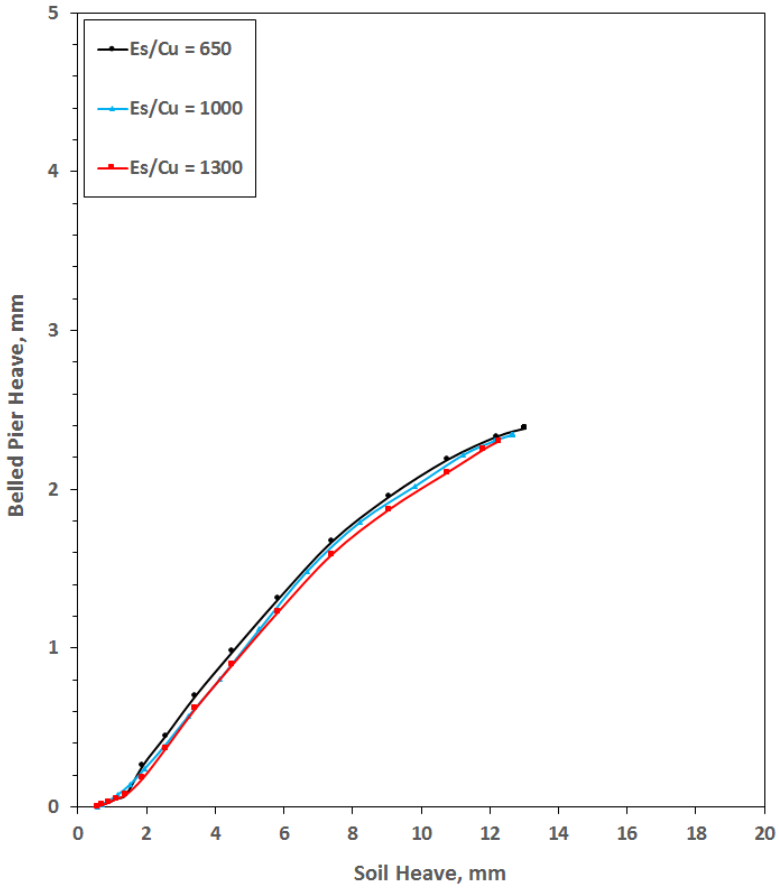

Figure 5.53: Effect of the ratio Es/Cu on Belled Pier Heave for $250kPa$ Swelling Pressure

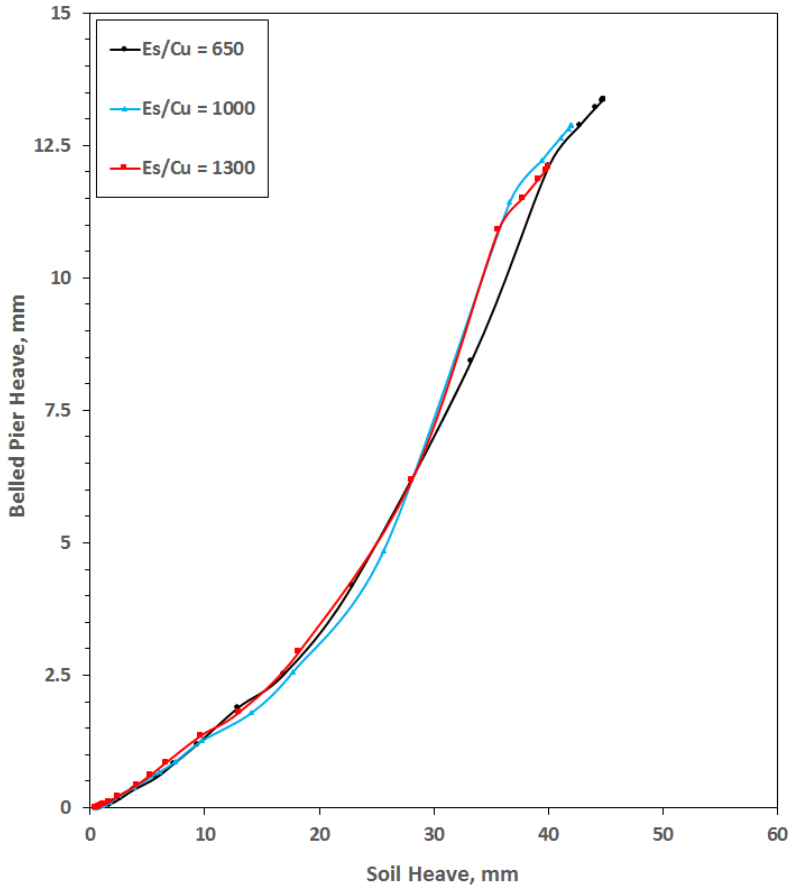

Figure 5.54: Effect of the ratio Es/Cu on Belled Pier Heave for $500kPa$ Swelling Pressure

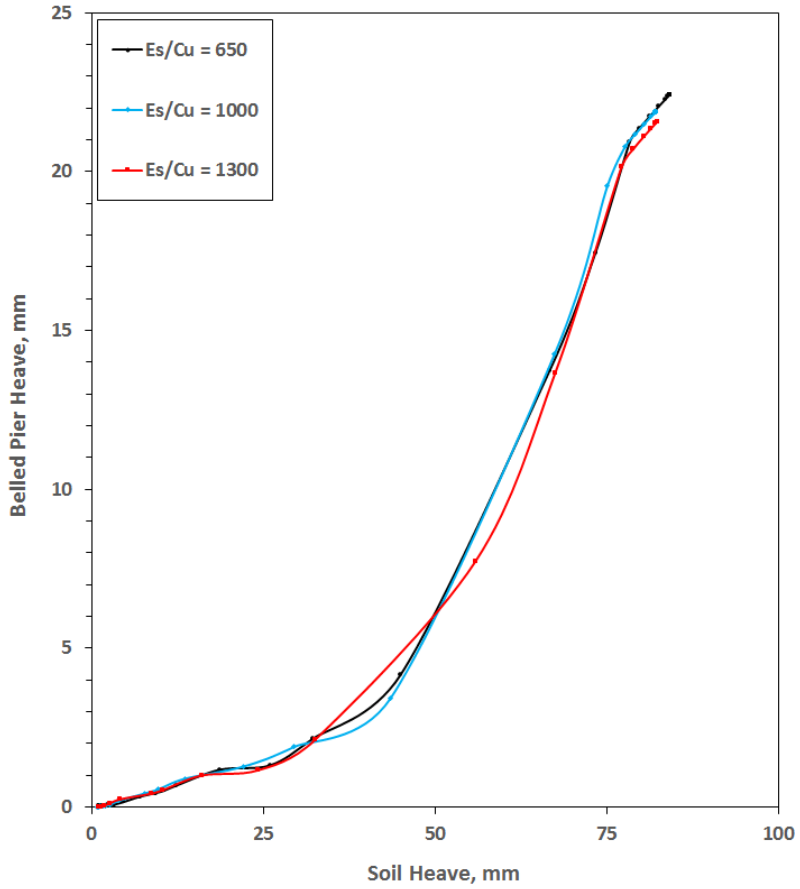

Figure 5.55: Effect of the ratio Es/Cu on Belled Pier Heave for $750kPa$ Swelling Pressure

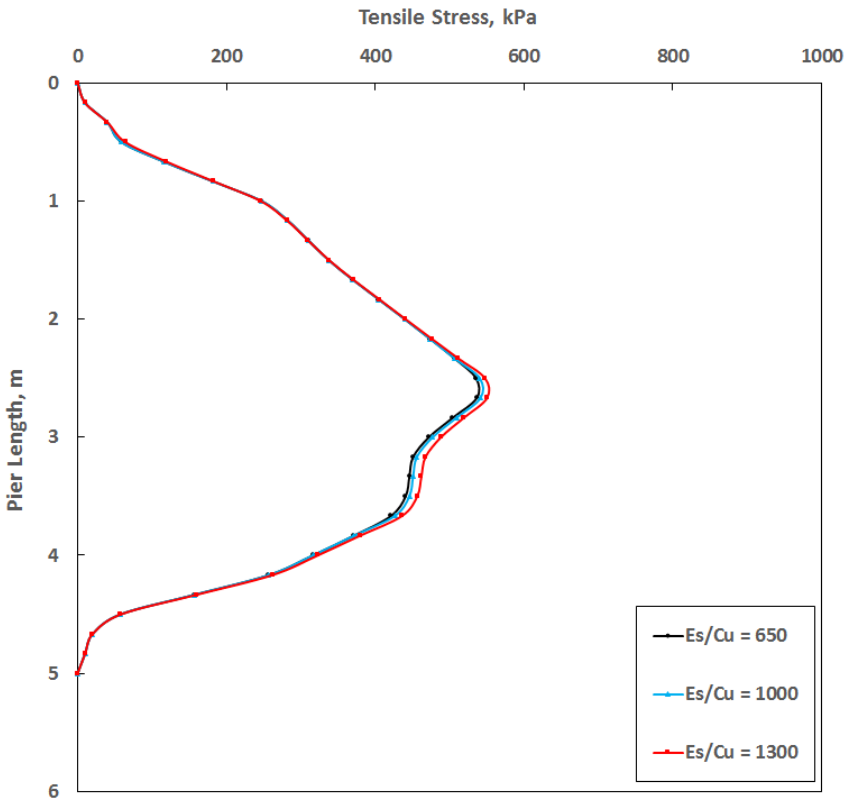

Figure 5.56: Effect of the ratio Es/Cu on Belled Pier Heave for $250kPa$ Swelling Pressure

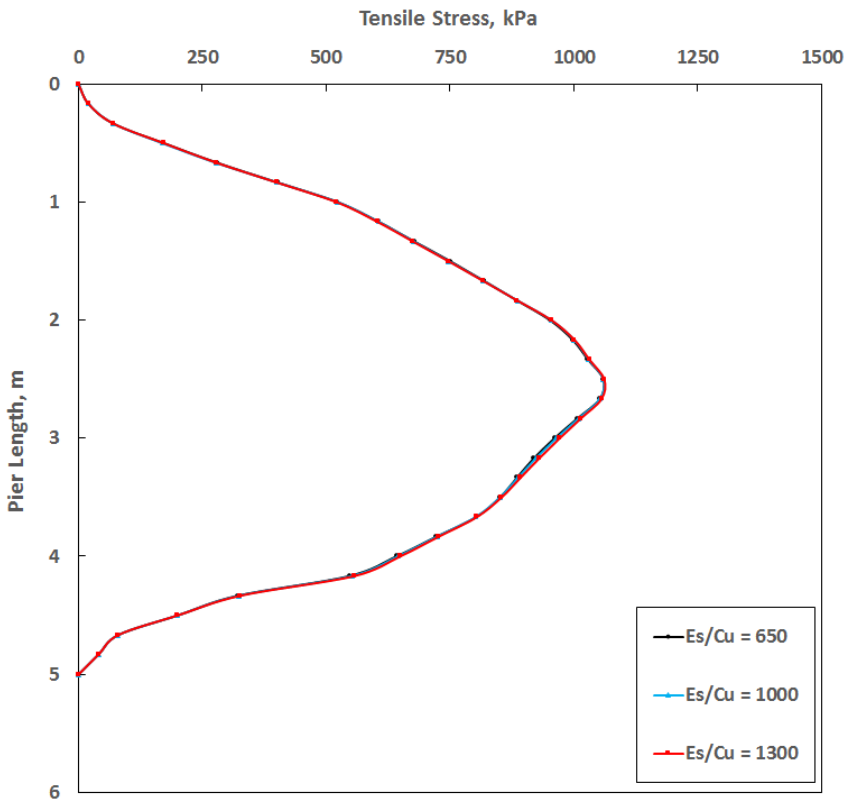

Figure 5.57: Effect of the ratio Es/Cu on Tensile Stresses Developed in Belled Piers for $500kPa$ Swelling Pressure

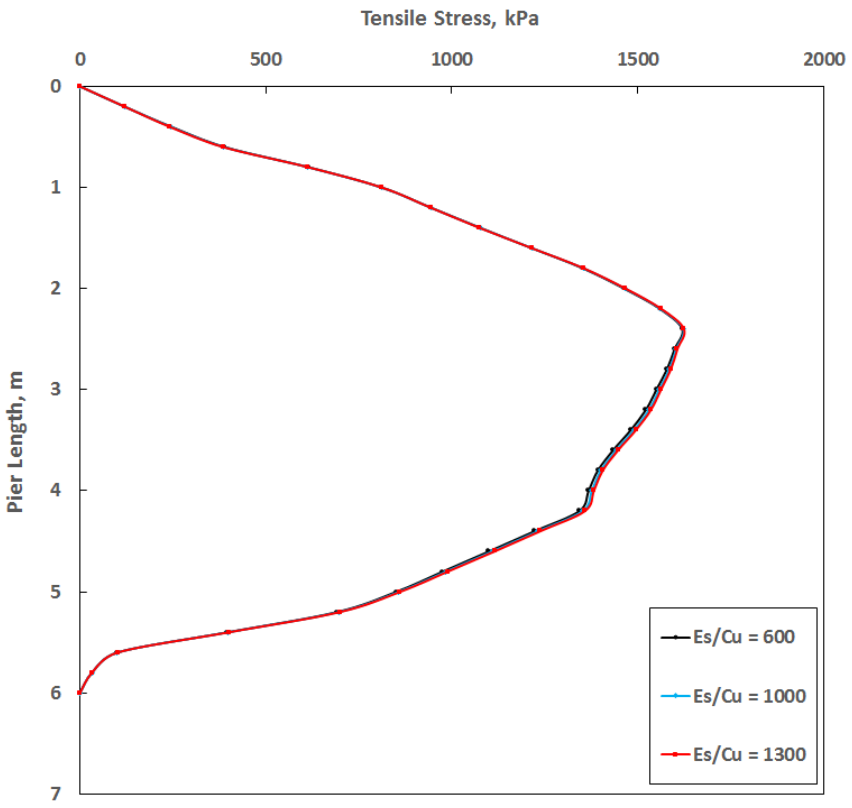

Figure 5.58: Effect of the ratio Es/Cu on Tensile Stresses Developed in Belled Piers for $750kPa$ Swelling Pressure

It can be observed from Figures 5.53 to 5.58 that changes in the ratio Es/Cu cause very small changes both in belled pier heave and tensile stresses developed in belled piers. For example, considering $750kPa$ swelling pressure, when the ratio Es/Cu increased from 650 to 1300, belled pier heave decreased by only about $1mm$ and maximum tensile stress in the belled piers increased by only $4.8kPa$. This shows that the investigations conducted up to this point and those done later are valid for hard clays having a range of young's modulus and undrained cohesion even though a hypothetical site is considered.

The effect of Es alone on straight shaft pier heave and tensile stresses developed in straight shaft piers was investigated by Nelson (2012). Variation in pier heave and tensile stresses developed were observed as Es varies. O'Neill (1988) considered that pier heave varies as Cu varies. But, as Cu varies, Es also varies as Es is dependent on Cu. Therefore, it's better to consider the effect of both parameters at the same time instead of considering their effects separately. Hence, the effect of the ratio Es/Cu is considered in this parametric investigation.

5.2.8 Effect of Applied Loads on Belled Pier Behaviour

There are two approaches to designing belled piers embedded in expansive soils against uplift. The first approach is to consider only a condition where there is no applied load acting on

the belled pier, i.e. free belled pier (Tomlinson and Woodward 2008). Only this condition is considered because it is assumed to be the governing condition. Note that the belled piers investigated up to this point are free belled piers. The second approach is to consider a condition where there is applied load acting on the belled pier in addition to the condition where there is no applied load acting on the belled pier (Murthy 2002). Therefore, the effect of applied loads on belled pier behavior must be investigated. This is done by considering the effect of the applied load pressure (q) on belled pier heave and axial stresses developed inside the belled piers. The results of the investigation are presented in Figures 5.59 to 5.64. For the investigation, belled piers of bell to shaft ratio (db/d) of 2, shaft diameter (d) of $0.6m$ and length (L) of $5m$ for $250kPa$ and $500kPa$ swelling pressures and $6m$ for $750kPa$ swelling pressure are considered. q is applied over a certain period of time ($1month$) instead of instantaneously.

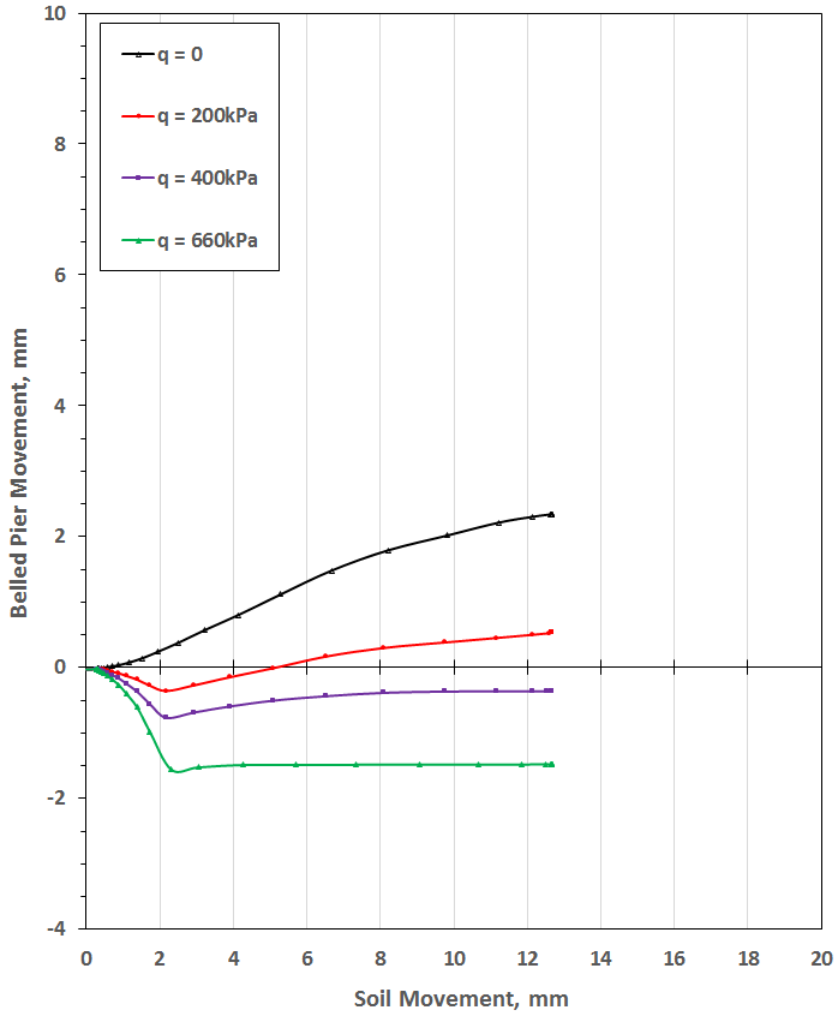

Figure 5.59: Effect of Applied Loads on Belled Pier Heave for $250kPa$ Swelling Pressure

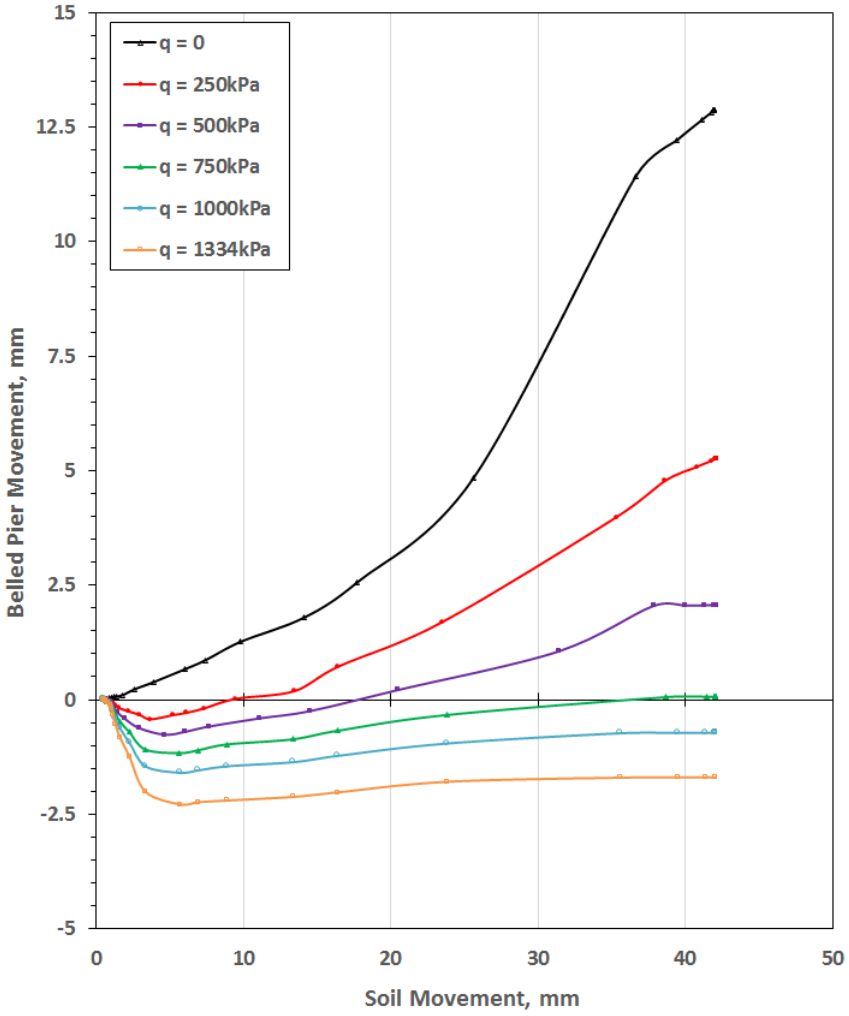

Figure 5.60: Effect of Applied Loads on Belled Pier Heave for $500kPa$ Swelling Pressure

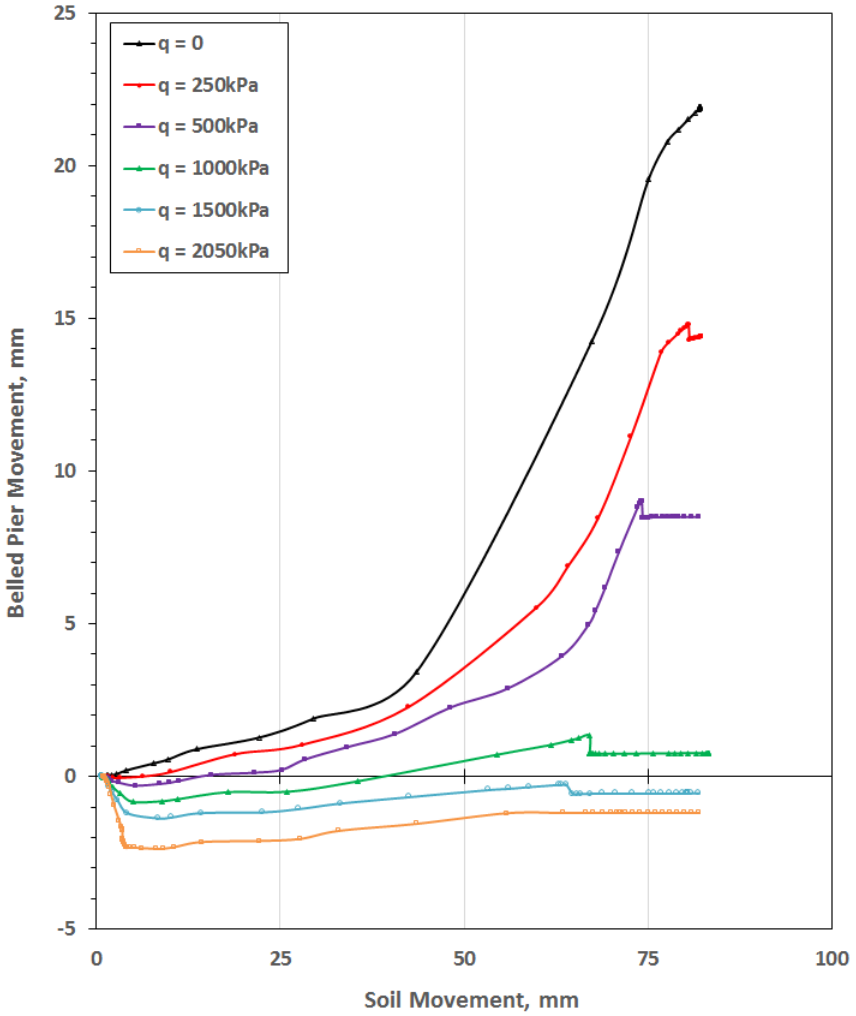

Figure 5.61: Effect of Applied Loads on Belled Pier Heave for $750kPa$ Swelling Pressure

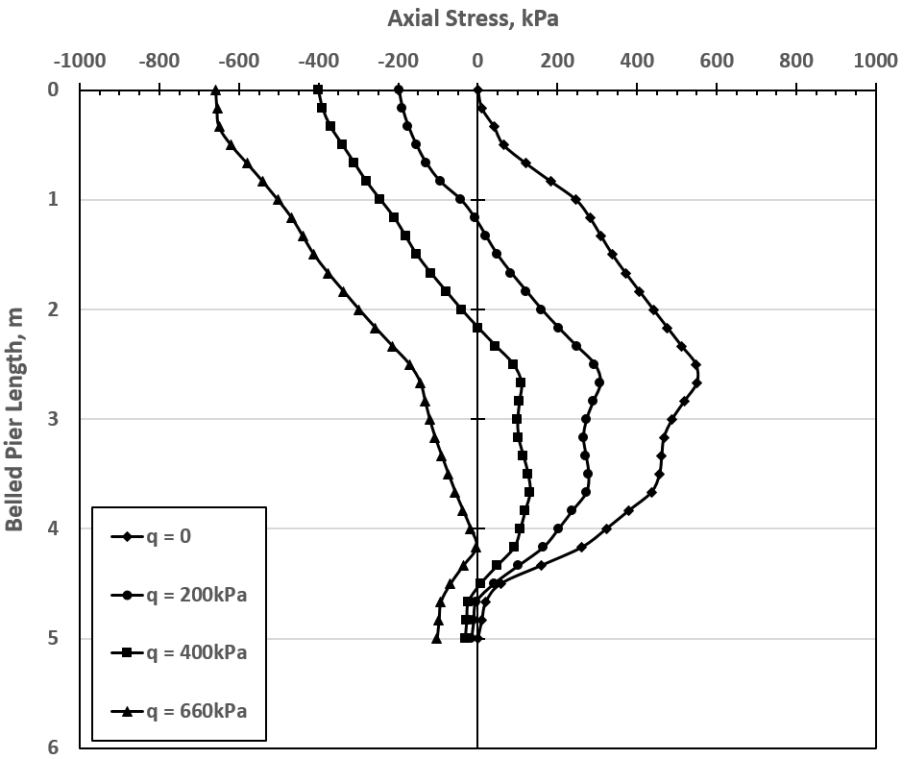

Figure 5.62: Effect of Applied Loads on Axial Stresses developed in Belled Piers for $250kPa$ Swelling Pressure

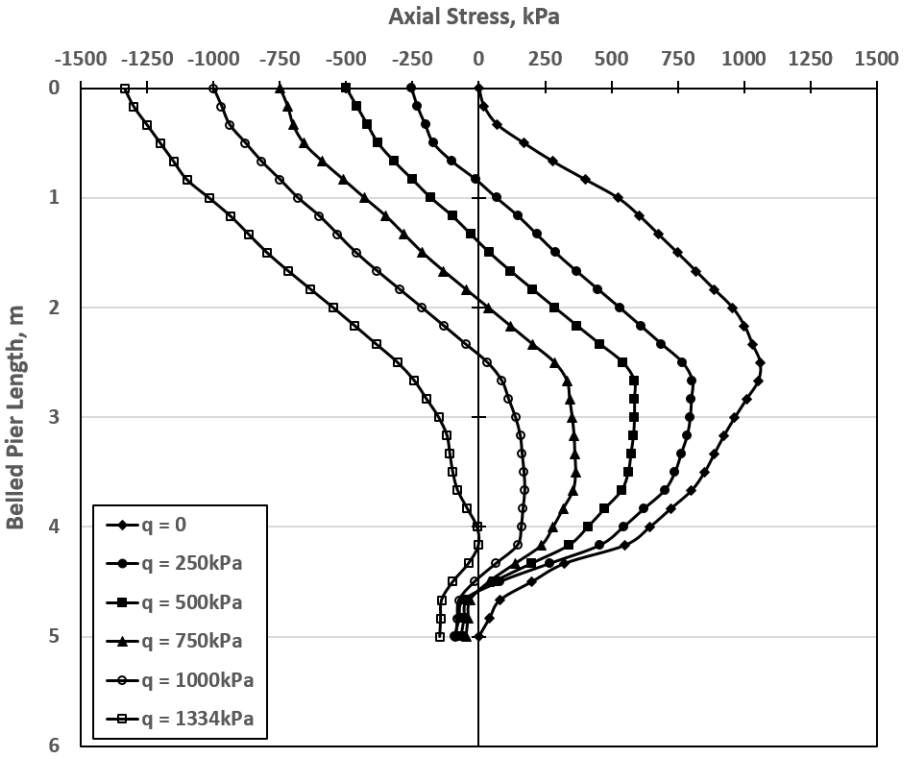

Figure 5.63: Effect of Applied Loads on Axial Stresses developed in Belled Piers for $500kPa$ Swelling Pressure

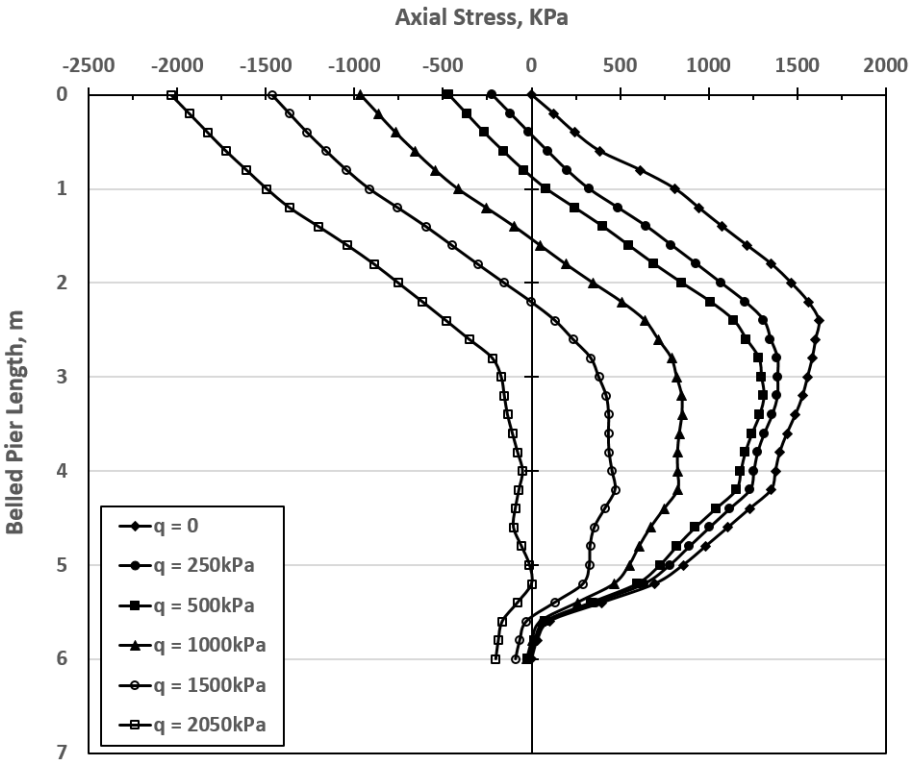

Figure 5.64: Effect of Applied Loads on Axial Stresses developed in Belled Piers for $750kPa$ Swelling Pressure

The following can be observed from Figures 5.59 to 5.64. As the value of the applied load pressure (q) increases, the belled pier heave decreases. In fact, if q is large enough, settlement (downward movement) occurs instead of heave. The same holds true for the tensile stresses developed in the belled piers, i.e. as the value of q increases, the tensile stresses decrease and if q is large enough, compressive stresses occur in the belled piers instead of tensile stresses.

Considering $750kPa$ swelling pressure, the maximum tensile stress in the free belled pier ($q = 0$) is $1622kPa$. The q needed to overcome this tensile stress so that only compressive stresses occur in the belled pier is $2050KPa$. The ratio of this q to the maximum tensile stress (t) will be 1.2. Therefore, applied load pressure (q) equal to 1.2 times the maximum tensile stress is needed to fully eliminate tensile stresses in the belled piers. This same value ($q/t = 1.2$) was obtained for swelling pressures of $250kPa$ and $500kPa$. This value is less than the value determined for straight shaft piers by Xiao et al. (2011). The value determine by Xiao et al. (2011) for straight shaft piers was $q/t = 2.5$.

The applied load (P) and the applied load pressure (q) are related by equation 5.7:

$$P = q\left(\pi\frac{d^2}{4}\right) \tag{5.7}$$

Belled pier heave decreases as applied load pressure (q) increases because q acts in opposite direction to belled pier heave and tends to cause downward movement (settlement) of

the belled pier. Or, one can consider the applied load P to be a resisting force in addition to the resisting forces mentioned in Section 5.2.1; and hence, its increment will result in belled pier heave decrement.

Tensile stresses developed in the belled piers decrease as q increases because the action of q puts the belled pier under **compression action instead of 'tensioning' action**. This will result in the reduction of tensile stresses developed and leads to the development of compressive stresses.

The effect of the applied load pressure (q) on the interface shear stresses developed on the belled pier shaft was also investigated. Results are presented in Figures 5.65 and 5.66.

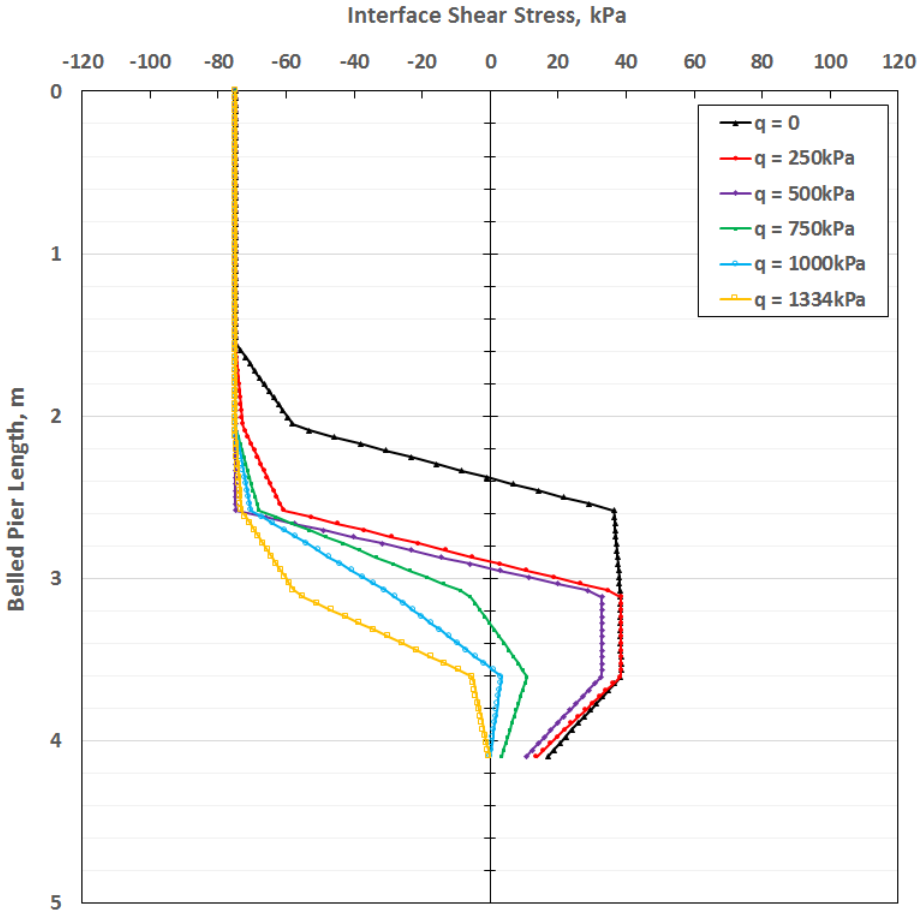

Figure 5.65: Effect of Applied Load on the Interface Shear Stress distribution on the Shaft for $500kPa$ Swelling Pressure

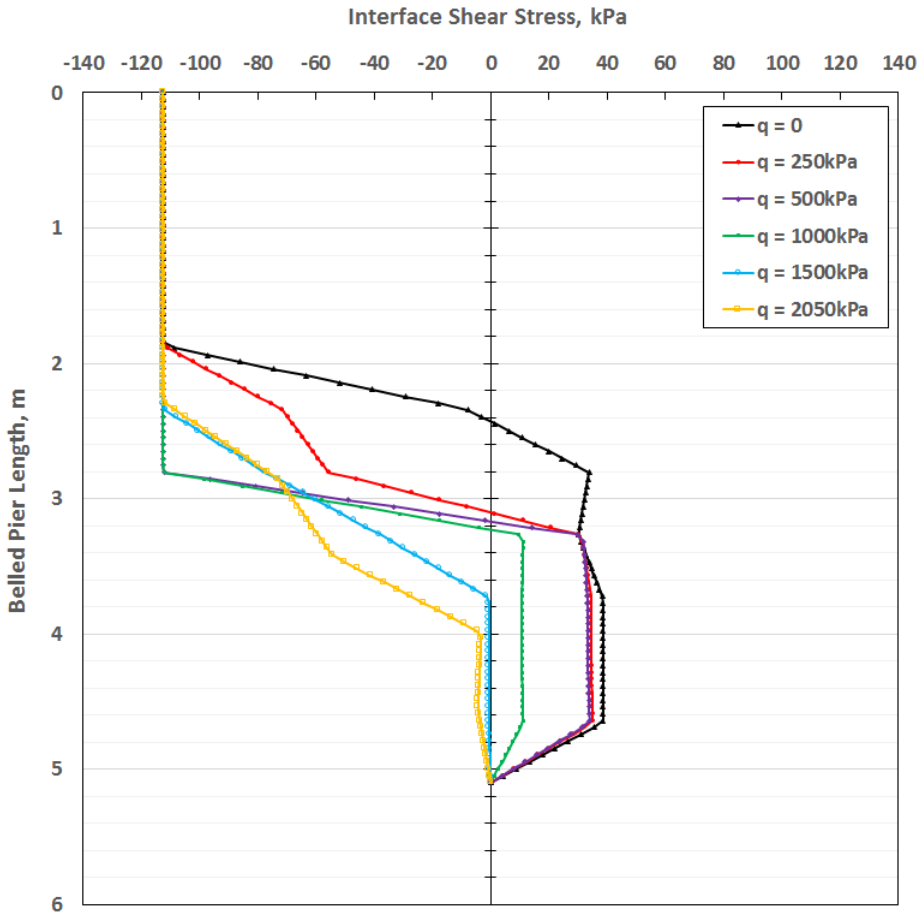

Figure 5.66: Effect of Applied Load on the Interface Shear Stress distribution on the Shaft for $750kPa$ Swelling Pressure

As can be observed form Figure 5.66 (for $q = 250kPa$, $q = 500kPa$ and $q = 1000kPa$), as q increases, resisting interface shear stresses (f_s) will not fully develop. This means most of the resistance to belled pier heave is provided by q itself. Again, considering 5.66 (for $q = 1500kPa$ and $q = 2050kPa$), only resisting interface shear stresses are developed. This is because downward movement (settlement) of the belled piers occurs for $q = 1500kPa$ and $q = 2050kPa$ as can be observed from Figure 5.61; note that for $q = 1500kPa$ and $q = 2050kPa$, the resisting shear stresses have negative values as the movement of the belled piers is in the downward direction this time around.

5.3 Cost Comparison

In the design of piers embedded in expansive soils, one can select straight shaft piers and small bell size piers with longer length or large bell size piers with shorter length depending on the amount of cost. To check which selection is better, a cost comparison is conducted. To conduct this cost comparison, costs of piers with the same heave are considered. The costs considered are concrete cost, reinforcement steel cost (Re-bar cost), shaft drilling cost

and bell drilling cost.

Costs are considered considering the construction market in Ethiopia in the year 2017 ($G.C.$) considering the local currency, Birr (ETB). Concrete cost is considered to be $3800 ETB/m^3$ considering concrete of cylindrical strength of $f_{ck} = 30 MPa$. Reinforcement steel cost is considered to be $42 ETB/kg$ considering Grade 60 steel. Shaft drilling cost is considered to be $2500 ETB/m^3$ considering shaft diameter (d) of $0.6m$. Bell drilling cost is considered to be $3000 ETB$ for large bell sizes, $2000 ETB$ for medium bell sizes and $1000 ETB$ for small bell sizes.

The results of the cost comparison are presented in Tables 5.1 to 5.3 and Figure 5.67. The volumes of the piers are calculated by considering Chen's (1988) recommendations on belled pier proportioning; see Section 2.4.1. Reinforcement areas, A_s and $A_{s,min}$ are calculated considering Nelson et al. (2007) and U.S. Army Corps of Engineers (1983) recommendations respectively; see Section 2.8.5.

Table 5.1: Cost Comparison of Piers considering $3m$ depth of the Swelling Zone and $250kPa$ Swelling Pressure

Designation	**Bell Size**	**Heave** (mm)	**Shaft Diameter** (m)	**Total Length** (m)	**Shaft Length** (m)	**Volume** (m^3)	**Maximum Tensile Stress** (kPa)	**Maximum Tensile Force** (kN)	$A_s(mm^2)$	$A_{s,min}(mm^2)$	**No. of Bars**	**Concrete Cost** (ETB)	**Re-Bar Cost** (ETB)	**Shaft Drilling Cost** (ETB)	**Bell Drilling Cost** (ETB)	**Total Cost** (ETB)
Large Bell	$db/d = 3$	1	0.6	4.5	3.1	2.988	579	163.7	608	2828	$9H20$	11354.4	466.2	11250	3000	26070.6
Medium Bell	$db/d = 2.5$	1	0.6	4.6	3.5	2.255	563	159.2	591	2828	$9H20$	8569	476.56	11500	2000	22545.56
Small Bell	$db/d = 2$	1	0.6	4.7	3.8	1.809	529	149.6	555	2828	$9H20$	6874.2	486.92	11750	1000	20111.12
Straight Shaft	$db/d = 1$	1	0.6	4.8	4.8	1.357	512	144.8	538	2828	$9H20$	5156.6	497.28	12000	0	17653.88

Table 5.2: Cost Comparison of Piers considering $3m$ depth of the Swelling Zone and $500kPa$ Swelling Pressure

Designation	**Bell Size**	**Heave** (mm)	**Shaft Diameter** (m)	**Total Length** (m)	**Shaft Length** (m)	**Volume** (m^3)	**Maximum Tensile Stress** (kPa)	**Maximum Tensile Force** (kN)	$A_s(mm^2)$	$A_{s,min}(mm^2)$	**No. of Bars**	**Concrete Cost** (ETB)	**Rebar Cost** (ETB)	**Shaft Drilling Cost** (ETB)	**Bell Drilling Cost** (ETB)	**Total Cost** (ETB)
Large Bell	$db/d = 3$	7	0.6	4.5	3.1	2.988	1208	341.6	1268	2828	$9H20$	11354.4	466.2	11250	3000	26070.6
Medium Bell	$db/d = 2.5$	7	0.6	5.8	4.7	2.594	1214	343.3	1274	2828	$9H20$	9857.2	600.88	14500	2000	26958.08
Small Bell	$db/d = 2$	7	0.6	6.6	5.7	2.347	1223	345.8	1283	2828	$9H20$	8918.6	683.76	16500	1000	27102.36
Straight Shaft	$db/d = 1$	7	0.6	7.8	7.8	2.2054	1208	341.6	1268	2828	$9H20$	8380.52	808.08	19500	0	28688.6

Table 5.3: Cost Comparison of Piers considering $4.5m$ depth of the Swelling Zone and $750kPa$ Swelling Pressure

Designation	**Bell Size**	**Heave** (mm)	**Shaft Diameter** (m)	**Total Length** (m)	**Shaft Length** (m)	**Volume** (m^3)	**Maximum Tensile Stress** (kPa)	**Maximum Tensile Force** (kN)	$A_s(mm^2)$	$A_{s,min}(mm^2)$	**No. of Bars**	**Concrete Cost** (ETB)	**Rebar Cost** (ETB)	**Shaft Drilling Cost** (ETB)	**Bell Drilling Cost** (ETB)	**Total Cost** (ETB)
Large Bell	$db/d = 3$	18	0.6	6.5	5.1	3.55	2689	760.3	2821	2828	$9H20$	13490	673.4	16250	3000	33413.4
Medium Bell	$db/d = 2.5$	18	0.6	9.9	8.8	3.753	2680	757.8	2811	2828	$9H20$	14261.4	1025.6	24750	2000	42037.04
Small Bell	$db/d = 2$	18	0.6	12.4	11.5	3.987	2673	755.8	2804	2828	$9H20$	15150.6	1284.6	31000	1000	48435.24
Straight Shaft	$db/d = 1$	18	0.6	14.1	14.1	3.987	2605	736.6	2733	2828	$9H20$	15150.6	1460.8	35250	0	51861.36

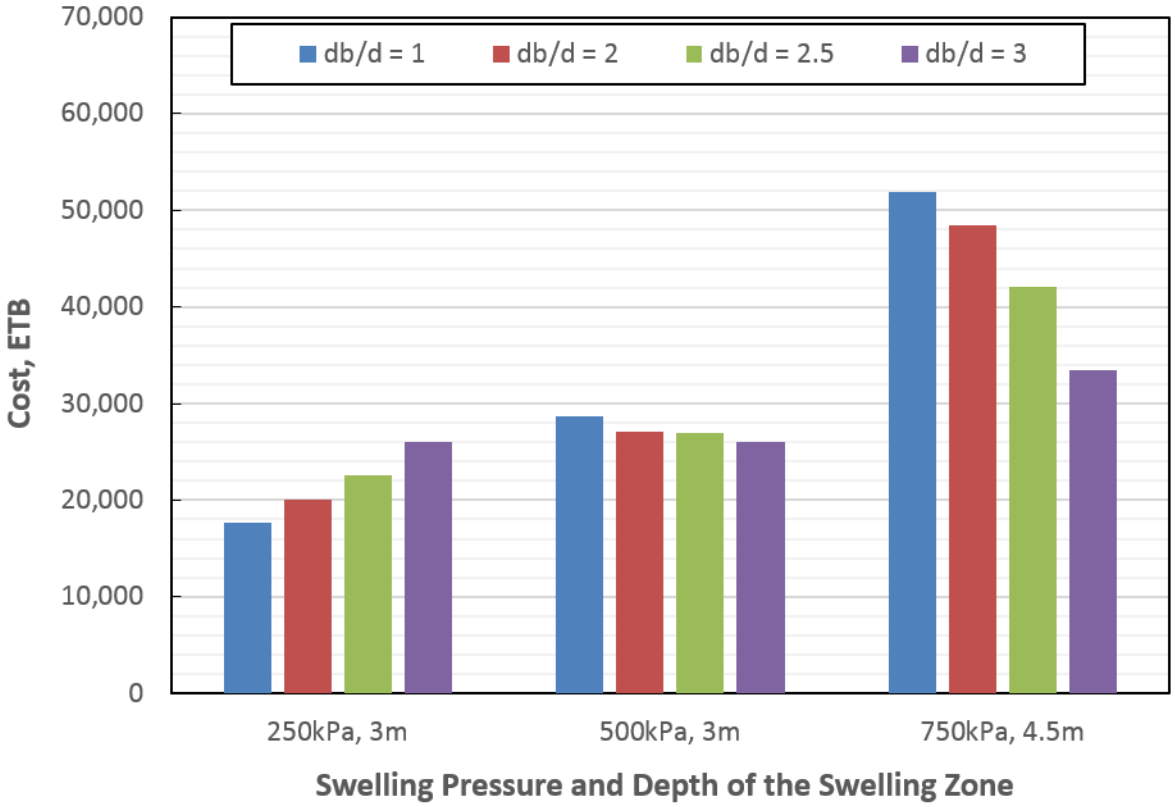

Figure 5.67: Cost Comparison of Piers

It can be observed from Figure 5.67 that **for smaller values of the swelling pressure and the depth of the swelling zone (less than $500kPa$ and $3m$ respectively), straight shaft piers are more cost effective; while for medium to large values of the swelling pressure and the depth of the swelling zone (greater than $500kPa$ and $3m$ respectively), large bell size belled piers are more cost effective.**

5.4 Trend Lines

The most common method that is used to design belled piers in expansive soils is the rigid pier method which is based on the equation proposed by O'Neill (1988), see Section 2.5.1. This method has major limitations which include:

- Pier heave is considered to be zero. If some pier heave were to be allowed, more economical designs can be obtained.
- No soil-pier slip is considered. But, some soil-pier slip is certain to exist in the actual soil-pier interaction.
- Bell friction is neglected.

- Interface shear stress is considered as a constant maximum value throughout the length of the belled pier in the swelling zone.
- Does not enable to determine the maximum tensile stresses developed inside the belled piers explicitly.

Therefore, a better method of designing belled piers in expansive soils is needed. This work addresses this issue by proposing trend lines which can be upgraded to design charts. These trend lines enable one to select the appropriate shaft diameters and lengths of belled piers in expansive soils. Furthermore, the trend lines also enable one to determine the maximum tensile stresses developed in belled piers in expansive soils. The trend lines eliminate all the limitations of O'Neill's approach. The trend lines are presented for different depths of the swelling zone (Za), different values of the swelling pressure (σ_s) and different values of the applied load pressure (q). The trend lines are presented in Figures 5.69 to 5.74. Comparison of the trend lines to the equation proposed by O'Neill (1988) is presented in Figure 5.68.

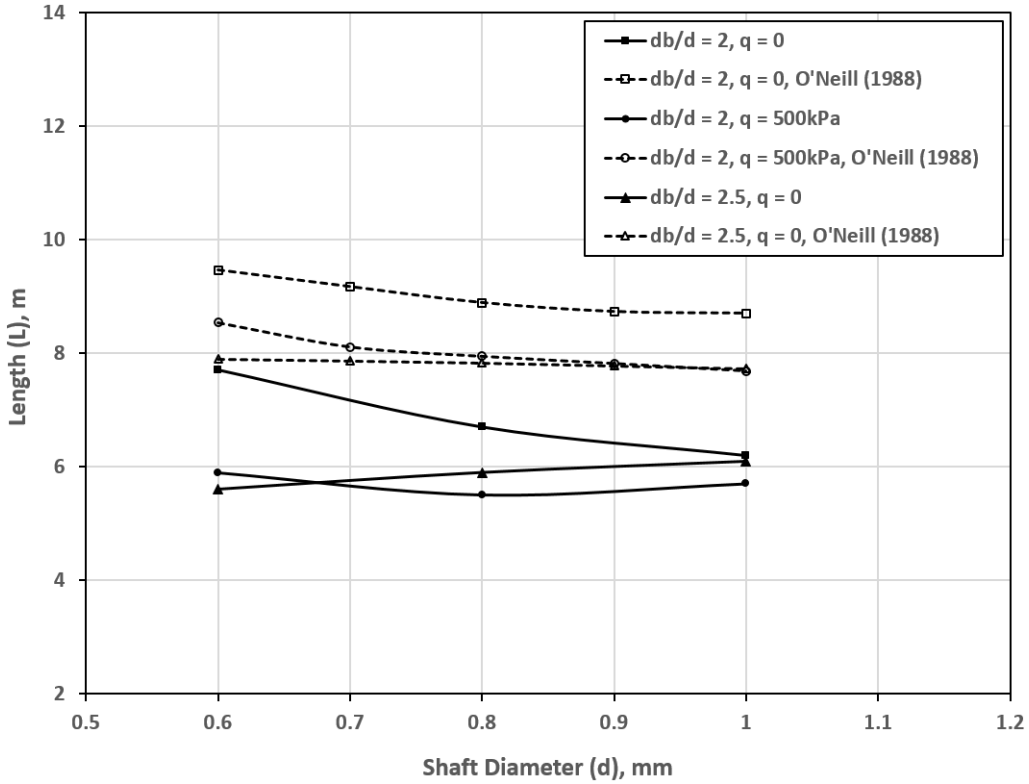

Figure 5.68: Comparison of Trend Lines to the equation proposed by O'Neill (1988)

Considering Figure 5.68, it is observed that the proposed trend lines give smaller values of length, i.e. are more economical, as compared to O'Neill's (1988) approach. This is because O'Neill's (1988) approach considers pier heave to be zero, neglects bell friction and considers the interface shear stress incorrectly. Nelson et al. (2007) concluded that O'Neill's (1988) approach was also uneconomical for the design of straight shaft piers in expansive soils.

The following points should be noted when using the proposed trend lines:

- Allowable heave is taken to be $50mm$ as per the recommendations of Nelson et al. (2007).
- It is suggested to reduce the applied dead load pressures by a factor of k as per the recommendations of O'Neill (1988) to account for the establishment of structural continuity.
- The trend lines must be used for belled piers fully embedded in hard, inorganic clay soils (CH); which is mostly the situation for belled piers in expansive soils.
- It is assumed that the most important parameters to consider in the design of belled piers in expansive soils are the depth of the swelling zone, the swelling pressure and the applied loads. Other soil parameters are neglected as their effect is assumed to be negligible (see Section 5.2.7). This assumption is reasonable because the neglected parameters **vary slightly** for the type of soils that represent belled piers in expansive soils and fully embedded in hard clay soils.
- It is assumed that the belled piers must not be entirely located inside the swelling zone. At least the bell portion must be in the non-swelling zone. Therefore, the belled piers considered in the trend lines will have a minimum allowable length based on the bell (enlarged base) dimension proportioning.
- It is assumed that it is possible to linearly interpolate between the depths of the swelling zone, swelling pressures and applied load pressures.
- Bell dimension proportioning must be conducted as per recommendations of Chen (1988); see Section 2.4.1.
- Minimum shaft diameter (d) of the belled piers is taken to be $0.6m$ and minimum base to shaft diameter ratio (db/d) is taken to be 2 as per the recommendations of Chen (1988).

5.4.1 $3m$ depth of the Swelling Zone

$750kPa$ Swelling Pressure

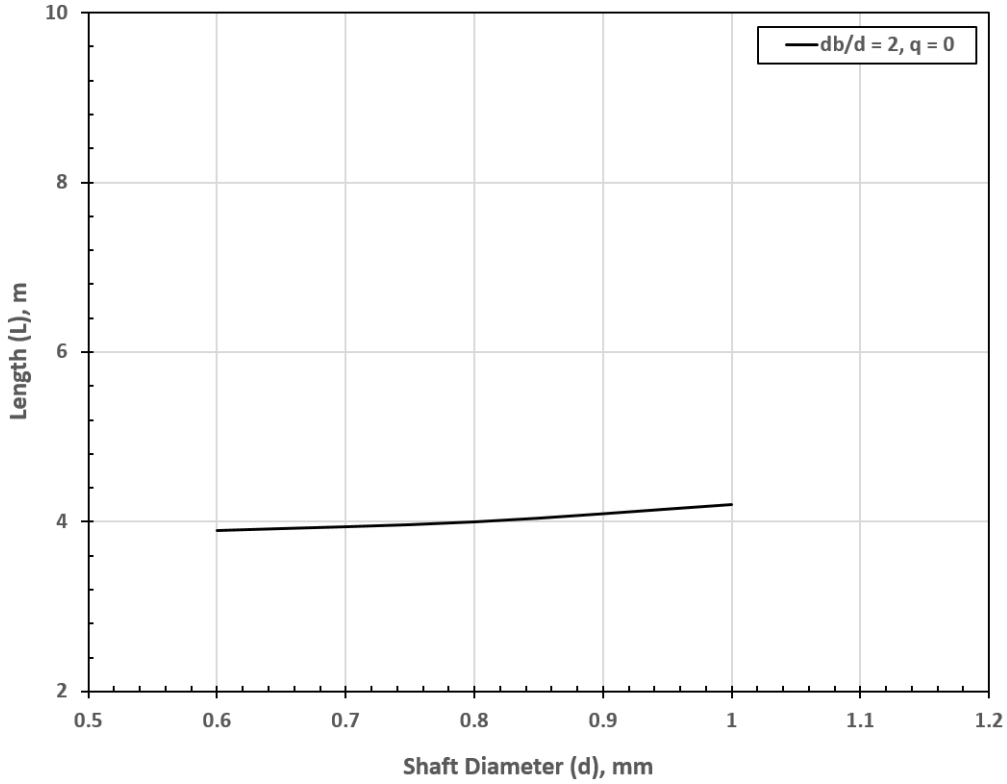

Figure 5.69: Trend Line for Shaft Diameter and Length, $3m$ depth of the swelling zone and $750kPa$ swelling pressure

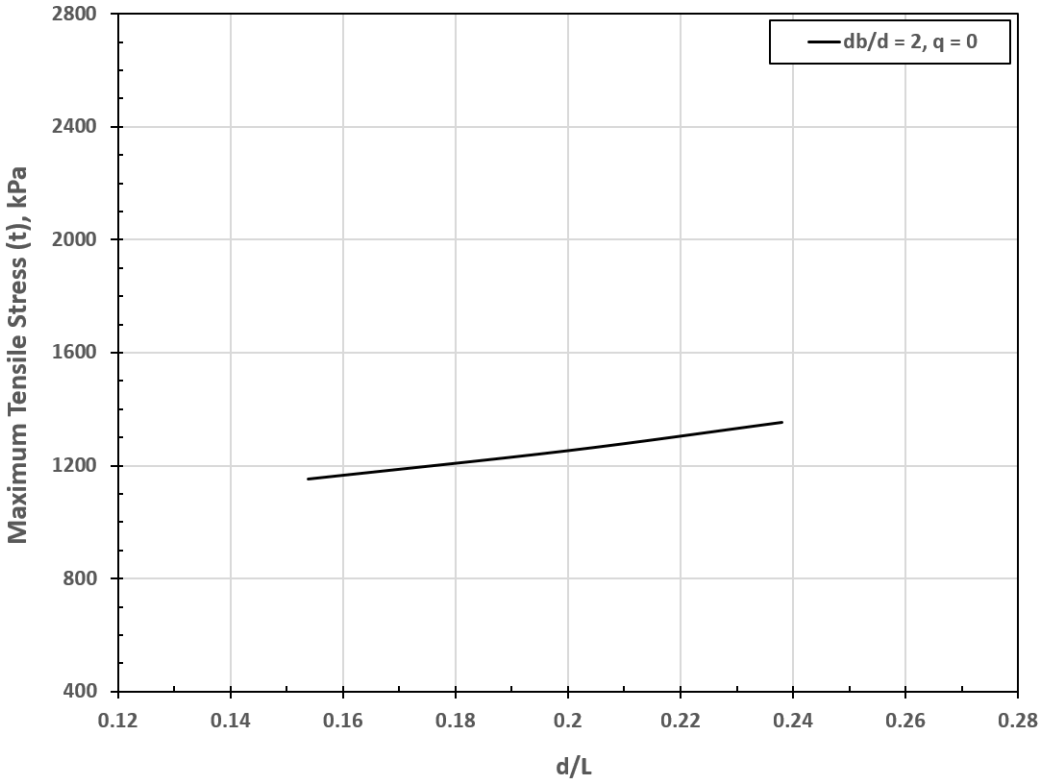

Figure 5.70: Trend Line for Maximum Tensile Stress, $3m$ depth of the swelling zone and $750kPa$ swelling pressure

Notes:

- The trend lines presented in Figures 5.69 and 5.70 can be used for $q > 0$ or $\sigma_s < 750kPa$ or both.
- Considering values of shaft diameter (d) larger than $0.6m$ or values of base to shaft diameter ratio (db/d) larger than 2 will result in uneconomical designs.

5.4.2 $4.5m$ depth of the swelling zone

$750kPa$ Swelling Pressure

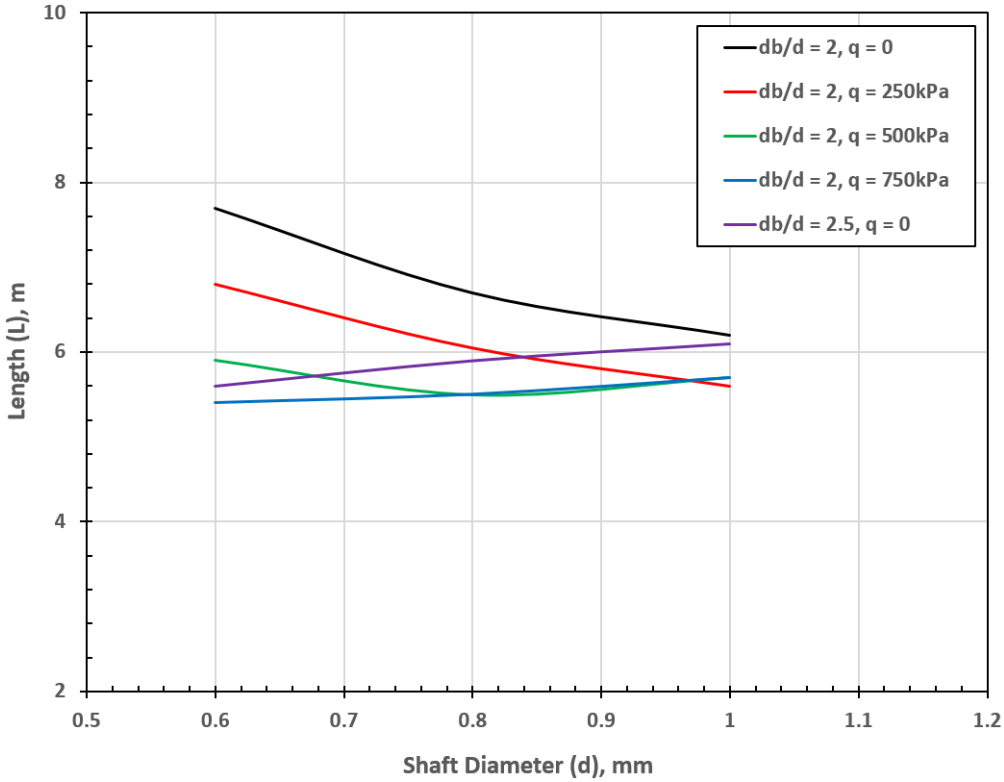

Figure 5.71: Trend Lines for Shaft Diameter and Length, $4.5m$ depth of the swelling zone and $750kPa$ swelling pressure

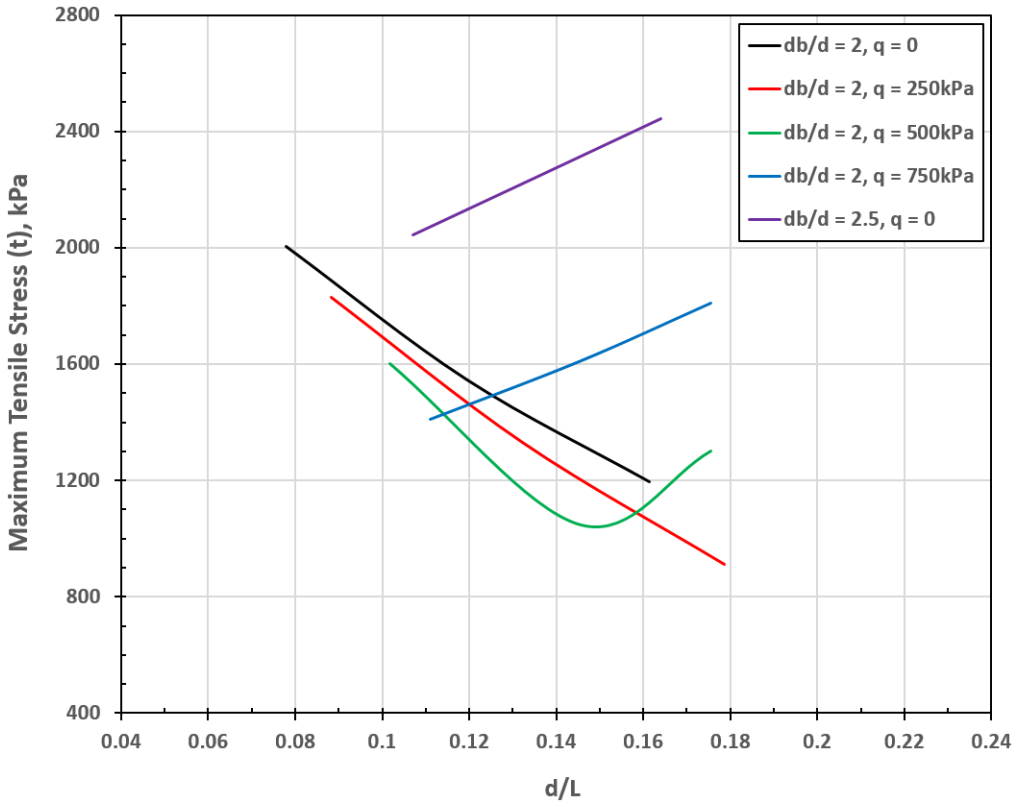

Figure 5.72: Trend Lines for Maximum Tensile Stress, $4.5m$ depth of the swelling zone and $750kPa$ swelling pressure

Notes:

- For $db/d = 2.5$ and $q > 0$, the trend lines presented for $q = 0$ shall be taken.
- For $db/d = 2$ and $q > 750kPa$, the trend lines presented for $q = 750kPa$ shall be taken.
- Upward shifting and upward progressing trend lines indicate uneconomical designs.

$500kPa$ Swelling Pressure

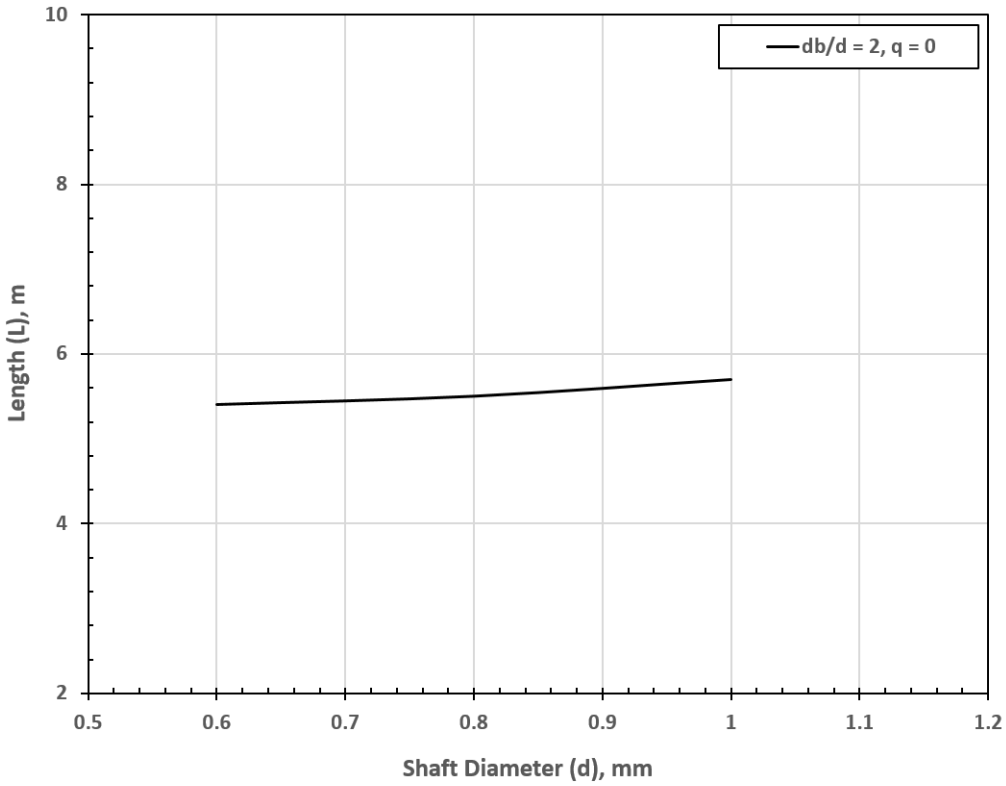

Figure 5.73: Trend Lines for Shaft Diameter and Length, $4.5m$ depth of the swelling zone and $500kPa$ swelling pressure

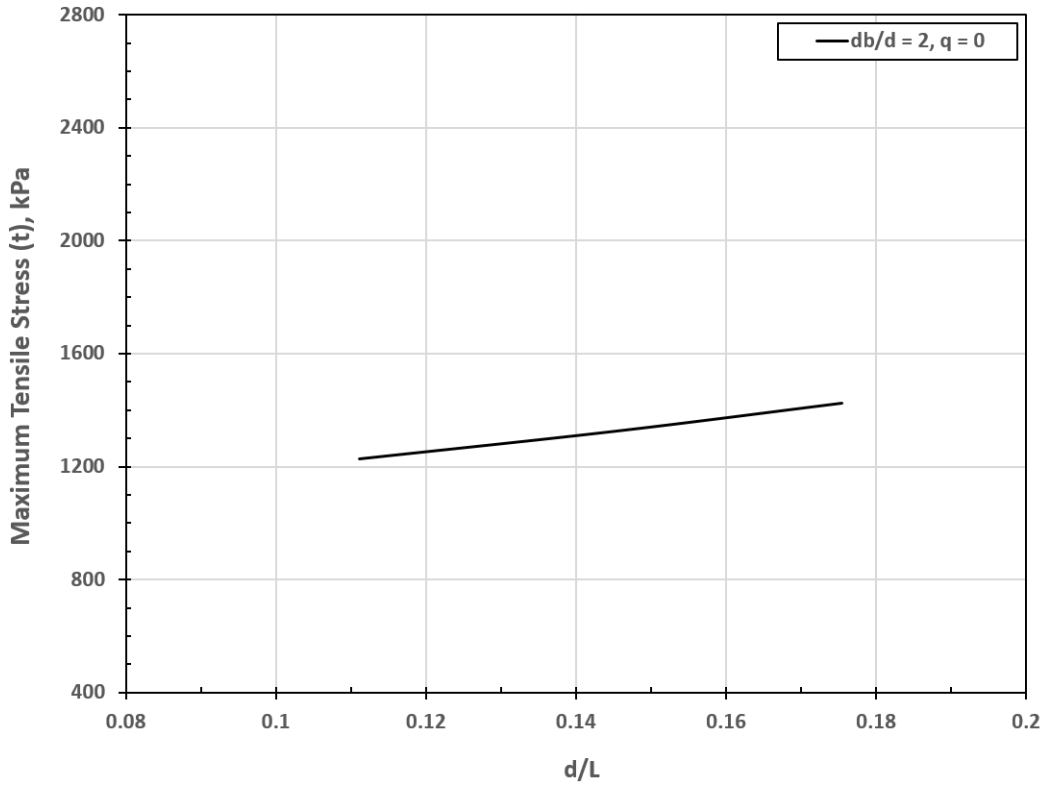

Figure 5.74: Trend Lines for Maximum Tensile Stress, $4.5m$ depth of the swelling zone and $500kPa$ swelling pressure

Notes:

- The trend lines presented in Figures 5.73 and 5.74 can be used for $q > 0$ or $\sigma_s < 500kPa$ or both.
- Considering values of shaft diameter (d) larger than $0.6m$ or values of base to shaft diameter ratio (db/d) larger than 2 will result in uneconomical designs.

Chapter 6

Conclusions and Recommendations

6.1 Conclusions

Belled piers in expansive soils were modelled using the finite element software Abaqus. The elasto-plastic and the swelling natures of the soil were considered in the modelling. Sampling and laboratory testing was conducted to determine some of these properties of the soil. Special attention was given to the contact between the belled piers and the soil. Soil-pier slip was allowed. The model was validated using different mechanisms. The effects of various parameters that can affect belled pier behaviors in expansive soils were investigated. A cost comparison of piers in expansive soils was conducted. Trend lines that can be used to design belled piers in expansive soils were proposed.

Based on the parametric investigations, cost comparisons and developed trend lines, the conclusions of the work can be summarized as follows:

- Increasing the shaft diameter decreases the pier heave. Furthermore, doing so also decreases the tensile stresses developed in the piers. Therefore, it is recommended to increase the shaft diameter instead of the length or the bell size to obtain safe designs when designing belled piers in expansive soils as increasing the length or the bell size increases the tensile stresses developed.

- The limiting diameter for belled piers ($d/L = 0.3$) is much higher than the limiting diameter for straight shaft piers ($d/L = 0.03$ or $d/L = 0.04$). Therefore, increasing the shaft diameter to obtain safe designs is more significant in belled piers than in straight shaft piers.

- Considering the usual case in Ethiopia where the swelling pressure is less than $500kPa$ and the depth of the swelling zone is less than $4.5m$, most belled piers in expansive soils in Ethiopia do not need tensile reinforcement, though reinforcement for shrinkage and temperature may still be necessary.

- Both pier heave and tensile stresses attain their maximum values within $7months$ of continuous saturation for $3m$ depth of the swelling zone.
- The applied load pressure needed to fully eliminate tensile stresses in belled piers is 1.2 times the maximum tensile stress in the corresponding free belled pier. This value is less than that observed for straight shaft piers where this value is 2.5 times the maximum tensile stress in the corresponding free straight shaft pier.
- For smaller values of the swelling pressure and the depth of the swelling zone, straight shaft piers are more cost effective; while for medium to large values of the swelling pressure and the depth of the swelling zone, large bell size belled piers are more cost effective.
- Again considering the usual case in Ethiopia where the swelling pressure is less than $500kPa$ and the depth of the swelling zone is about $3m$, belled piers with the minimum possible values of the shaft diameter, base to shaft diameter ratio and length can be used considering an allowable pier heave of $50mm$.

6.2 Recommendations

The following topics are recommended for future works by considering relations to the current work:

- Conduct field investigations or obtain field measured data of the behavior of belled piers in expansive soils and compare with the finite element analysis results.
- Develop a finite element code to investigate the behavior of belled piers in expansive soils.
- Investigate the effect of the installation process of belled piers on the behavior of belled piers in expansive soils.
- Investigate the effect of number of bells on belled pier behavior in expansive soils.
- Investigate belled piers under tension loading.

Bibliography

[1] Abaqus 6.14 Online Documentation (2014). Dassault Systèmes.

[2] Aljorany, A. N., and Noori, F. S. (2013). "Effect of Swelling Soil on Load Carrying Capacity of a Single Pile." *Journal of Engineering*, 7(19), 896-905.

[3] Al-Rawas, A. A., and Goosen, M. F. A. (2006). *Expansive soils: Recent advances in characterization and treatment*, Taylor & Francis, London.

[4] Al-shamrani, M. A., and Al-mhaidib, A. I. (1999). "Comparison of vertical and volumetric swells of compacted expansive soils." College of Engineering, King Saud University, Riyadh.

[5] American Standards for Testing Materials (2003).

[6] Averjanov, S. F., (1950), "About permeability of subsurface soils in case of complete saturation," *English Collection*, 7, 19–21

[7] Bowles, J. E., (2001). *Foundation analysis and design*, McGraw-hill, New York.

[8] Casagrande, A. (1936). "The determination of the Preconsolidation Load and its Practical Significance" *Proc. First Int. Conf. Soil Mech. Found Eng*, 3.

[9] Challa, P. K., and Poulos, H. G. (1991). "Behaviour of single pile in expansive clay." *Geotech. Eng.,* 22(2), 189–216.

[10] Chen, F. H. (1988). *Foundations on expansive soils*, Elsevier, New York.

[11] Chen, Y., Chang, H., Kulhawy, F. H., (2008). "Evaluation of Uplift Interpretation Criteria for Drilled Shaft Capacity", *Journal of geotechnical and geoenvironmental engineering, ASCE,* 134(October), 1459–1468.

[12] DE Bruyn, B. C. M. A., and Collins, L. E. (1956). "The specific surface, water affinity, and potential expansiveness of clays." National Building Research Institute, Pretoria, S. Africa., 120–128.

[13] Fan, Z. H., Wang, Y. H., Xiao, H. B., and Zhang, C. S. (2007). "Analytical method of load-transfer of single pile under expansive soil swelling." *J. Central South Univ. Technol.*, 14(4), 575–580.

[14] Farokhi, A. S., and Alielahi, H. (2014). Optimizing the Performance of Under- reamed Piles in Clay using Numerical Method, *EJGE*, 19(2014), 1507–1520.

[15] Jones, D.E. and Holtz, W. D. (1973). "Expansive soils - The hidden disaster." *ASCE*, 43(8), 49-51.

[16] Helwany S., (2007). *Applied soil mechanics with Abaqus applications*, John Wiley & Sons, Inc., Hoboken, New Jersey.

[17] Kaufmann, K. L., Nielsen, B. N., and Augustesen, A. H. (2010). "Finite element investigations on the interaction between a pile and swelling clay." *Tech. Rep. No. 104*, Dept. of Civil Engineering, Aalborg Univ., Aalborg, Denmark.

[18] PRE Technologies Ltd. (2014).

[19] Mohamedzein, Y. E. A., Mohamed, M. G., and Sharief, A. M. E. (1999). "Finite element analysis of short piles in expansive soils." *Comput. Geotech.*, 24(3), 231–243.

[20] Mosley, B., Bungey, J., Hulse, R. (2007), *Reinforced Concrete Design to Eurocode 2*, Palgrave Macmillan Publishing, Houndmills, Hampshire.

[21] Murray, E. J., and Sivakumar, V. (2010). *Unsaturated soils: A fundamental interpretation of soil behavior*, Wiley-Blackwell.

[22] Murthy, V. N. S. (2002). *Geotechnical engineering: Principles and practices of soil mechanics and foundation engineering*, CRC Press.

[23] Nelson. J. D., Schaut, R. W., Asce, M., Chao, K., Overton, D. D., ... Asce, A. M. (2012). "Design Procedure and Considerations for Piers in Expansive Soils." *Journal of geotechnical and geoenvironmental engineering, ASCE*, 138(August), 945–956.

[24] Nelson J. D., D. D. Overton, and K. Chao, (2010). "An empirical method for predicting foundation heave rate in expansive soil." *Geoshanghai International Conference*, Shanghai, China, June.

[25] Nelson, J. D., Chao, K. C., and Overton, D. D. (2007). "Design of pier foundations on expansive soils." *Proc., 3rd Asian Conf. on Unsaturated Soils*, Science Press, Beijing.

[26] Nelson, J. D., and Miller, D. J. (1992). *Expansive soils. Problems and practice in foundation and pavement engineering*, Wiley, New York.

[27] O'Neill, M. W. (1988). "Adaptive model for drilled shafts in expansive clay." *Proc., Geotech. Eng. Div. National Convention*, ASCE, New York, 1–22.

[28] Poulos, H. G. (1993). "Piled rafts in swelling or consolidating soils." *J. Geotech. Eng.*, 119, 374–380.

[29] Poulos, H.G. and Davis, E.H. (1980). *Pile Foundation Analysis and Design*. New York: John Wiley.

[30] Puppala, A. J., Manosuthikij, T.,and Chittoori, B. C. S. (2014). Swell and shrinkage strain prediction models for expansive clays. *Engineering Geology*, 168(2013), 1–8.

[31] Schmertmann, J.H. (1955). "The Undisturbed Consolidation Behavior of Clay," *Trans. ASCE, No. 120*.

[32] Seepage Modeling with SEEP/W (2007).

[33] Sisay, A., and Haile, M. (2004). "Assesment of damage of buildings constructed in expansive soil areas of Addis Ababa." Addis Ababa Institute of Technology.

[34] Skempton, A. W. (1953). *The colloidal activity of clays. Proc. 3rd Int. Conf. Soil Mech. Found. Eng.*, Switzerland. V.l:57-6l.

[35] Soundara, B., and Robinson, R. G. (2012). "Swelling Pressure and Uplift of Piles in Expansive Soils".

[36] Teferra, A. (1992). *Foundation Engineering*, Addis Ababa University.

[37] Tomlinson, M. and Woodward, J. (2008). *Pile Design and Construction Practice (5th edition)*. Taylor & Francis, London & New York.

[38] U.S. Army Corps of Engineers. (1983). *Technical manual TM 5-818-7*, Foundations in Expansive Soils, Washington, DC.

[39] Xiao, H., Zhang, C., Acse, S. M., Wang, Y., & Fan, Z. (2011). "Pile-Soil Interaction in Expansive Soil Foundation: Analytical Solution and Numerical Simulation". *Int. J. Geomech*, 11(June), 159–166.

[40] Xu, K. J., and Poulos, H. G. (2001). "3D elastic analysis of vertical piles subjected to 'passive' loadings." *Comput. Geotech.*, 28, 349–375.

[41] Zhan, Y. G., Wang, H., Liu, F. C. (2012). "Modelling vertical bearing capacity of pile foundation by using Abaqus." *EJGE*, 17(2012), 1855-1865